2003

Analysis of laboratory and field pull-out tests of geosynthetics in clayey soils

Ather Mohiuddin
Louisiana State University and Agricultural and Mechanical College, amohiu1@lsu.edu

ANALYSIS OF LABORATORY AND FIELD PULL-OUT TESTS OF GEOSYNHTHETICS IN CLAYEY SOILS

A Thesis

Submitted to the Graduate Faculty of the
Louisiana State University and
Agricultural and Mechanical College
in partial fulfillment of the
requirements for the degree of
Master of Science in Civil Engineering

in

The Department of Civil and Environmental Engineering

by
Ather Mohiuddin
B.E., Osmania University, 2001
August 2003

ACKNOWLEDGEMENTS

This thesis would not have seen the light of the day without the help and support of many people. I would like to take this opportunity to thank all the people who made this possible. First of all, I would like to thank the Louisiana Transportation Research Center (LTRC) for providing the necessary funds during my research program. I would like to express my sincere gratitude to my advisors Dr. Murad Abu-Farsakh and Dr. Mehmet Tumay. Dr. Murad was always willing to share his great knowledge and expertise with me. I also thank him for being patient with me during this endeavor. I feel fortunate in getting the opportunity to work under him and the experience was both enlightening and memorable. I will also be eternally grateful to Dr. Mehmet Tumay who was always willing to lend an ear to the issues and problems that I faced during the course of this thesis.

I would also like to thank Dr. Khalid Farrag for allowing me to work on his project, and provide me with the pull-out test results for the analysis I have done in this thesis. I would also like to extend my thanks and appreciations to Dr. Khalid Alshibli and Dr. Louay Mohammad for serving on the committee.

My special appreciations to my father Khader Mohiuddin, mother Qaiser-unisa Begum and grand mother Ahmedi Begum for their love, care and prayers that has brought me to this level. My love and thanks to Ahmed, Ayub, Junaid, Waleed and all of my friends for being there when I needed them, and showing me the meaning of true friendship.

TABLE OF CONTENTS

LIST OF TABLES

LIST OF FIGURES

ABSTRACT

Soil reinforcement interaction is a key issue in the design of reinforced soil structures. Therefore, it is important to analyze the pull-out mechanism, and to evaluate the interaction between the soil and geosynthetic reinforcement. Majority of pull-out tests performed to date were in granular soils, and very few tests were reported in cohesive soils. The shortage of in-situ granular materials and the availability of cohesive soils in Louisiana have initiated a growing interest in using the marginal soils as backfill material. To investigate the soil-geosynthetic interaction parameters, series of laboratory and field pull-out tests were conducted using various geosynthetics (geogrids: UX750, UX1500, UX1700, Stratagrid-500, and geotextiles: Woven (4x4), Woven (6x6) and Non-woven) with different lengths under various confining pressures. This research program is based on the analysis of the pull-out tests, which includes (i) the comparison of laboratory and field pull-out tests, (ii) the contribution of passive bearing resistance to the total pull-out resistance, (iii) the evaluation of coefficient of interaction (C_i), and (iv) the evaluation of the scale correction factor (α).

The results of this study indicate that (i) the laboratory and field pull-out test results are close to each other and show more consistency for high strength geosynthetics compared to weak strength geosynthetics, (ii) the contribution of passive bearing resistance ranges from 5-30 percent of the total pull-out resistance, (iii) the coefficient of interaction (C_i) ranged from 0.5 to 1.0 for laboratory tests and 0.3 to 1.2 for field pull-out tests, and decreases with increasing length and increasing confining pressure, and (iv) the scale correction factor (α) values estimated for the geogrids ranges from 0.32 to 0.82.

CHAPTER 1

INTRODUCTION

1.1 Introduction

The use of various reinforcements to improve the tensile capacity of soils has been widely used in many soil structures, especially in the construction of reinforced earth walls, reinforced slopes, embankments on soft soils, vertical landfills and foundation soils. The interface friction between the soil and geosynthetics is a very important factor for design of these structures. The use of reinforcements will provide additional shear stress in the soil mass through the tensile force in the reinforcement, which will increase the strength of soil-reinforcement mass, and hence reduce the horizontal deformations, and thereby increasing the overall stability of the structure. Geosynthetics were first introduced as reinforcement material for reinforced soil structures in the 1970s (Holtz et al., 1997). The considerable increase in the use of geosynthetics in the reinforced soil structures led to the development of testing procedures to evaluate their interaction properties. Research to date has been focused on the evaluation of the interaction properties of the reinforcement in granular soils. This is primarily due to the extensive use of granular backfill in reinforced soil walls and embankments. The advantages of using granular materials are their higher frictional resistance, their stable soil properties with time and with changes in moisture content, and to provide free-drainage backfill.

However, the shortage of in-situ granular materials and the availability of cohesive soils in Louisiana, as well as, in some other states, have initiated the growing interest in the use of the available cohesive soils in the construction of the reinforced soil

structures. The utilization of lower quality backfill in reinforced soil structures could significantly reduce the cost of these structures. This economical consideration could be a major importance when the available cohesive soils are used with different reinforced soil structures (Farrag, 1996). The advantages of geosynthetic reinforcement over conventional steel reinforcements were given by Lee (2000) as:

1. Geosynthetic reinforcements are more tolerant to differential movements than conventional reinforcements, because of the excellent flexibility and uniformity of geosynthetics.
2. Geosynthetics are more resistant to corrosion and other chemical reactions.

However, one of the major disadvantage of geosynthetics is that it has a considerable creep with time, especially in regions that experience higher temperatures, which should be considered in the design by applying a factor of safety that include creep effects.

One of the predominant causes of failure in the geosynthetic reinforced soil walls is the pull-out resistance of geosynthetics. Therefore the evaluation of pull-out resistance is an essential factor in the design of the geosynthetic reinforced soil structures. Many methods have been developed to predict the pull-out resistance of geosynthetics. The illustration of these evaluations and their usage in the design of reinforced soil structures will be discussed in detail in Chapter 6.

Although there is an increased interest in the use cohesive soils in reinforced walls and slopes, limited research had been done relevant to the evaluation of the interaction parameters (i.e. pull-out resistance and shear stress-strain characteristics) between the cohesive soils and the geosynthetics. Due to the lack of granular backfill

material and the availability of silty clay in Louisiana, a comprehensive testing program was conducted at Louisiana Transportation and Research Center, LTRC, to evaluate the potential use of cohesive soils in reinforced walls and slopes. Laboratory pull-out tests were conducted on silty clay soils in the Geosynthetic Engineering Research Laboratory, GERL, at the LTRC using large size pull-out boxes. Also a full-scale instrumented test wall, called the LTRC-test wall, has been constructed at the Accelerated Loading Facility (ALF) site under the supervision of Dr. Khalid Farrag to perform field pull-out tests, under in-situ conditions, and to evaluate the reliability of using silty clay as backfill material for reinforced walls and slopes. A summary of the equipment and procedures used in determining the clay-geosynthetics interface parameters is presented in Chapter 3. The evaluation of the effect of the testing parameters on the interaction mechanism was mainly conducted on the geogrid and geotextiles using large boxes for pull-out tests. There were four different types of geogrids, and three different types of geotextiles tested for pull-out tests. The test results of pull-out tests are presented in Chapter 5, which are then analyzed to determine the influencing factors on the pull-out resistance and the interface shear resistance along the length of geosynthetic. The analysis presented in Chapter 6 will provide a selection criterion for the design parameters of geosynthetics in cohesive soils, and evaluation of pull-out and interface shear resistance under different testing conditions.

The second phase of this research program was focused on the evaluation of the laboratory pull-out resistance and the interpretation through a comparison with the field pull-out test results. The field tests were performed on various types of geosynthetics in an instrumented test wall constructed using cohesive soil as backfill material. Both the

laboratory and the field tests were conducted on the same soil using the same geosynthetics to compare the effects of in-situ conditions, and to have the luxury of using the laboratory tests in future.

1.2 Objectives

The main objective of this study is to analyze the field and laboratory pull-out tests of geosynthetics, which includes:

i. Comparison of laboratory and field pull-out tests,

ii. Contribution of passive bearing resistance to the total pull-out resistance,

iii. Evaluation of coefficient of interaction (C_i),

iv. Evaluation of shear stress distribution along the length of the geosynthetic, and

v. Evaluation of pull-out resistance design parameters (F^* and α).

CHAPTER 2

LITERATURE REVIEW

2.1 Literature Review

Several researchers have carried out the pull-out tests of reinforcements in soils (Ingold, 1983; Rowe et al., 1985; Juran, 1988; Fannin and Raju, 1993; Farrag, 1993; Bergado et al., 1992; Mallick et al., 1995; and Ochiai et al., 1996). These pull-out tests were originally carried out for the purpose of clarifying the pull-out mechanism of the reinforced soils. The method of preparing the sample, soil utilized, reinforcement material, testing procedure and the size of the pull-out test apparatus were among the factors studied. A comparative study was conducted by Juran et al. (1988), but because of the different test conditions such as soils and apparatus used in each test, their studies were restricted to qualitative rather than quantitative basis. The results of pull-out tests have been used for investigating the mechanism and evaluating the design and analysis parameters of reinforced soil structures. The test conditions are very important for the determination of these parameters. The interaction between soil and reinforcement is frequently evaluated in terms of apparent interface friction factor evaluated from the pull-out tests as recommended by Ingold, 1983; Rowe et al. 1985; Juran, 1988; and Christopher, 1988.

Rowe et al. (1985) evaluated the soil-geosynthetic interface strength properties of geosynthetics in conventional granular fill and light weight (saw dust) fill. They conducted series of direct shear tests and pull-out tests, which were performed to determine these properties for a number of different geotextiles and geogrids in both granular fill and saw dust. For both woven and non-woven fabrics, the interface friction

angle (δ) was the same in both direct shear and pull-out modes. But for geogrid "Tensar SR2", the interface friction angle (δ) measured by direct shear test was essentially the same as that of the soil (i.e. $\delta = \Phi = 30^o$), and the interface friction angle measured by pull-out test was significantly lower (i.e. $\delta = 18^o$).

Koutsourais et al. (1998) also compared the results of pull-out and direct shear tests of geosynthetic reinforcement in marginal cohesive soil, in terms of interface friction angle (δ). They concluded that the pull-out tests truly simulate the pull-out failure, and the pull-out tests provide approximately 13% to 17 % higher soil interaction values at low confining pressures (< 4 psi) and provide essentially the same soil interaction values at higher confining pressures.

Cowell and Sprague (1993) compared the pull-out performance of geogrids and geotextiles in uniformly fine sand. They investigated the differences in the pull-out performance for geogrids with and without junctions and for geogrids and geotextiles with similar stress-strain characteristics when tested in uniform fine sand. The pull-out resistance at 0.75 inches of displacement for the geotextiles tested was significantly 50% to 67% lower than that obtained for geogrids of similar strengths. The removal of the junctions from the geogrid tested reduced the pull-out resistance of the geogrids by less than 10%.

Bergado et al. (1992) conducted pull-out tests of steel geogrids in weathered clay, and compared the laboratory and field pull-out test results. The laboratory pull-out tests were conducted on various reinforcement sizes, mesh geometry, and compaction conditions of the weathered clay. The field pull-out tests provided higher pull-out resistance than the laboratory tests. The total pull-out resistance of the geogrids is the

combination of the frictional resistance and the passive bearing resistance. Though the tests were conducted with steel geogrids, they provided the effect of cohesive nature of the soils and provided the necessary formulations for passive bearing resistance for cohesive soils. The passive bearing resistance (F_b) was related to the bearing capacity factors in the Terzaghi-Buisman bearing capacity equation. Two failure models were adopted to evaluate the bearing capacity factors, namely the bearing capacity failure model (Peterson and Anderson, 1980) and the punching shear failure model (Jewell et al. 1984). The prediction for passive bearing associated with the bearing capacity failure model formed the upper boundary while the prediction associated with the punching shear failure model provided the lower boundary. Lin et al. (1996) studied the performance of polymeric geogrids in compacted cohesive lateritic soil and complemented the analysis done by Bergado et al. (1992) and presented identical conclusions. Lin et al. (1996) used the same failure models to evaluate the passive bearing resistance of polymer geogrids and came up with conclusion similar to Bergado et al. (1992), i.e., the bearing capacity failure and the punching failure modes appeared to be an upper bound and lower bound envelope for the pull-out capacities of the polymer grid reinforcements, respectively. The passive bearing resistance and the frictional resistance are discussed in detail in Chapter 6, Section 6.4.

The total pull-out resistance for geotextiles is contributed only by the frictional resistance. The frictional resistance for geotextiles is evaluated using Mohr-Coulomb yield criterion, which depends on the soil properties (i.e. soil friction angle and soil cohesion intercept), interface friction angle, interface adhesion, the embedded area and applied confining pressure (Koutsourais et al., 1998).

Ochiai et al. (1996) evaluated the pull-out resistance from pull-out tests of geogrids in uniform fine sand. In their study, both field and laboratory pull-out tests were carried out in order to clarify the pull-out mechanism, and to determine the parameters needed for design and analysis of the reinforced soil structures. In order to evaluate the pull-out resistance, two evaluation methods were defined the Mobilizing process method and the Average resistance method. Based on the pull-out mechanism, the Average resistance method was further sub-divided in to three methods which are called the Total area method, the Effective area method and the Maximum slope method. For practical use, the pull-out test with small vertical stress is recommended, together with the total area method, for evaluating the average resistance from the test results (Ochiai et al., 1996). These methods are further discussed in detail in Chapter 6, Section 6.5.

Many researchers have discussed the importance of using the coefficient of interaction (C_i) as a design parameter (Cowell et al., 1993; Koutsourais et al., 1998; Tatlisoz et al., 1998). According to these researchers, the coefficient of interaction is the ratio of interface strength between the soil and reinforcement to shear strength of the soil. Cowell et al. (1993) evaluated the soil interaction coefficients of geotextiles and geogrids in sand, the C_i values ranged from 0.8 to 1.0. However, Koutsourais et al. (1998) evaluated the coefficient of interaction (C_i) of geotextiles and geogrids in clay, and they obtained C_i values that ranged from 0.5 to 0.9. Tatlisoz et al. (1998) studied the interaction between reinforcing geosynthetics and soil-tire chip mixtures. In there study, they evaluated the coefficient of interaction for different geosynthetics with different soil combinations. The C_i values obtained in the study ranged from 0.3 to 1.5. An interaction coefficient greater than unity ($C_i > 1$) indicates that there is an efficient bond between the

soil and the geosynthetic and that the interface strength between the soil and the reinforcement is greater than shear strength of the soil (Tatlisoz et al., 1998). Similarly, if the interaction coefficient is less than 0.5 ($C_i < 0.5$) indicates weak bonding between soil and geosynthetic or breakage of geosynthetic layer (Tatlisoz et al., 1998).

The shear stress distribution along the length of geosynthetics using pull-out tests was first introduced by Holtz (1977). In his laboratory study of reinforced earth using woven polyester fabric, he conducted friction tests, and in these tests a system of small magnets was attached to test specimen at every 150 mm to measure deformation. The location of each magnet relative to its initial position was observed and recorded several times during the pull-out test. Thus, the difference between any two relative moments represents the measure of the net deformation in a given section of test specimen. After measuring the deformation along the length of the test specimen, the corresponding strain and then the corresponding stress in a given section of the test specimen was calibrated. Ochiai et al. (1996) also evaluated the shear stress distribution of geogrids tested in sand. The deformation along the length of the geogrid was measured using LVDTs, and therefore the average shear stress between the given sections was calculated. Both studies concluded that the shear stress is maximum at the face of the geosynthetic and gradually decreases along its length.

The normalized method to determine the pull-out resistance factors was recommended in the FHWA 1996 manual (Elias and Christopher, 1996). In the FHWA 1996 manual, the pull-out resistance factors F^* (friction-bearing interaction factor) and α (scale correction factor) were evaluated, both theoretically and experimentally. The experimental procedure recommended laboratory or field pull-out tests to evaluate these

factors. To determine the scale correction factor (α), the pull-out tests was recommended for different lengths with varying confining pressure. For geosynthetic reinforcements, the F^* was referred as the interaction coefficient (C_i). The recommended value of α for design using geosynthetics was recommended in the range of 0.6 to 0.8. The pull-out resistance factors are further reviewed in detail in Chapter 6, Section 6.7.

CHAPTER 3

LABORATORY TESTS

3.1 General

The laboratory pull-out testing facility at LTRC was originally constructed in 1993 for the evaluation of interaction parameters of geosynthetics in granular soils under the supervision of Dr. Khalid Farrag and Dr. Ilan Juran. A pull-out testing program was conducted to evaluate the performance of the facility and to assess the effect of testing parameters on the pull-out characteristics of geosynthetics with the cohesive silty clay. The pull-out testing equipment consisted mainly of two large pull-out boxes. The pull-out boxes were designed with the consideration of the following objectives:

i. To provide the capability of conducting both load-controlled and displacement-rate controlled pull-out tests,

ii. To provide through modular design of the box, flexibility in testing with various sample/box dimensions for evaluation of boundary effects,

iii. To minimize the effect of the rigid front facing by incorporating sleeves of appropriate lengths at the front wall,

iv. To allow for testing under different confining pressure,

v. To insure confinement of the geosynthetic specimens during the test by extending the clamping plates inside the soil,

vi. To establish reliable instrumentation scheme to measure displacements and pressures.

3.2 Laboratory Test Set-up

In the laboratory, pull-out tests were modified to facilitate the testing of compacted cohesive soils. Two pull-out boxes were utilized in the evaluation of the pull-out resistance of the geosynthetics. The large pull-out box has internal dimensions of 60-inch length, 36 inch width, and 36 inch height. The small pull-out box has the dimensions of 48 inch length, 24 inch width, and 18 inch height. The small box is movable, to facilitate compaction and moisture control of the cohesive soil. When testing, the small box is placed inside the large box. A typical schematic diagram of the pull-out boxes is shown in Figure 3.2.1 and Figure 3.2.2.

The reduction in the influence of the top boundary and a uniform distribution of the applied confining pressure (vertical overburden pressure) was achieved with a 2-inch thick inflatable air bag. The sleeve plates of 4 inches in width were used to minimize the lateral stress transfer to the rigid front wall of the pull-out box. Metal plates were clamped to the geosynthetic specimens and were extended through the box. A minimum of 6-inch plate length was left inside the soil to allow the pull-out displacement of the geosynthetic specimen within the soil. The hydraulic ram (Model Miller H67B) was mounted on the loading frames to apply a pull-out through the clamping plates. To reduce the boundary effects, geosynthetic specimens of 3 ft long and 1ft wide were tested. Furthermore these geosynthetic specimens were connected with LVDT (Linear Variable differential Transformers) model ‘Schaevitz’ with stroke length of 10 inches. These LVDT were placed at 1 ft spacing along the length of the geosynthetic specimen to measure the deformations of the geosynthetic specimen with respect to increasing confining pressure.

The pull-out box was filled to level of the sleeve with the soil compacted in 6-inch lifts. The geosynthetic specimen was then placed in between the sleeves, and the rest of the soil was then compacted with 6-inch layers until the box was filled with the compacted cohesive soil. The pull-out force was applied through hydraulic ram with a constant displacement rate of 1.5mm/min. The data was recorded by the data acquisition system in the computer, which recorded the load and displacement. The test was stopped when the pull-out load stopped increasing.

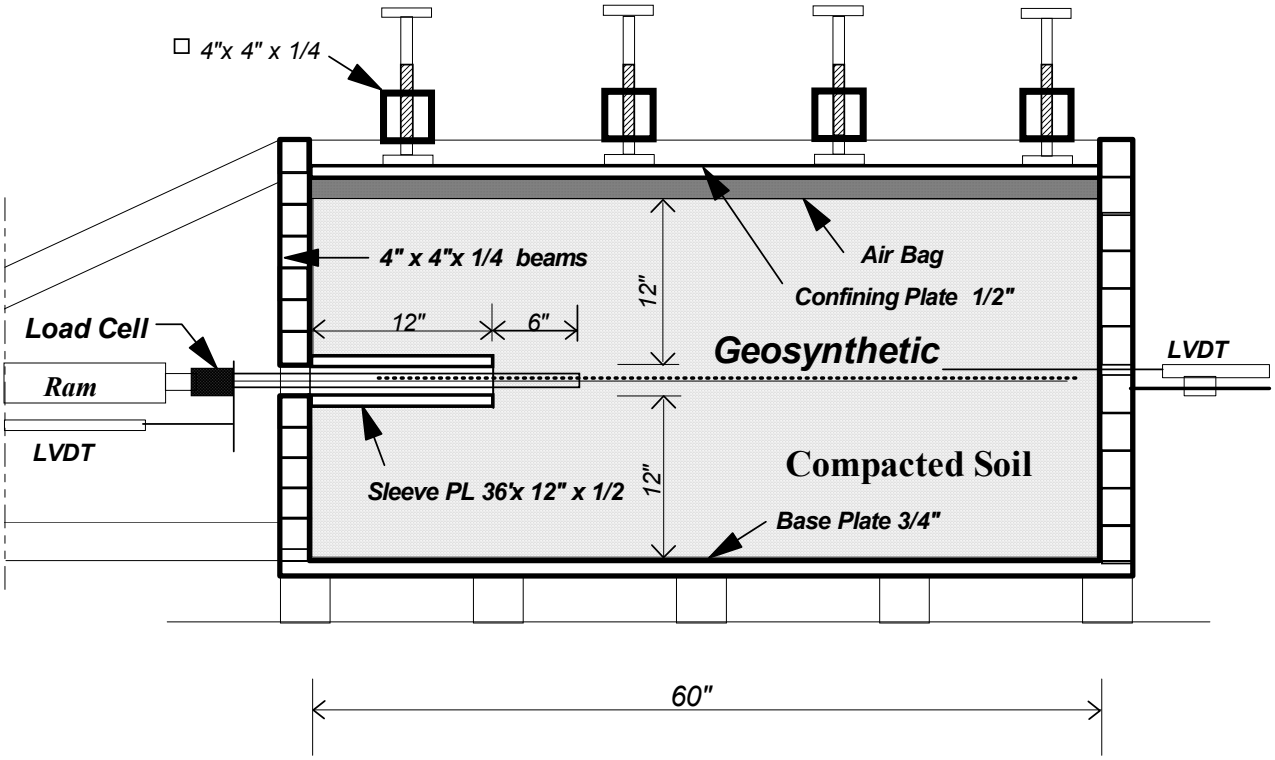

Figure 3.2.1: Cross section of the large pull-out box (Farrag, 1993)

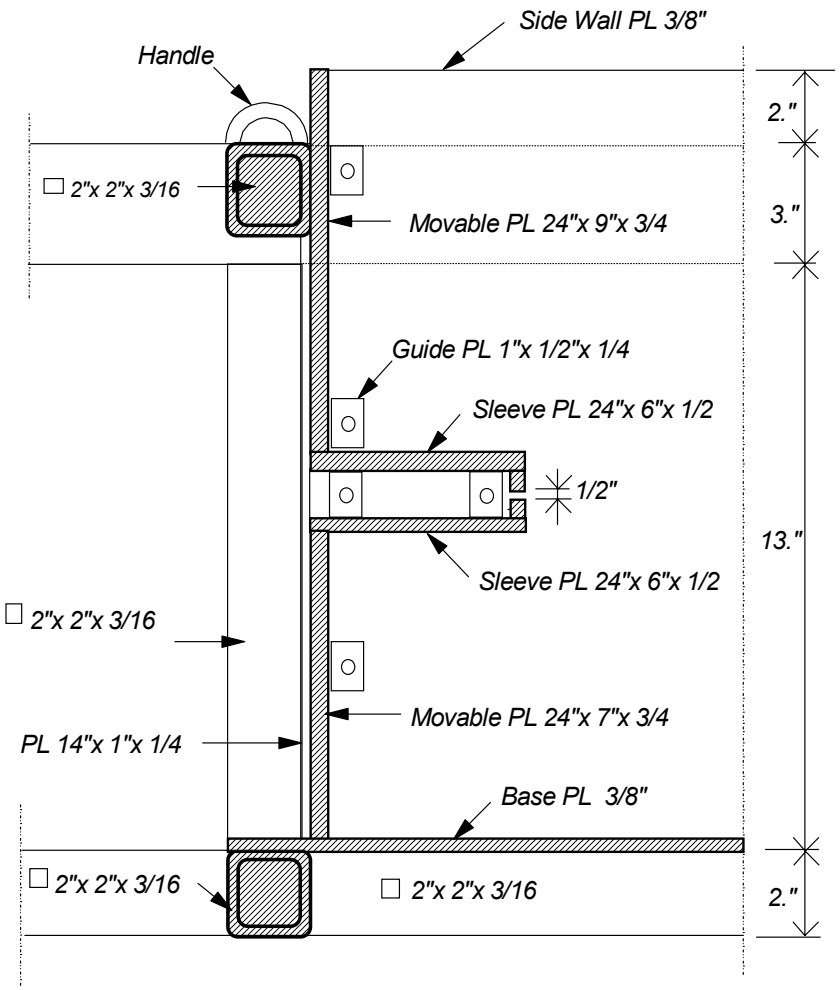

Figure 3.2.2: Cross-section in the front wall of small pull-out box (Farrag, 2003)

3.3 Material Properties

The soil properties which were obtained using the direct shear test are given in the Table 3.3.1, and Figure 3.3.3 presents the behavior of soil with respect to water content obtained from the standard proctor test. Figure 3.3.4 shows the grid structure of the uniaxial geogrid, where TD is the transverse direction and MD is the machine direction.

Table 3.3.1: Soil properties

Liquid limit	Plasticity Index	% Silt	% Clay	Cohesion Intercept (C) psi	Φ' (degrees)	w_{opt} (%)	γ_{max} (pcf)
27	6	72.0	19.0	3.0	24	18.75	104

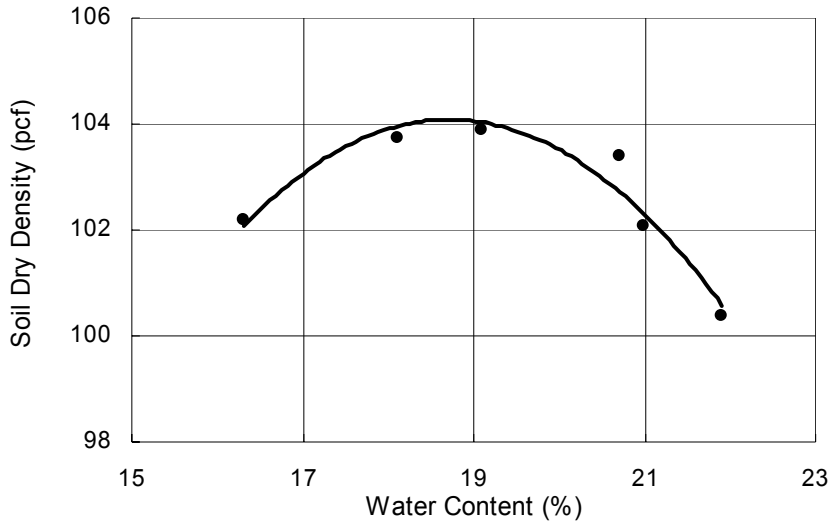

Figure 3.3.3: Water content versus soil dry density for silty clay.

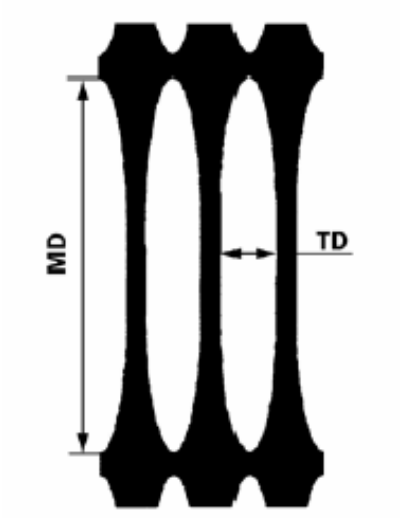

Figure 3.3.4: Grid structure of a uniaxial geogrid
MD is the machine direction, and TD transverse direction.

The properties of seven different geosynthetics provided by the respective manufacturers are summarized in Tables 3.3.2 and 3.3.3. Table 3.3.2 presents the properties of the four different geogrids, where UX750, UX1500 and UX1700 are the products of Tensar Technologies Ltd and Strata-500 is the product of Strata Systems Inc. Table 3.3.3 presents the properties of the Woven (4x4), Woven (6x6) and Non-woven (TG700) geotextiles.

Table 3.3.2: Properties of uniaxial geogrids

Type	Apertures (inch)		Open area (%)	Thickness (inch)		Tensile Modulus (lb/ft) per 1ft width
	MD	TD		ribs	junctions	
UX1500HS	14.5	0.66	68	0.065	0.167	90,000
UX1700HS	14.5	0.66	68	0.125	0.283	160,000
UX750SB	6	0.66	60	0.018	0.072	27,000
Strata 500	2.30	1.00	55	.050	.060	22,000

Table 3.3.3: Properties of woven and non-woven geotextiles

Product Name	Polymer Type	Mass per unit area (gm/m^2)	Strength at 5% Strain (lb/in)/ft width		Ultimate Strength (lb/in)/1ft width	
			MD	XD	MD	XD
Geotex(4x4)	Polypropylene	440	110	130	400	400
Geotex(6x6)	Polyester	455	150	250	600	600
TG 700 (NW)	Polypropylene	271	NP	NP	NP	NP

The strength properties for non-woven geotextile (TG-700) were not provided by the manufactures (Evergreen technologies). However, the wide width tensile test for this geotextile was conducted in the laboratory. Figure 3.3.11 shows the load strain relationship for the non-woven geotextile (TG-700).

The wide width tensile tests were conducted for five different geosynthetics (UX750, Strata-500, Woven (4x4), Woven (6x6) and Non-woven (TG-700)) to determine the tensile modulus at 2% strain, 5% strain and at ultimate strain. The tests were conducted on geosynthetic samples of 8 inch width and 18 inch length. The load-strain relationship for other two geogrids (UX1500 and UX1700) was provided by Tensar Ltd (the manufacturer). The load was calibrated with respect to 1 ft width. The load-strain curves for the seven different geosynthetics used in this study are shown in Figures 3.3.5 through 3.3.11.

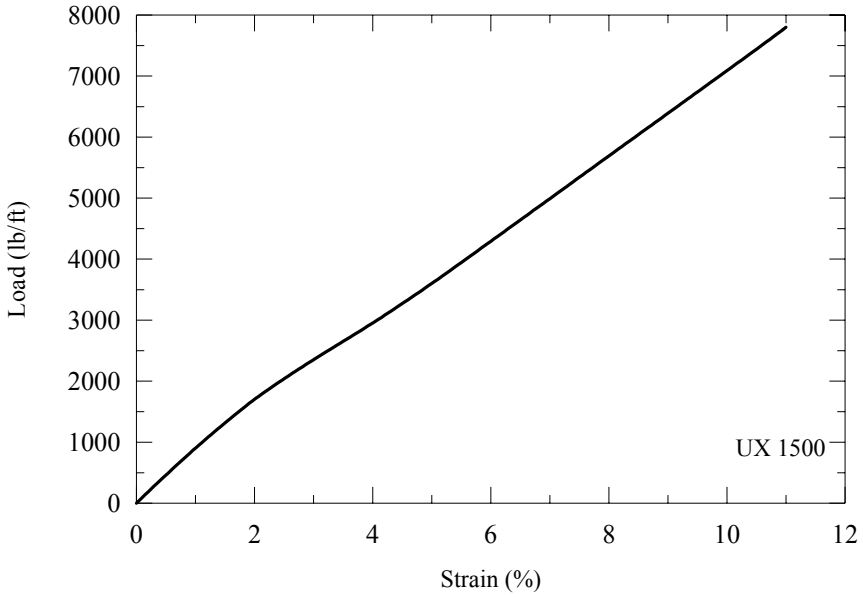

Figure 3.3.5: Load-strain relationship for UX 1500 (Tensar Ltd).

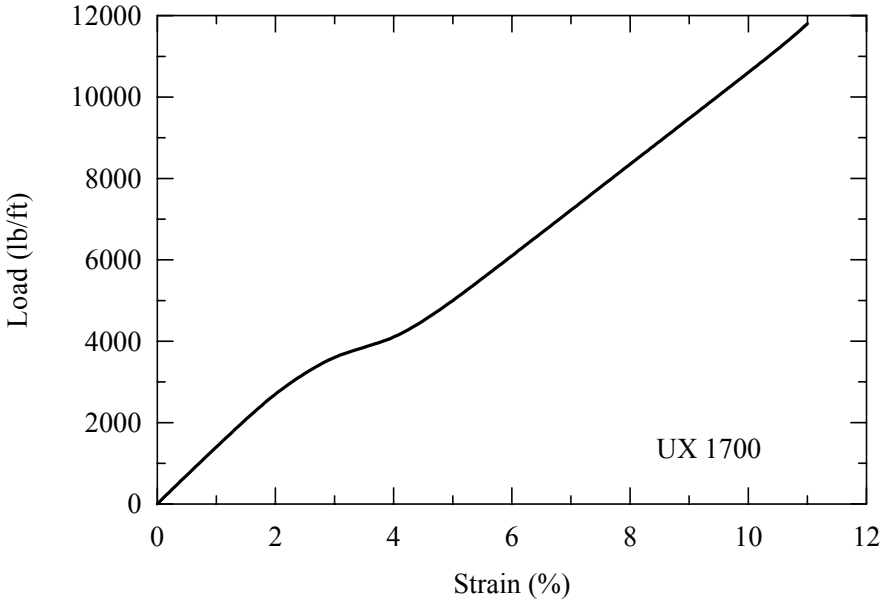

Figure 3.3.6: Load-strain relationship for UX 1700 (Tensar Ltd).

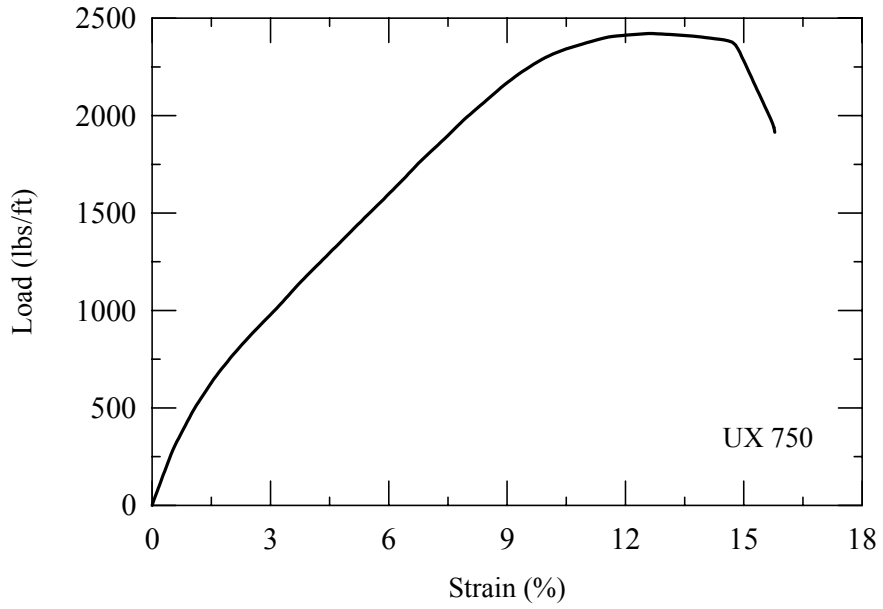

Figure 3.3.7: Load-strain relationship for UX 750.

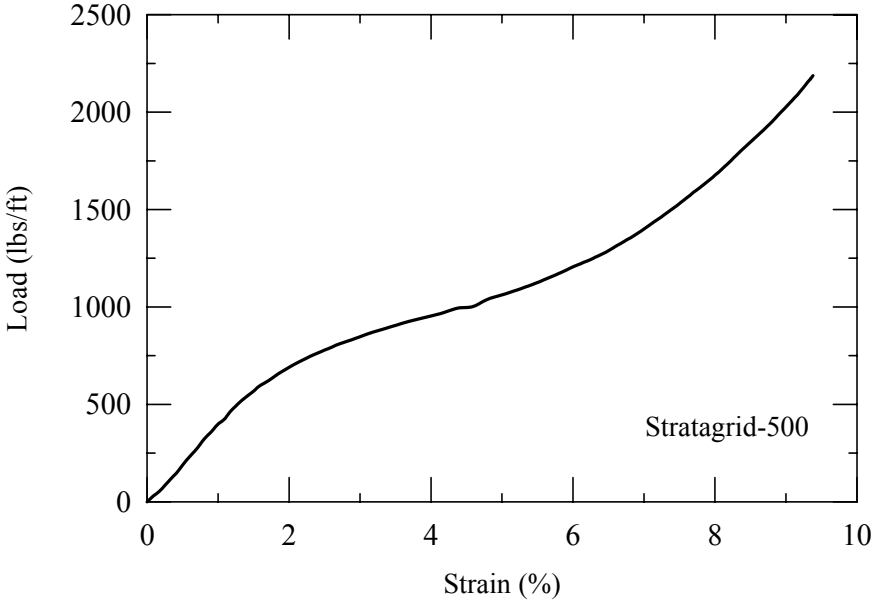

Figure 3.3.8: Load-strain relationship for Stratagrid-500.

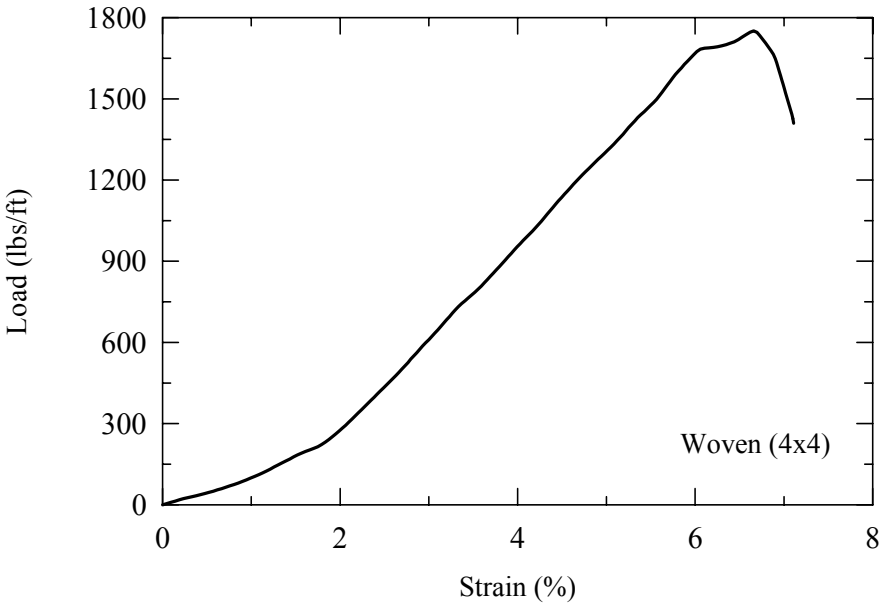

Figure 3.3.9: Load strain relationship for Woven (4x4) geotextile.

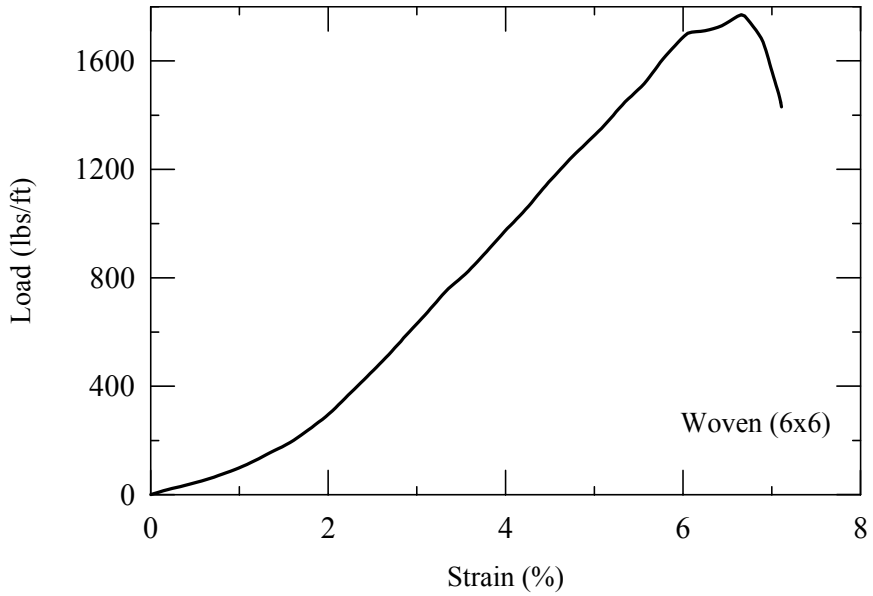

Figure 3.3.10: Load strain relationship for Woven (6x6) geotextile.

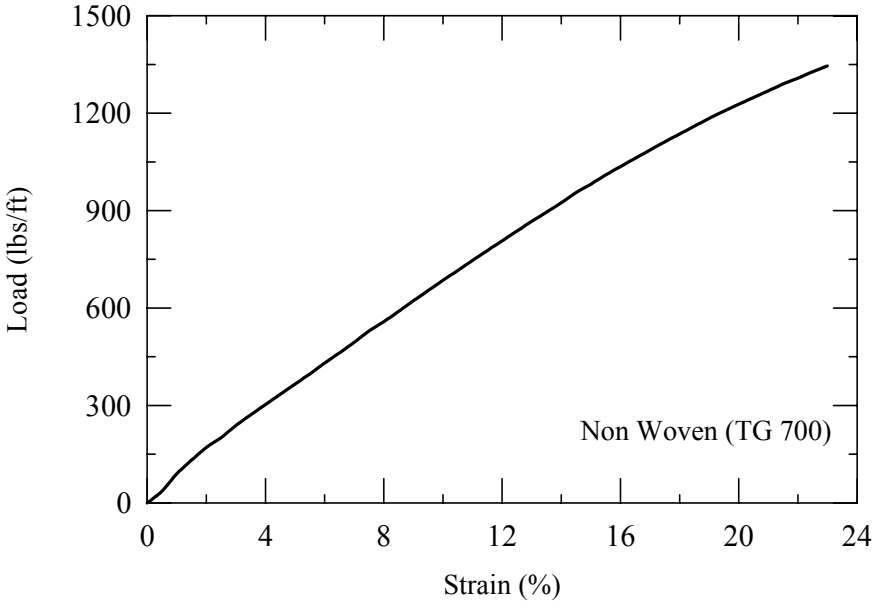

Figure 3.3.11: Load strain relationship for Non-woven TG 700 geotextile.

CHAPTER 4

FIELD PULL-OUT TESTS

4.1 General

The reinforced-soil test wall and reinforced soil slope was constructed at the LTRC-ALF test site under the supervision of Dr. Khalid Farrag (1998) to provide the necessary data to evaluate design parameters and to compare the field pull-out test results with laboratory pull-out test results conducted using the same cohesive soil. The wall is 20 ft (6.1 m) high and 154 ft (47 m) long. The front facing of the wall consisted of modular blocks reinforced with various types of geogrids. The back facing of the wall is a one to one (1:1) slope reinforced with two types of geotextile reinforcements. Figure 4.1.1 shows the plan and elevation views of the LTRC-test wall.

The vertical facing is divided into four zones. The first zone is dedicated to perform field pull-out tests on seven different types of geosynthetics (geogrids: Strata-500, UX750, UX1500, UX1700, and geotextiles: Woven (4x4), Woven (6x6) and Non-woven). The facing blocks at various locations in this zone are replaced by wooden boxes that allow the geosynthetic specimens to be pulled out from the wall. Figure 4.1.2 shows the elevation of LTRC-test wall with the arrangement of pull-out boxes. The second zone is constructed with HDPE geogrid (UX1400) placed at maximum vertical spacing of 40 inches (1 m) between the layers. The third zone is constructed with compact size modular blocks and weaker HDPE geogrid (UX750) placed at minimum vertical spacing of 16 inches (0.4 m). The partial safety factors, F.S, of the reinforcement of these layers are reduced to minimum (F.S=1.0) to assure deformation readings. The reinforcement is instrumented with strain gages to monitor deformation. The instrumentation of the wall is

discussed in the next section of this chapter. The south side of the test wall is constructed with a geoweb gravity wall. The function of this section is to evaluate the construction and performance of a geoweb wall, which is beyond the scope of this research program. Geosynthetic specimens of length 3ft, 4ft and 5ft were tested. All the geosynthetic specimens were glued with the strain gages to monitor the deformation of the geosynthetic specimen at the desired positions.

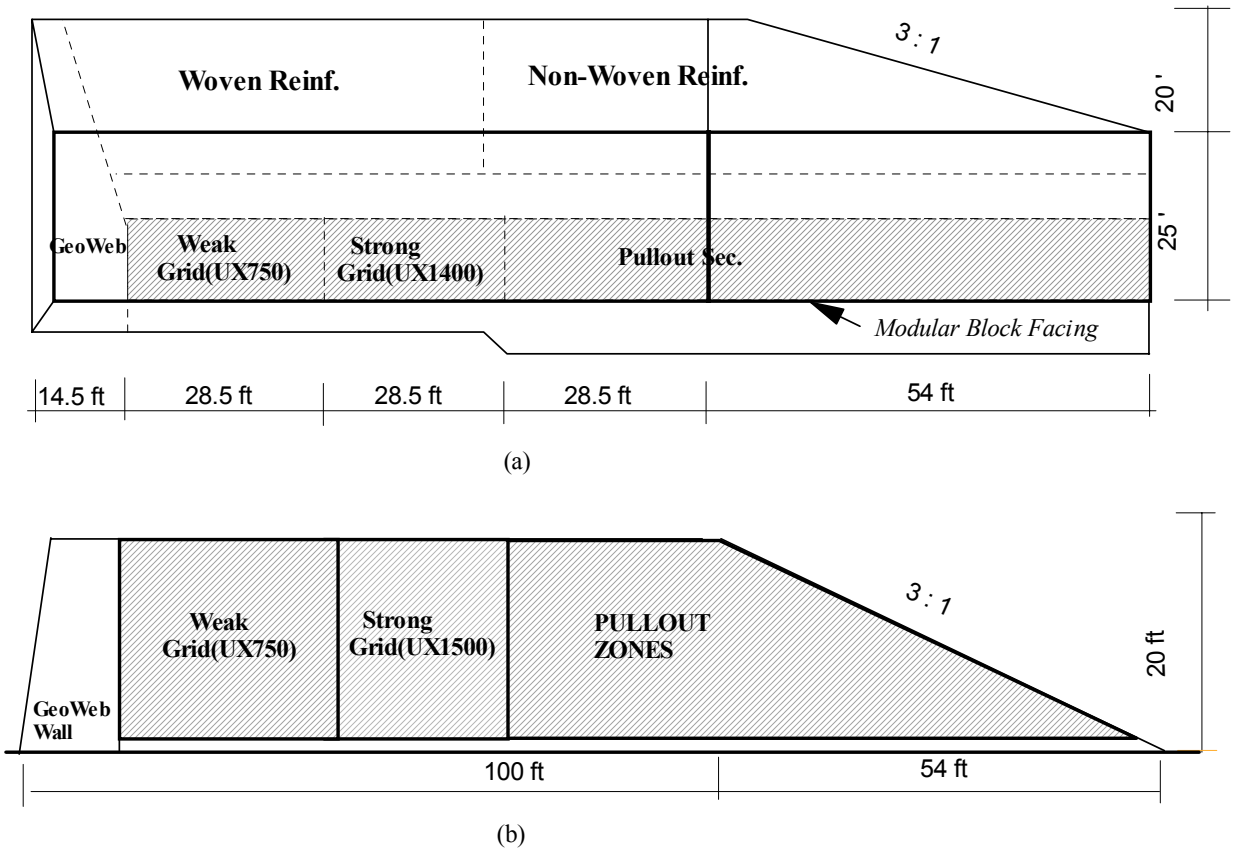

Figure 4.1.1: Schematics of the LTRC test wall (a) Plan of the LTRC test wall; (b) Elevation of the LTRC test wall (Farrag, 2003).

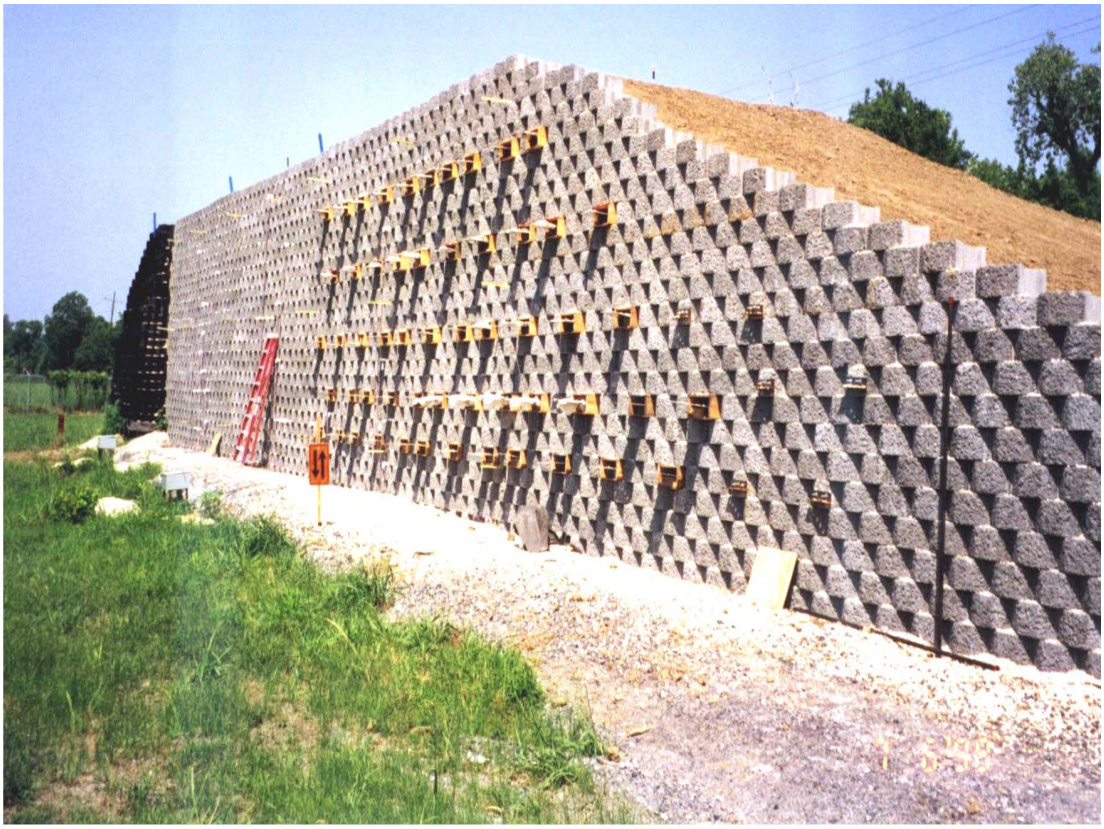

Figure 4.1.2: Elevation of LTRC test wall with the wooden pull-out test boxes.

4.2 Instrumentation of LTRC Test Wall

Figure 4.2.1, describes the instrumentation of the LTRC test wall. The vertical settlement of the wall was monitored during and after the construction using two horizontal inclinometers placed under the wall. The measurements of the inclinometers were complimented and verified by the survey of the vertical settlement at the front of the wall and by settlement plates placed at various locations at the base of the structure. In order to monitor the settlement profile of the soft foundations under the wall, two horizontal inclinometer pipes were installed in the longitudinal and latitudinal directions of the wall.

Seven survey points were selected to measure the magnitude of the lateral deformation at the facing. Vertical inclinometers were installed at various locations near the wall facings to monitor its horizontal deformation. The horizontal deformation was complimented using the survey points installed at the vertical side of the wall. Along each survey point there were three points at distances of 2.7 ft, 9.3 ft, and 16 ft along the vertical length of the wall.

Earth pressure cells were installed to measure vertical soil stresses in the soil mass. These pressure cells were used to evaluate the lateral earth pressure distribution.

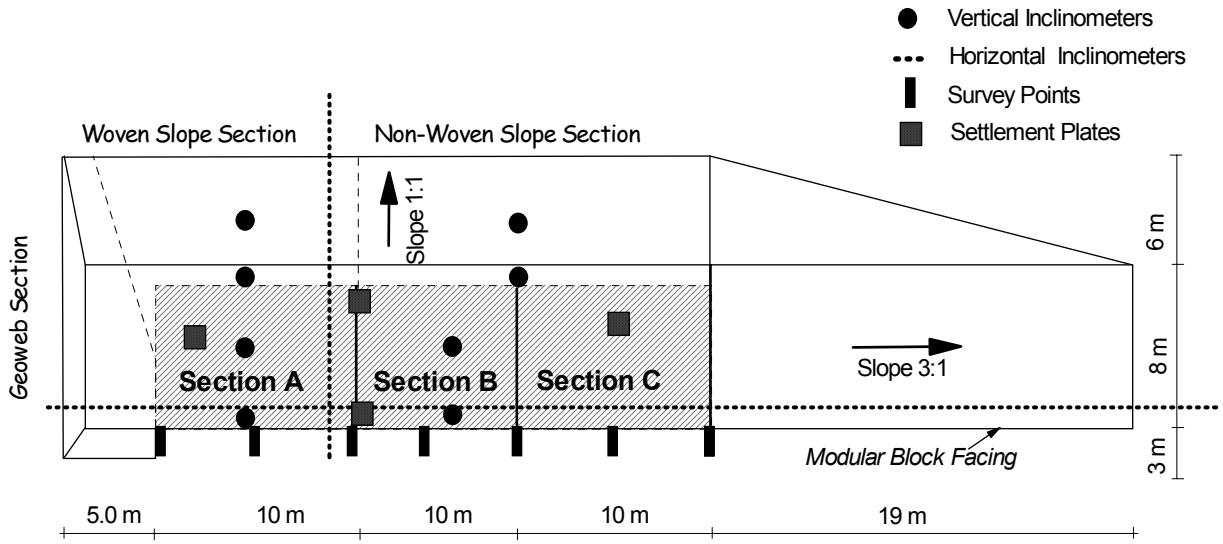

Figure 4.2.1: Plan of the wall showing the instrumentation at different locations with in the wall (Farrag, 2003).

Section A of the LTRC test wall was reinforced using weak geogrid (UX750) at a spacing of 400 mm (16 in). Section B was reinforced by a stronger geogrid (UX1400) at a spacing of 1000 mm (40 in). And Section C was reinforced with a much stronger and

standard geogrid (UX1500) with a spacing of 1000 mm (40 in). An array of strain gages is installed to measure the strains along the reinforcement specimen. The strain gages are mainly located near the wall facing where high strain levels are expected. The arrangements of the strain gage in Section A, Section B and Section C is illustrated in Figure 4.2.2, Figure 4.2.3 and Figure 4.2.4 respectively. The strain gages in sections A and B were glued along the junctions (transverse members) of each reinforcement layer, whereas the locations of strain gages in section A was non-uniform with bulk of the strain gages in front of the wall facing.

Strain gages were glued to each reinforcement layer in order to predict the maximum strains in each layer, and thereby to determine the maximum stress in each layer with respect to its placement. The wall was designed with a minimum factor of safety (i.e. 1.0) to experience deformations, which are further used to measure the maximum loads in each reinforcement layer.

4.3 Field Test Set-up

Field pull-out tests were conducted (Farrag, 1998) to investigate the pull-out resistance of different geosynthetic embedded at respective overburden pressures i.e. with respect to height of the wall. The pull-out testing mechanism in the field was the same as that of the laboratory, with all the arrangements made on a platform that was movable to facilitate easy testing at higher levels (Figure 4.3.1). The overburden pressure at each reinforcement layer was calculated as γH, where γ is the soil unit weight and H is the height of the backfill over the respective layer. Strain gauges and extensometers were instrumented to record the displacements and axial strains along the length of the specimen. The pull-out test results are presented in chapter 4, where the effect of

confining pressure is presented. Chapter 5 continues with the analysis of the pull-out test results, including the comparison of field and laboratory pull-out tests.

Table 4.3.1 shows the pull-out test location for different geosynthetics that were tested in the field. For example, geosynthetic non-woven [3A] indicates that the non-woven geotextile of 3ft length tested at level A of the wall. Where, the level A, B, C, D and E are the levels starting from the base of the wall, respectively. Table 4.3.1 also indicates the number of blocks (Modular blocks) in each case to measure the vertical overburden pressure, which is tabulated in the adjacent column. Since there is a slope above the pull-out zone, the confining pressure at each level varies depending on its location, which is evident in the Table 4.3.1.

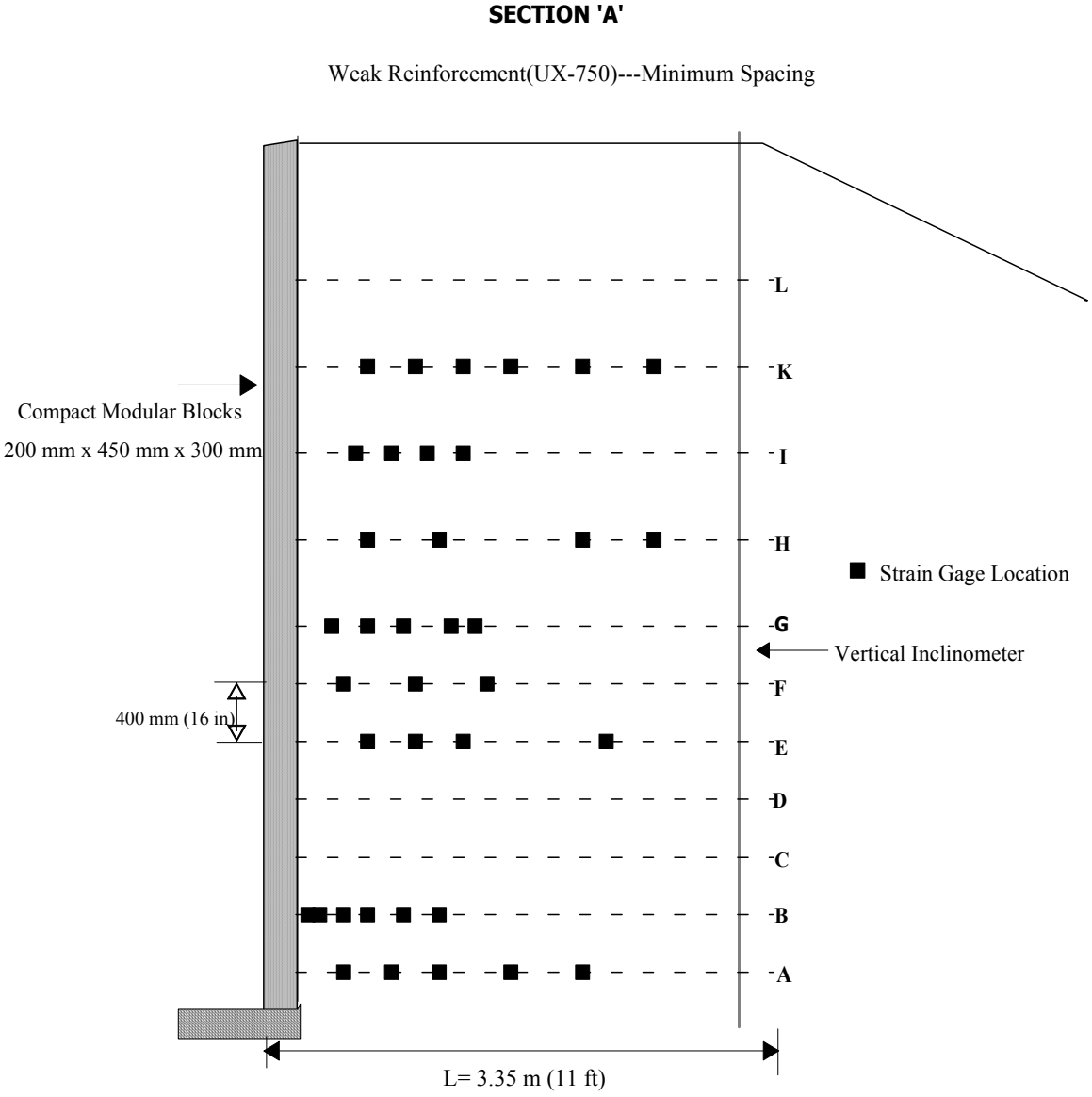

Figure 4.2.2: Layout of the strain gages in Section A (UX750)

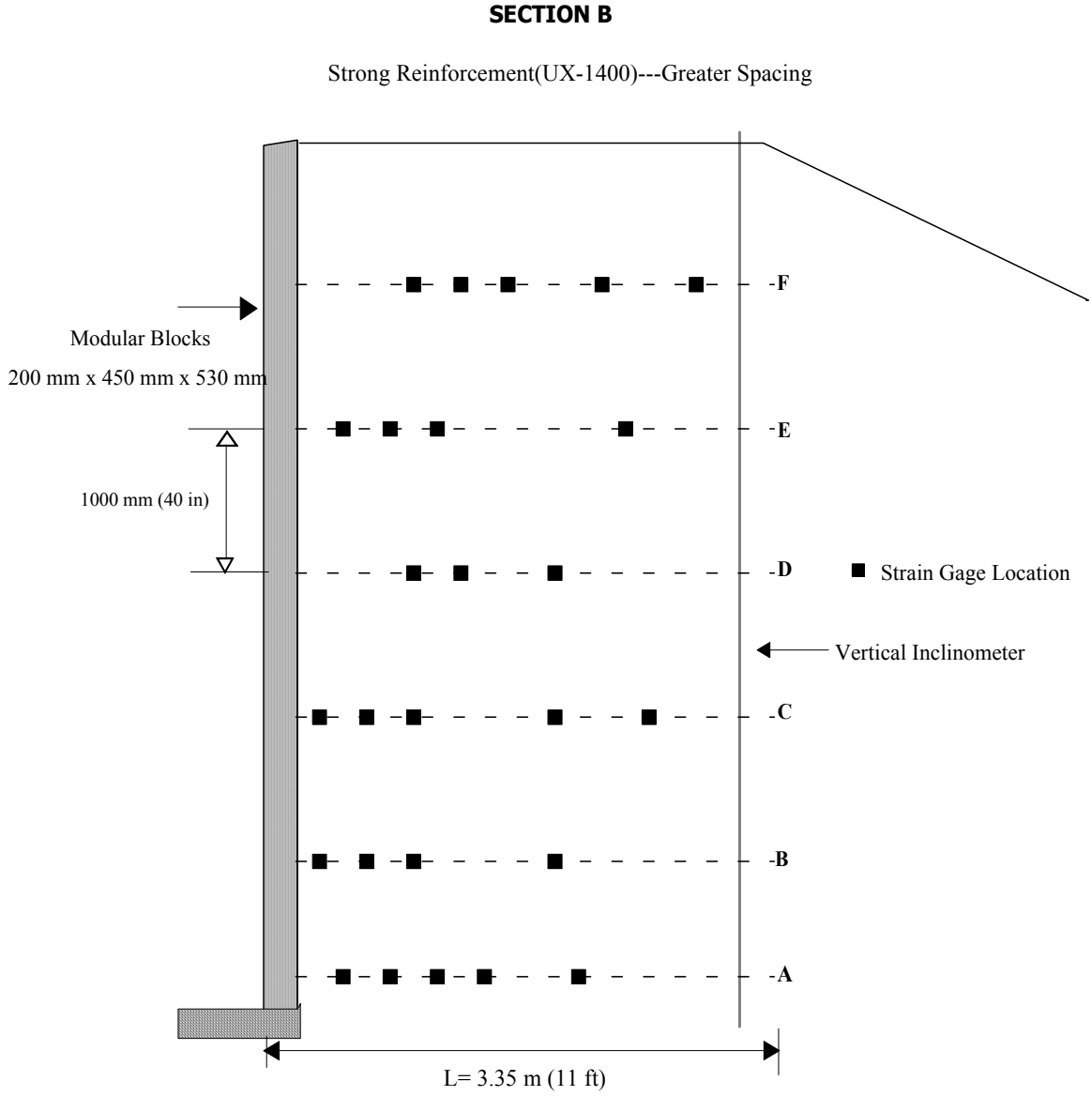

Figure 4.2.3: Layout of the strain gages in Section B (UX1400)

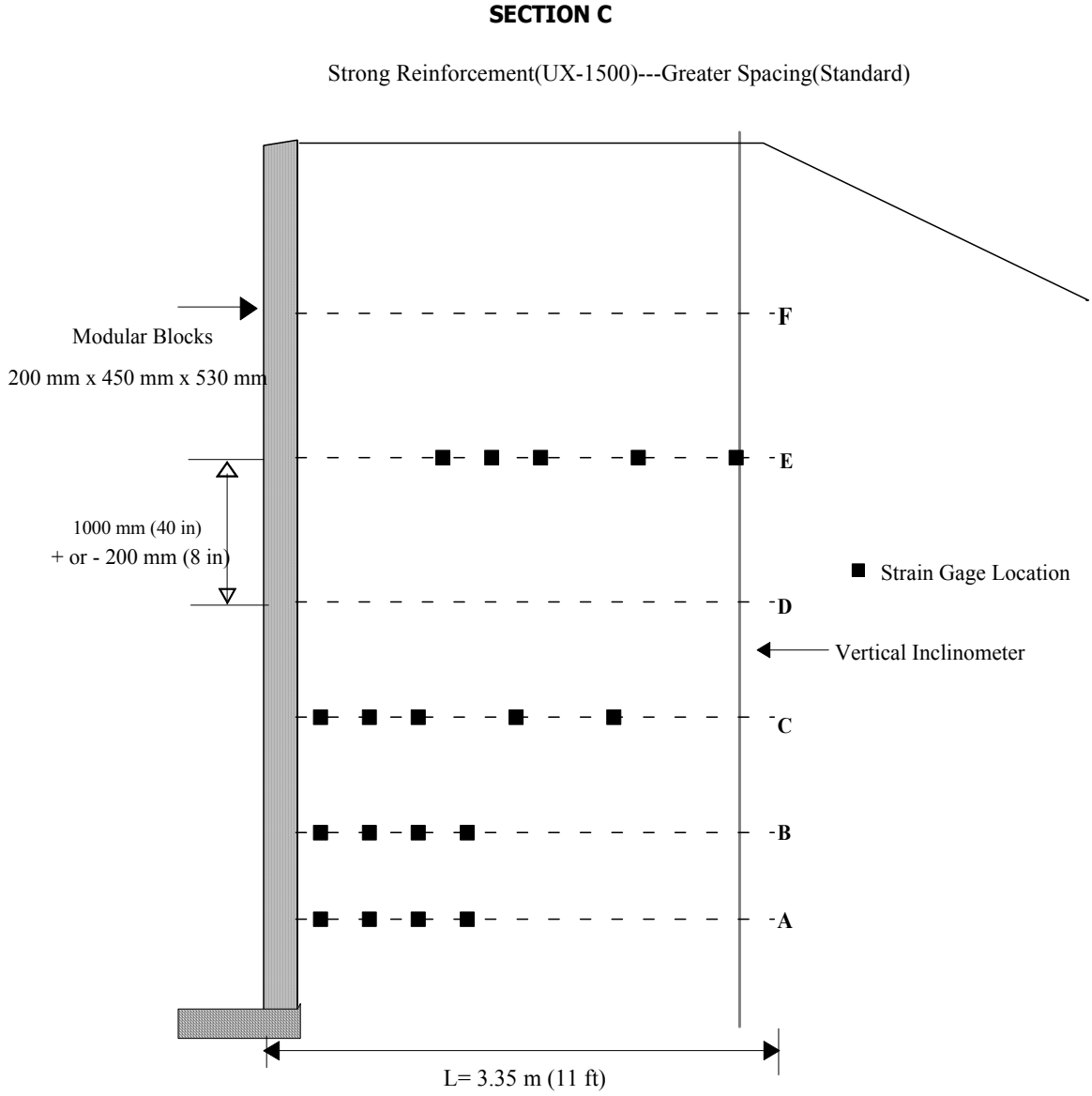

Figure 4.2.4: Layout of the strain gages in Section C (UX1500)

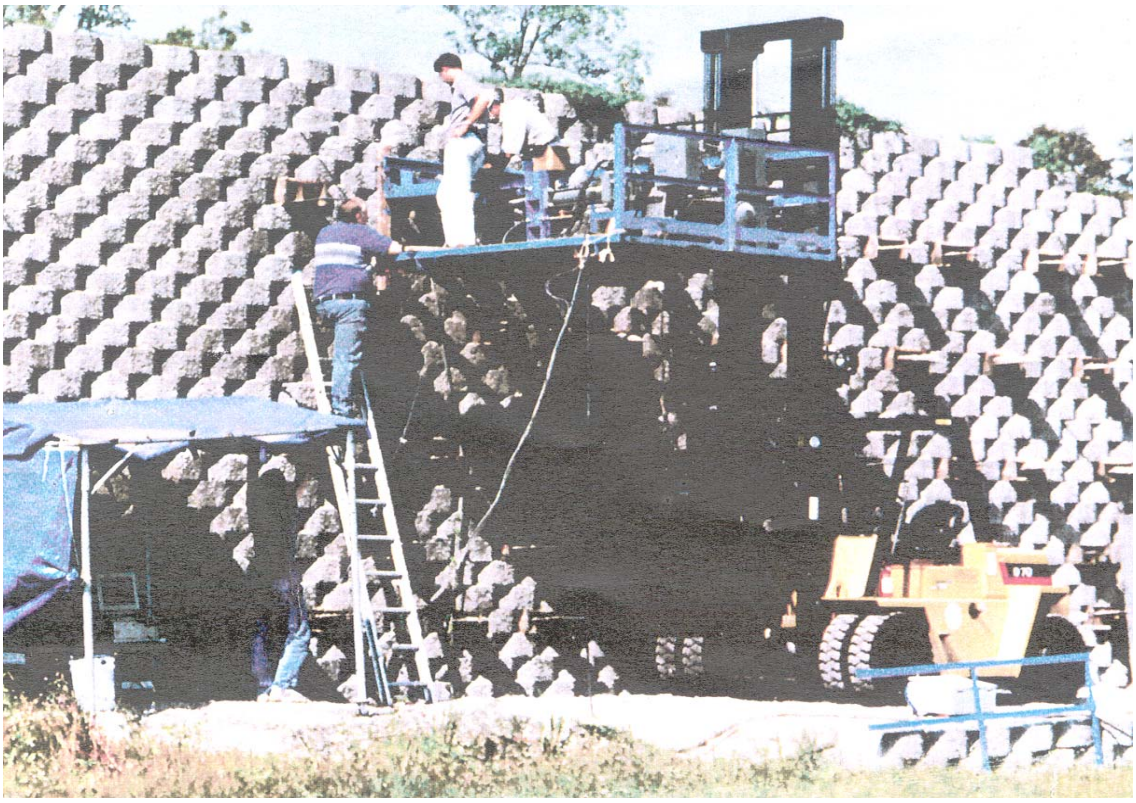

Figure 4.3.1: Platform to facilitate pull-out testing.

Table 4.3.1: Pull-out test locations for different geosynthetics

(a) For non-woven (TG-700) geotextiles

Test	Soil Height (Modular Blocks)	Overburden Pressure (psi)
Non-woven [3A]	19	10.56
Non-woven [4A]	15.5	8.61
Non-woven [3B]	14	7.78
Non-woven [4B]	12	6.67
Non-woven [3C]	11.5	6.39
Non-woven [4D]	5	2.78

(b) For woven (4x4) geotextiles

Test	Soil Height (Modular Blocks)	Overburden Pressure (psi)
Woven (4x4) [3A]	20.5	11.12
Woven (4x4) [4D]	5	2.78
Woven (4x4) [5D]	5	2.78
Woven (4x4) [4E]	2	1.12
Woven (4x4) [5E]	2	1.12

(table con'd.)

(c) For woven (6x6) geotextiles:

Test	Soil Height (Modular Blocks)	Overburden Pressure (psi)
Woven (6x6) [3A]	20.5	11.12
Woven (6x6) [4A]	15.5	8.34
Woven (6x6) [3B]	12	6.62
Woven (6x6) [4B]	11.5	6.39
Woven (6x6) [3C]	10	5.5
Woven (6x6) [3D]	5	2.78

(d) For Stratagrid-500:

Test	Soil Height (Modular Blocks)	Overburden Pressure (psi)
Stratagrid-500 [3A]	22	12.23
Stratagrid-500 [3B]	19	10.56
Stratagrid-500 [3C]	15	8.33
Stratagrid-500 [4A]	22	12.23
Stratagrid-500 [4B]	19	10.56
Stratagrid-500 [5A]	22	12.23
Stratagrid-500 [5B]	19	10.56

(table con’d.)

(e) For UX1700:

Test	Soil Height (Modular Blocks)	Overburden Pressure (psi)
UX1700 [3A]	22	12.23
UX1700 [3B]	19	10.56
UX1700 [3C]	15	8.33
UX1700 [4A]	22	12.23
UX1700 [4B]	19	10.56
UX1700 [5A]	22	12.23

(f) For UX1500:

Test	Soil Height (Modular Blocks)	Overburden Pressure (psi)
UX1500 [3B]	19	10.56
UX1500 [3C]	15	8.33
UX1500 [3D]	10	5.56
UX1500 [3E]	5	2.78
UX1500 [4C]	15	8.33
UX1500 [4D]	10	5.56
UX1500 [4E]	5	2.78
UX1500 [5D]	10	5.56
UX1500 [5E]	5	2.78

. (table con'd.)

(g) For UX750:

Test	Soil Height (Modular Blocks)	Overburden Pressure (psi)
UX750 [3D]	10	5.56
UX750 [3E]	5	2.78
UX750 [4D]	10	5.56
UX750 [4E]	5	2.78
UX750 [5E]	5	2.78

* Each Modular block has a height of 0.77 ft.

CHAPTER 5

PULL-OUT TEST RESULTS

5.1 Laboratory Pull-out Test Results

The laboratory pull-out tests were conducted on 5 types of geosynthetics (Stratgrid500, UX750, UX1500, UX1700 and Woven (4x4) geotextile) at different confining pressures (ranging from 1.12 to 12.23 psi). Laboratory pull-out test results included load and displacement measurements of the geosynthetic specimen with respect to different confining pressures, and at a constant pull-out rate of 1.5mm/min. LVDTs were placed at different locations along the length of the specimen to provide records of the displacements that determine the strain and tensile force profiles during the pull-out of the geosynthetic.

Figures 5.1.1 through 5.1.5 show the results of pull-out load-displacement curves at different confining pressures for Stratgrid500, UX750, UX1500, UX1700 and Woven (4x4) geotextile, respectively, each of which tested at different confining pressures. It can be clearly seen that the pull-out load increases with the level of confining pressure. However, the results of Woven (4x4) and UX750, Figures 5.1.1 and 5.1.2, respectively showed that the pull-out load at higher confining pressures could be less than that at lower confining pressures. This may be due to the reduced confining pressure and soil dilation effects that are more pronounced at lower confining pressures than at higher confining pressures. One can even notice that after reaching the peak pull-out load, the geosynthetic comes out with a smaller load (residual load). This is the residual strength and it is mostly present at lower confining pressures. This means the geosynthetic still has the ability to resist even after the maximum pull-out is reached. Therefore this

resistance could be the function of soil geosynthetic interaction or the function of the soil friction angle.

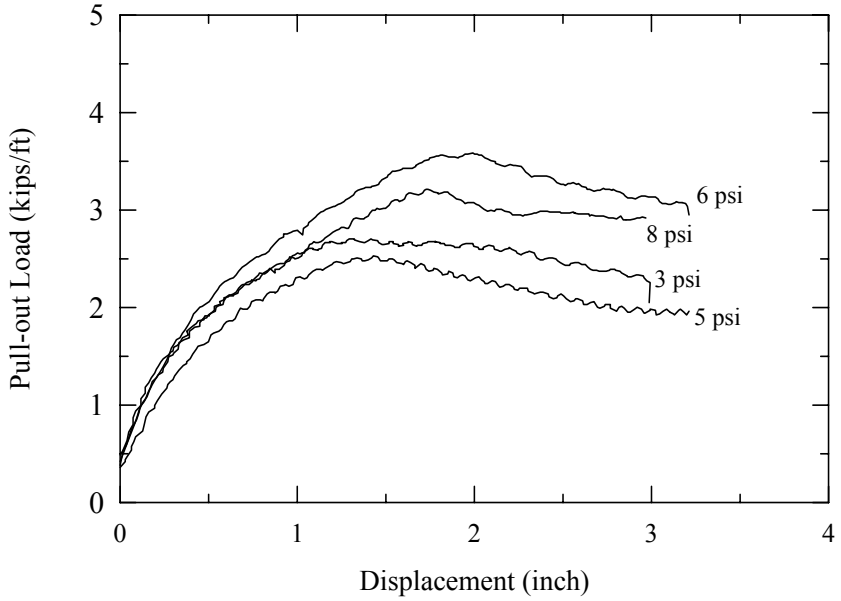

Figure 5.1.1: Displacement versus pull-out load for Woven (4x4) geotextile.

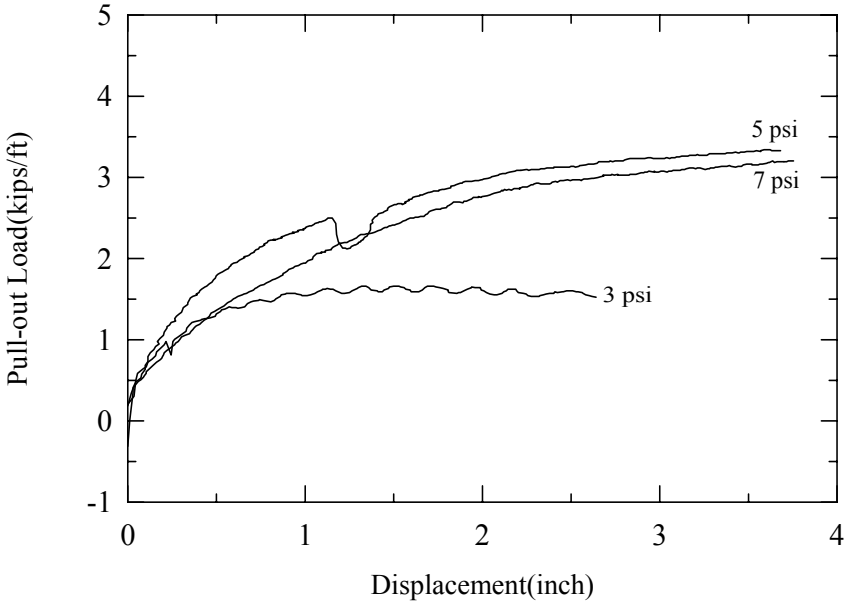

Figure 5.1.2: Displacement versus pull-out load for UX750.

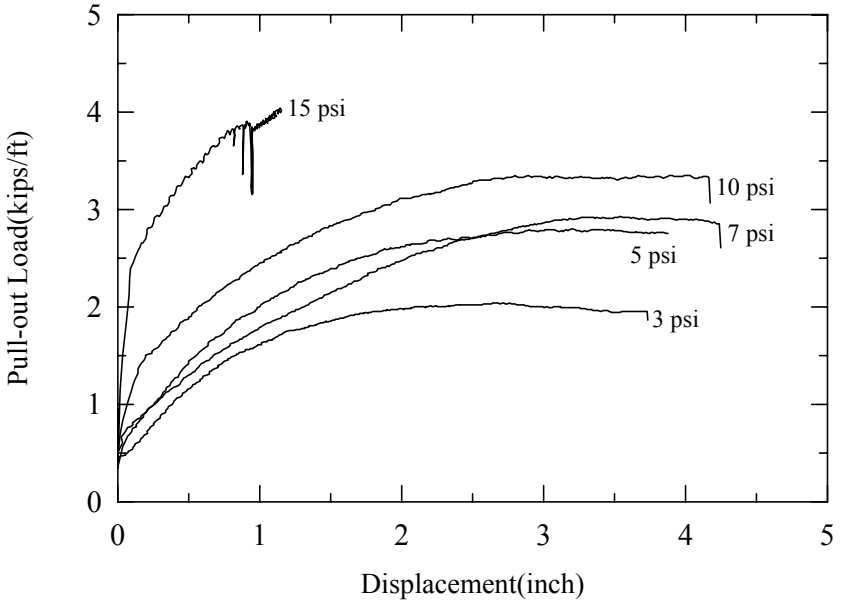

Figure 5.1.3: Displacement versus pull-out load for UX1500.

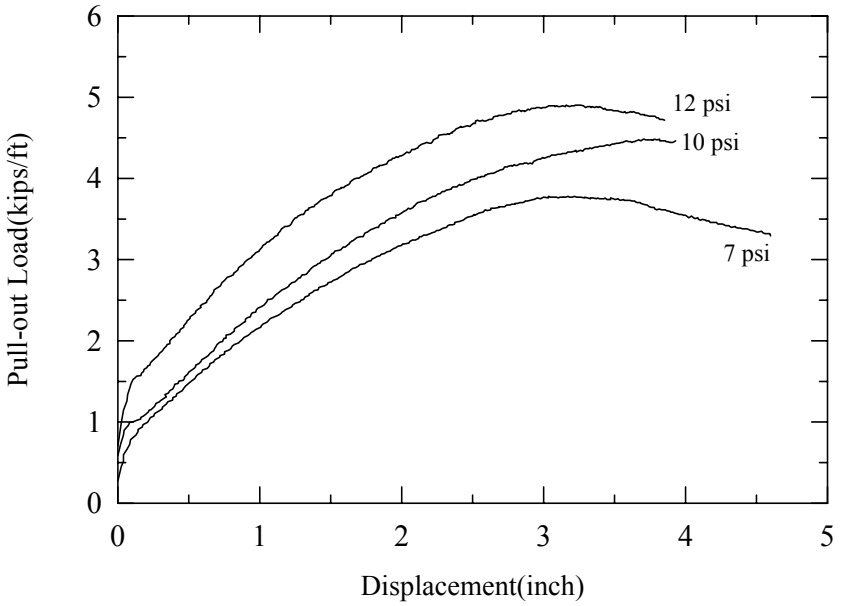

Figure 5.1.4: Displacement versus pull-out load for UX1700.

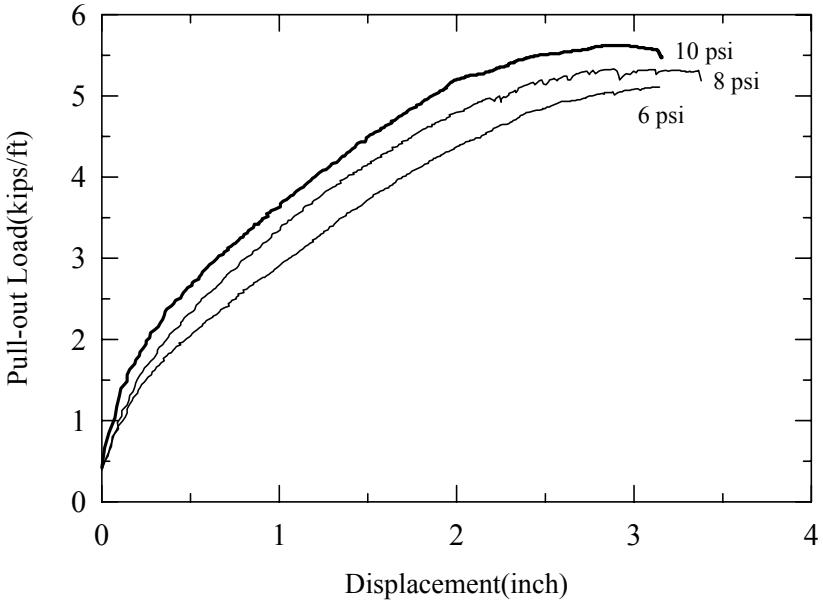

Figure 5.1.5: Displacement versus pull-out load for Stratagrid-500.

Figures 5.1.6 through 5.1.22 show the results of the time-displacement curves for the displacements along the length of the specimen. The displacement was recorded at the front of the geosynthetic specimen, at 1 feet distance, and at two feet distance from the face along the length of the specimen. The LVDTs located at 2-ft showed no movements (Figures 5.1.6 through 5.1.9), and the displacements occurred only within the first 1-ft of the geosynthetic specimen. This is mainly due to the lack of stiffness of the geosynthetic material, and this indicates that there are no shear stresses after the 2-ft length of the specimen. The results in the figures show that the slope of the time-displacement curve at the front is practically constant and equals the displacement-rate. At an early stage of pull-out, most of the load is carried out between first two points and high strains are mobilized at the front part of the geosynthetic specimen. The interaction mechanism progressively transfers to the rear nodes as the pull-out load increases to its peak (demonstrated by both material elongation and shear resistance at the interface).

Figures 5.1.13 through 5.1.19 indicates that the reinforcement has been pulled out of the soil. It also indicates that there is a displacement at the 2-ft length, and therefore the shear stresses occur beyond the 2-ft point. The geosynthetic was totally pulled out from the soil due to the higher stiffness of the geosynthetic material (i.e., high strength geogrids were totally pulled out). The other reason might be due to the weak interface friction, which made the geosynthetic specimen to be pulled out without any tension failure. Figures 5.1.20 through 5.1.22 was not pulled out of the soil, but there was hint of shear stress beyond the 2-ft point. In this case, the geosynthetic was not pulled out due to the lower stiffness of the geosynthetic material.

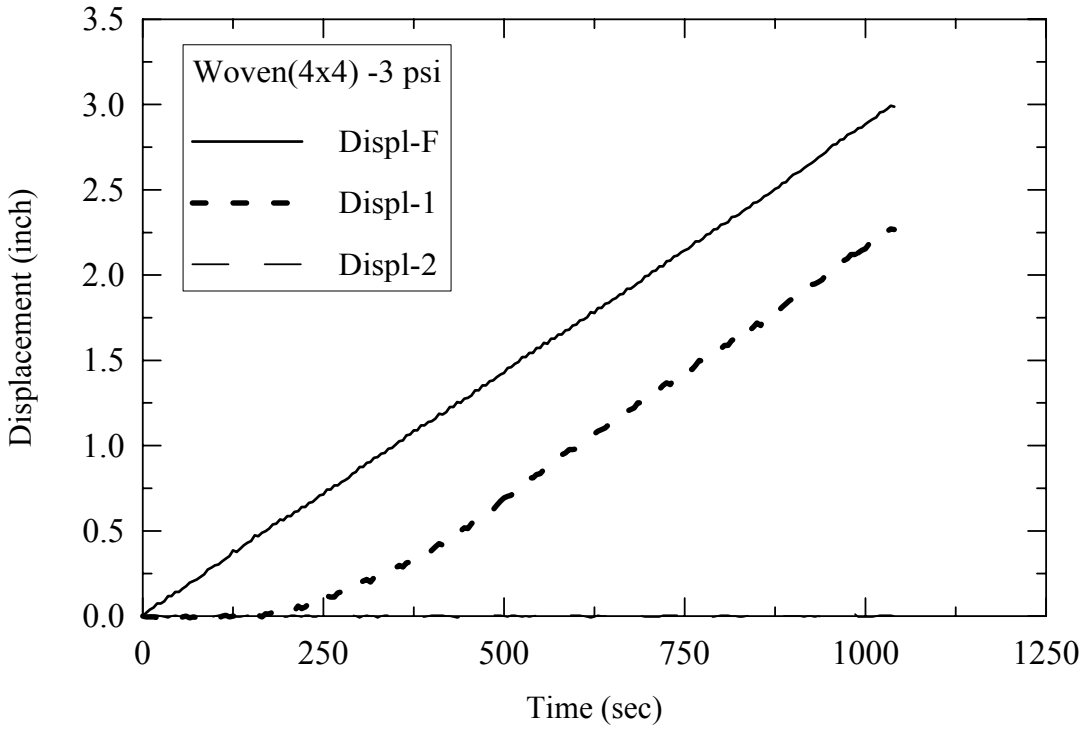

Figure 5.1.6: Woven (4x4) geotextile under a confining pressure of 3 psi

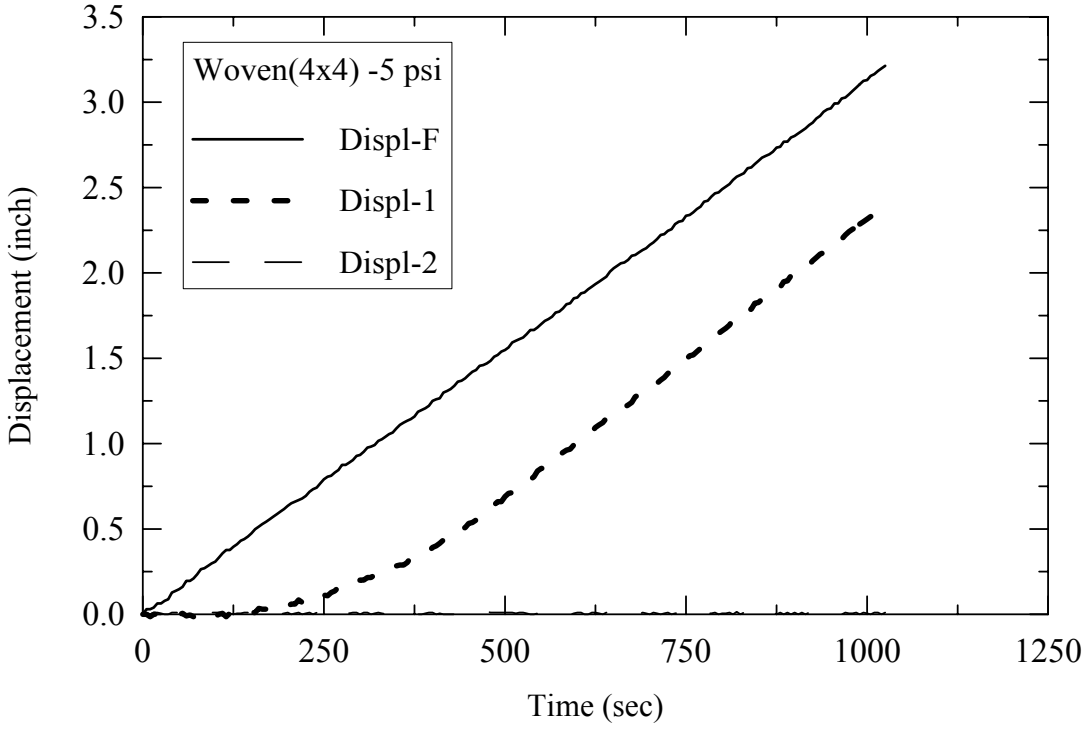

Figure 5.1.7: Woven (4x4) geotextile under a confining pressure of 5 psi.

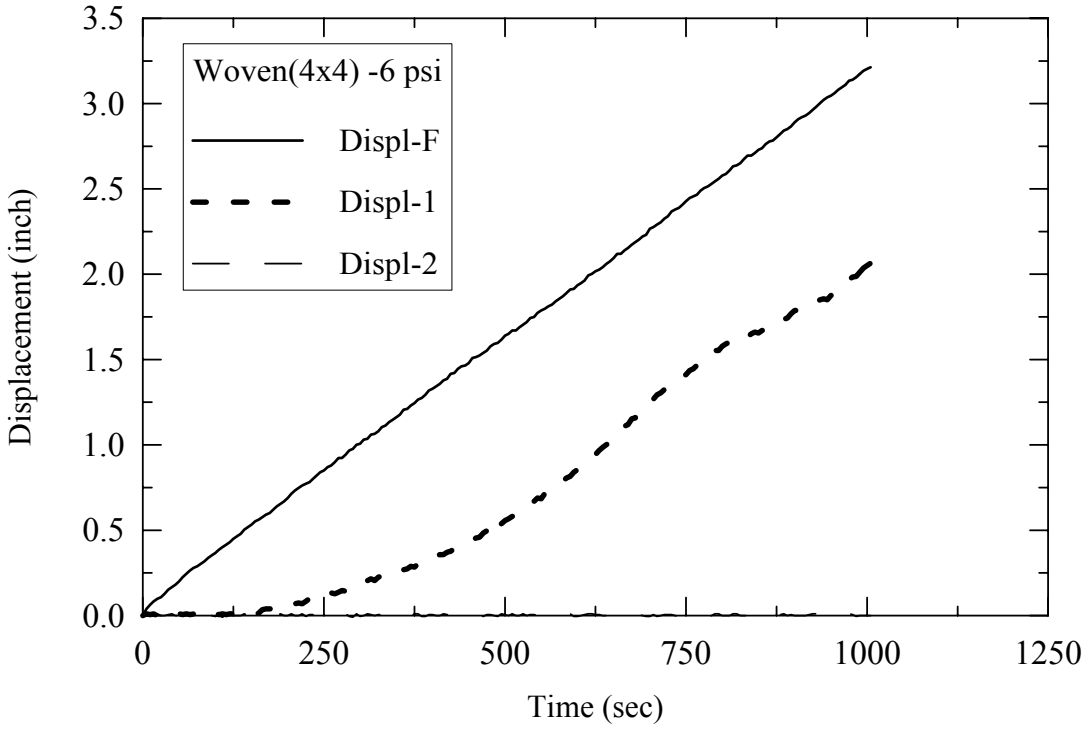

Figure 5.1.8: Woven (4x4) geotextile under a confining pressure of 6 psi.

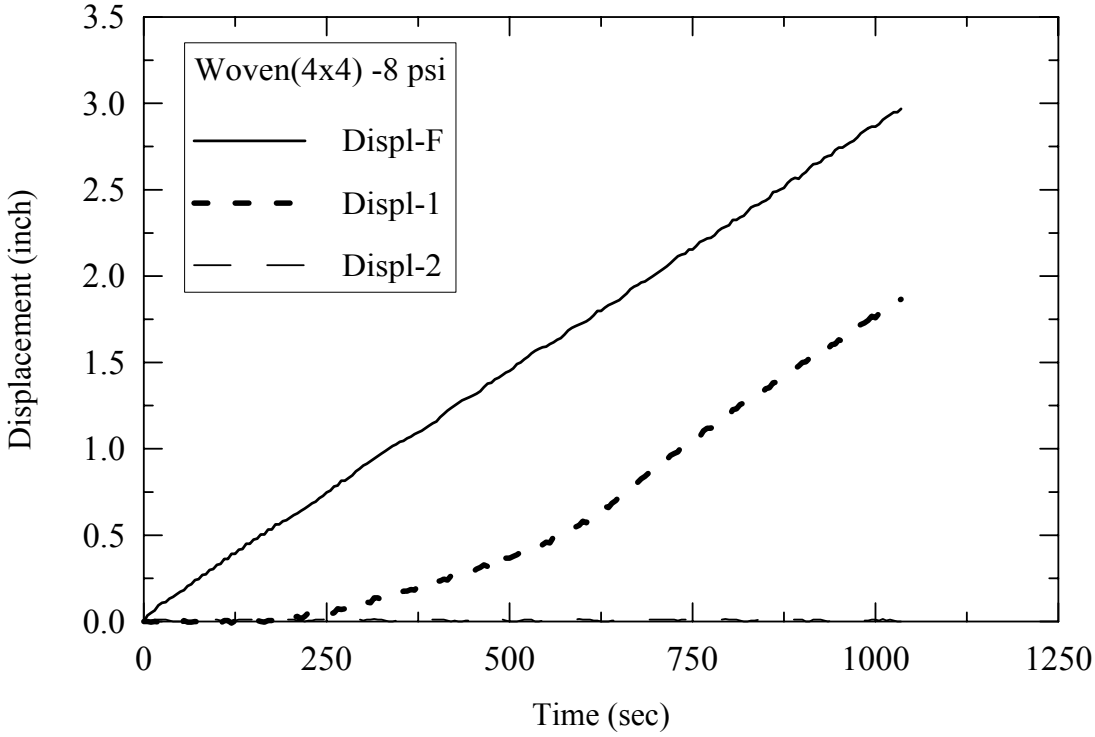

Figure 5.1.9: Woven (4x4) geotextile under a confining pressure of 8 psi.

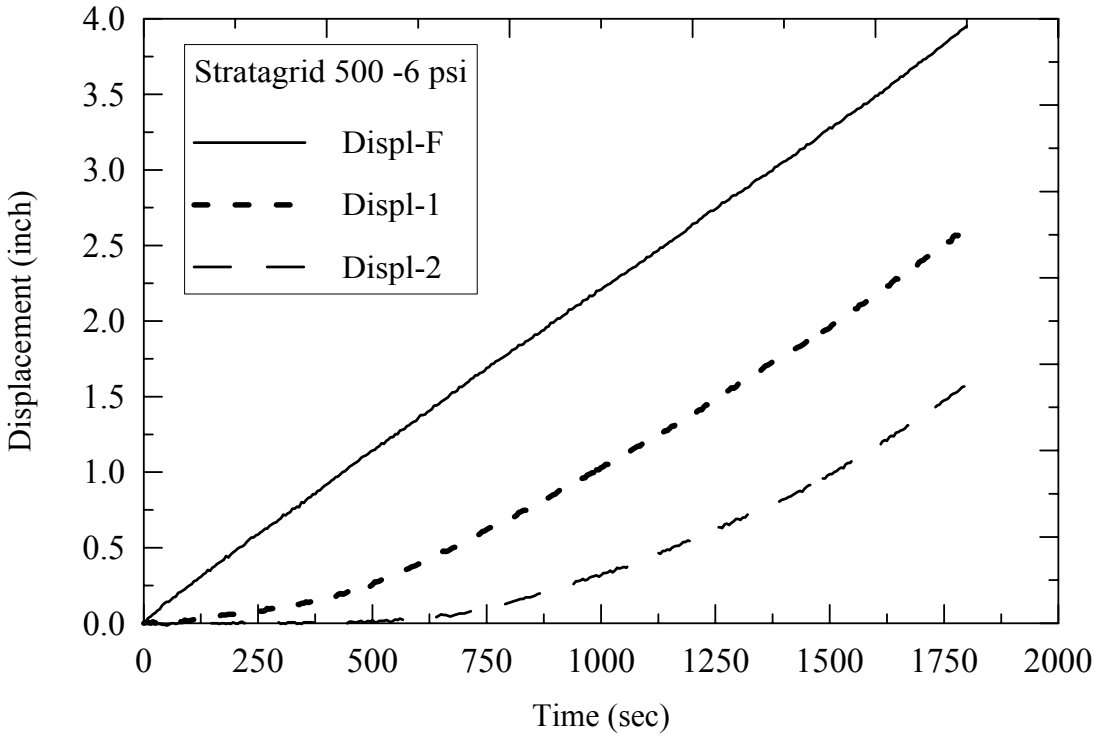

Figure 5.1.10: Stratagrid-500 under a confining pressure of 6 psi.

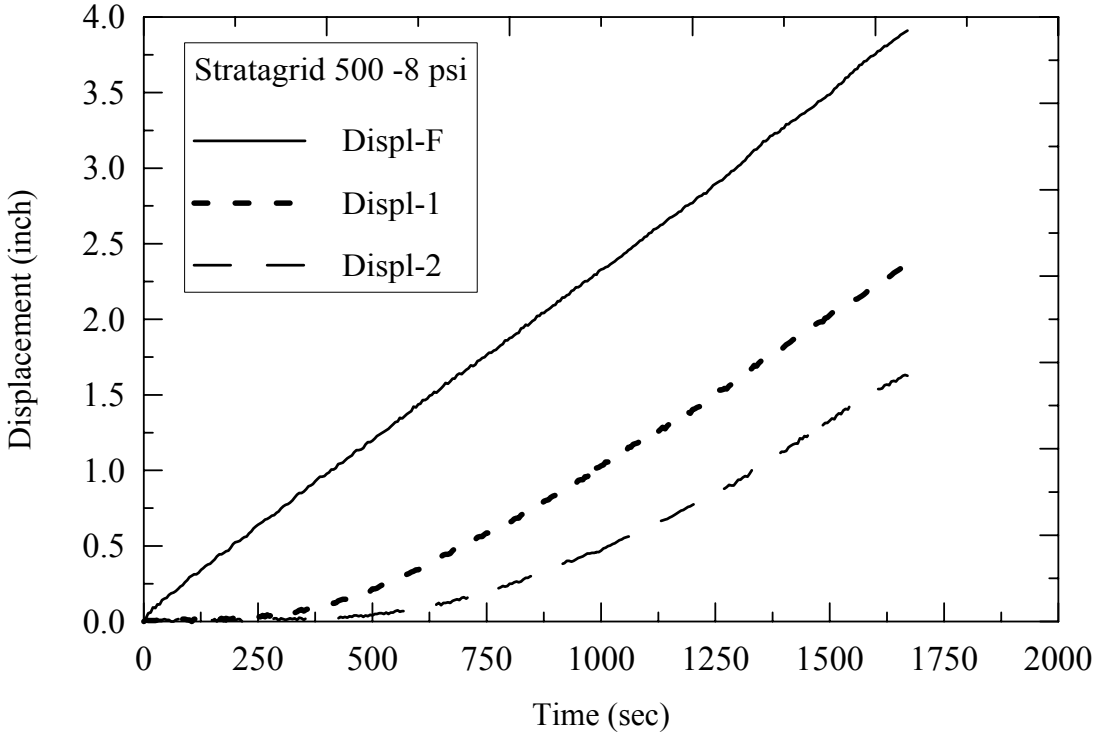

Figure 5.1.11: Stratagrid-500 under a confining pressure of 8 psi.

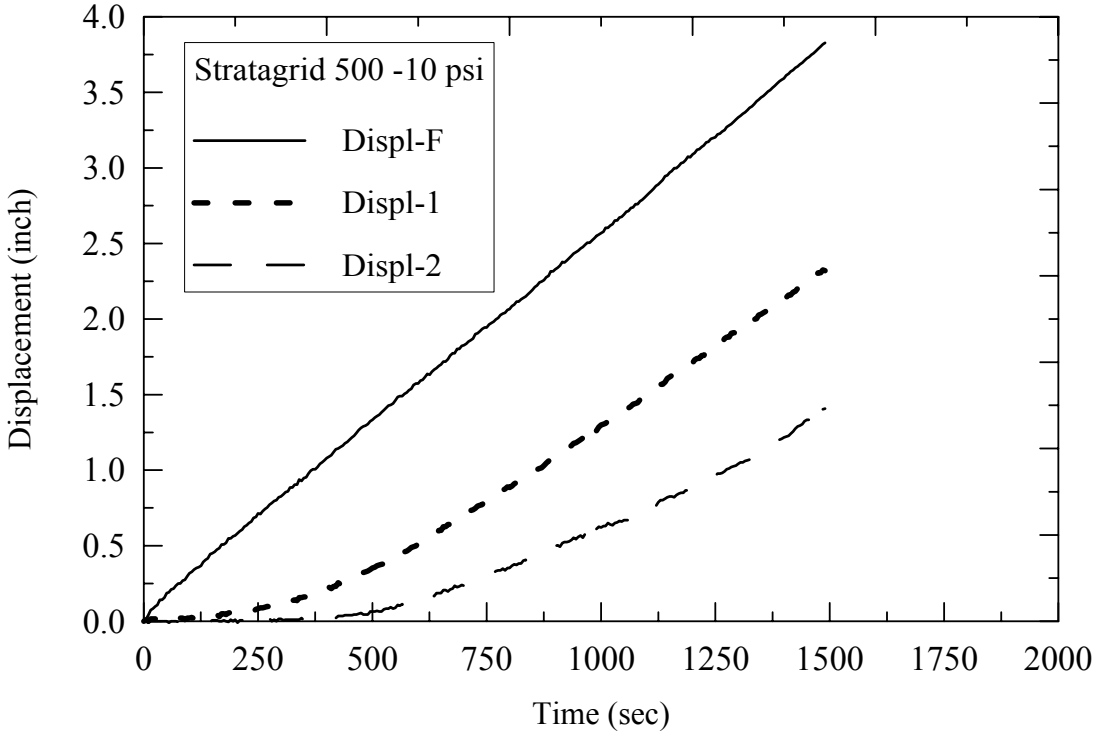

Figure 5.1.12: Stratagrid-500 under a confining pressure of 10 psi.

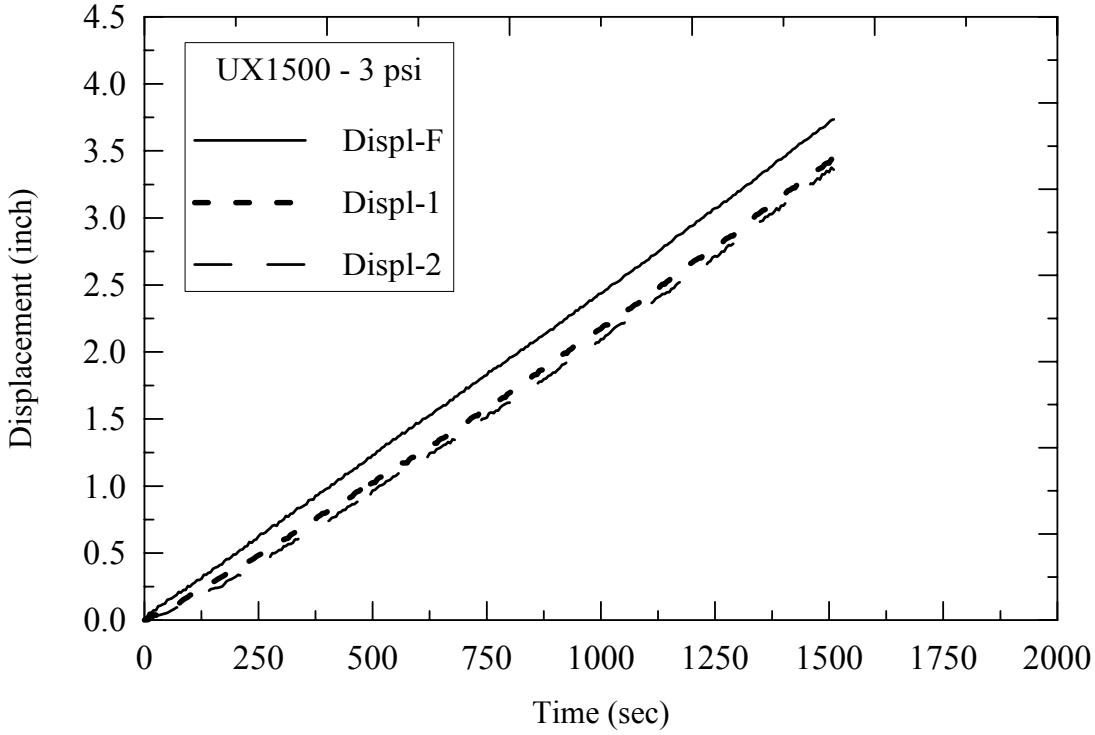

Figure 5.1.13: UX1500 under a confining pressure of 3 psi.

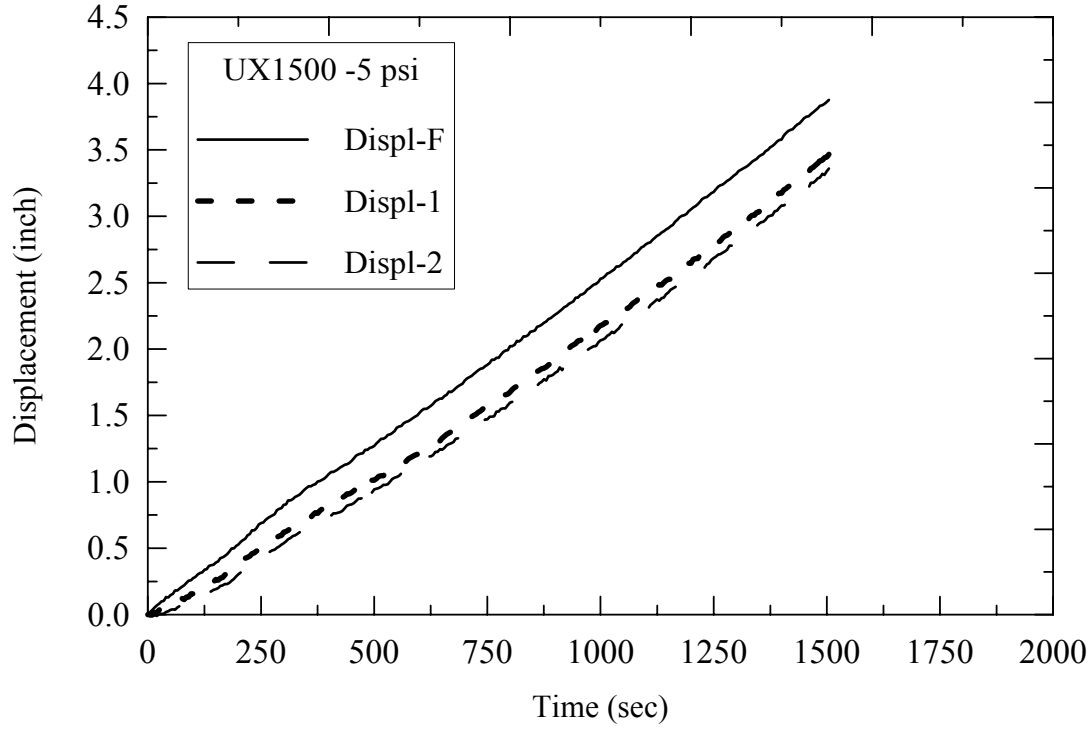

Figure 5.1.14: UX1500 under a confining pressure of 5 psi.

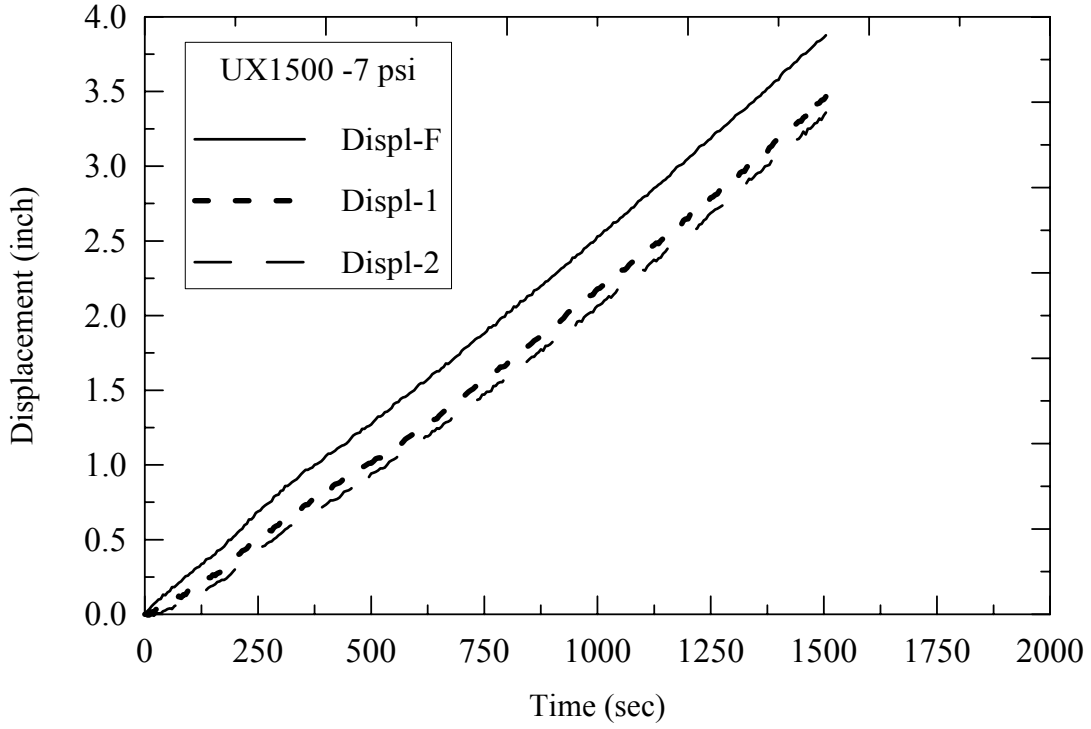

Figure 5.1.15: UX1500 under a confining pressure of 7 psi.

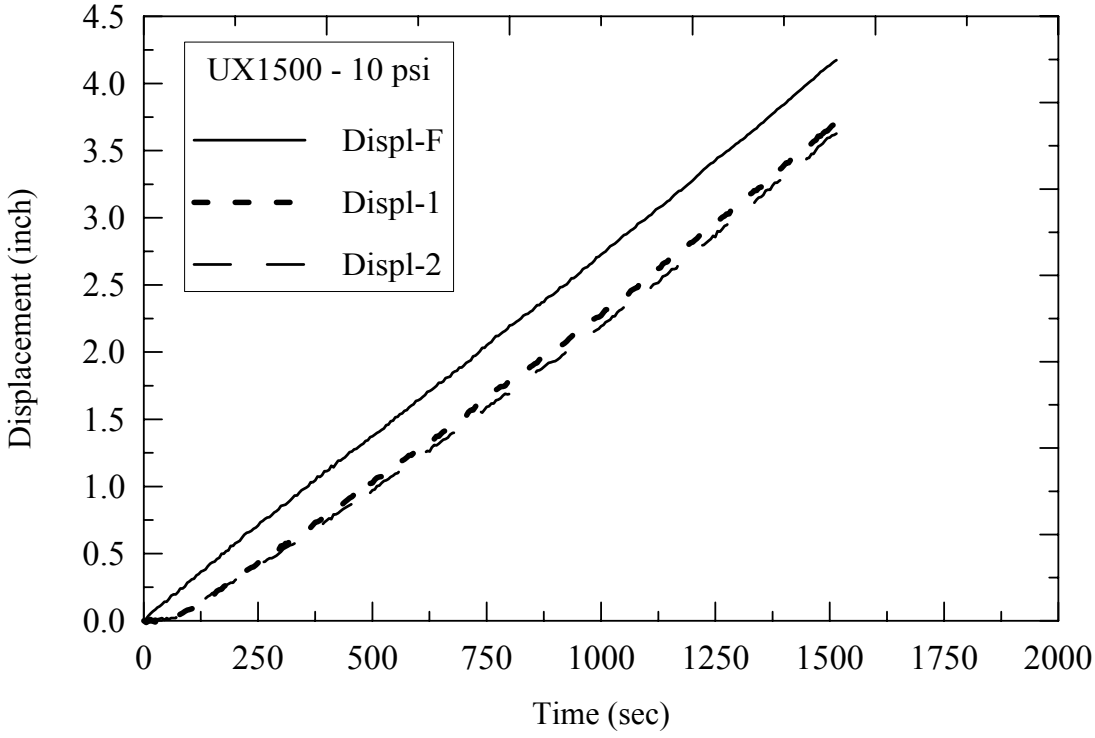

Figure 5.1.16: UX1500 under a confining pressure of 10 psi.

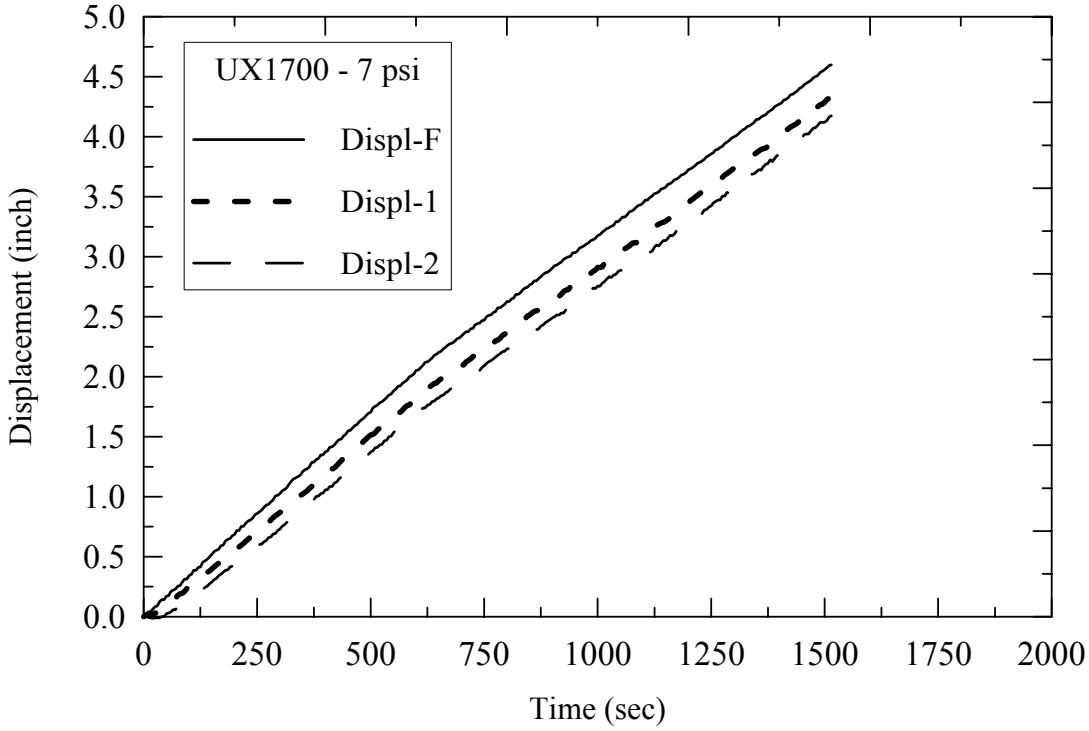

Figure 5.1.15: UX1700 under a confining pressure of 7 psi.

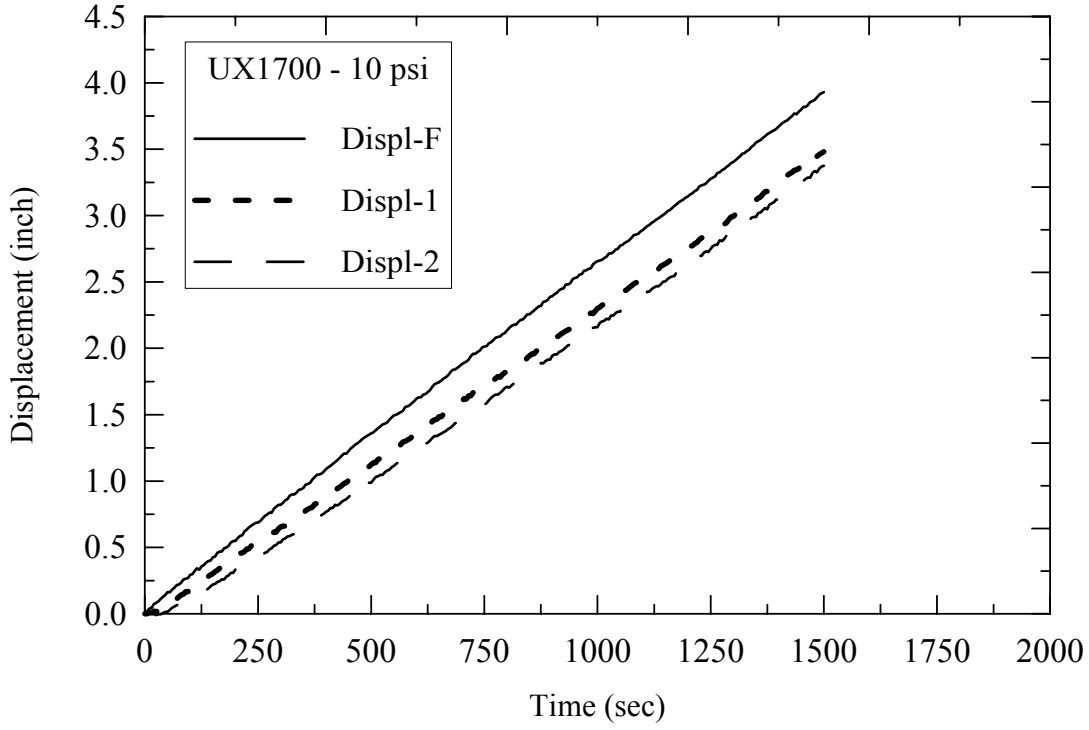

Figure 5.1.18: UX1700 under a confining pressure of 10 psi.

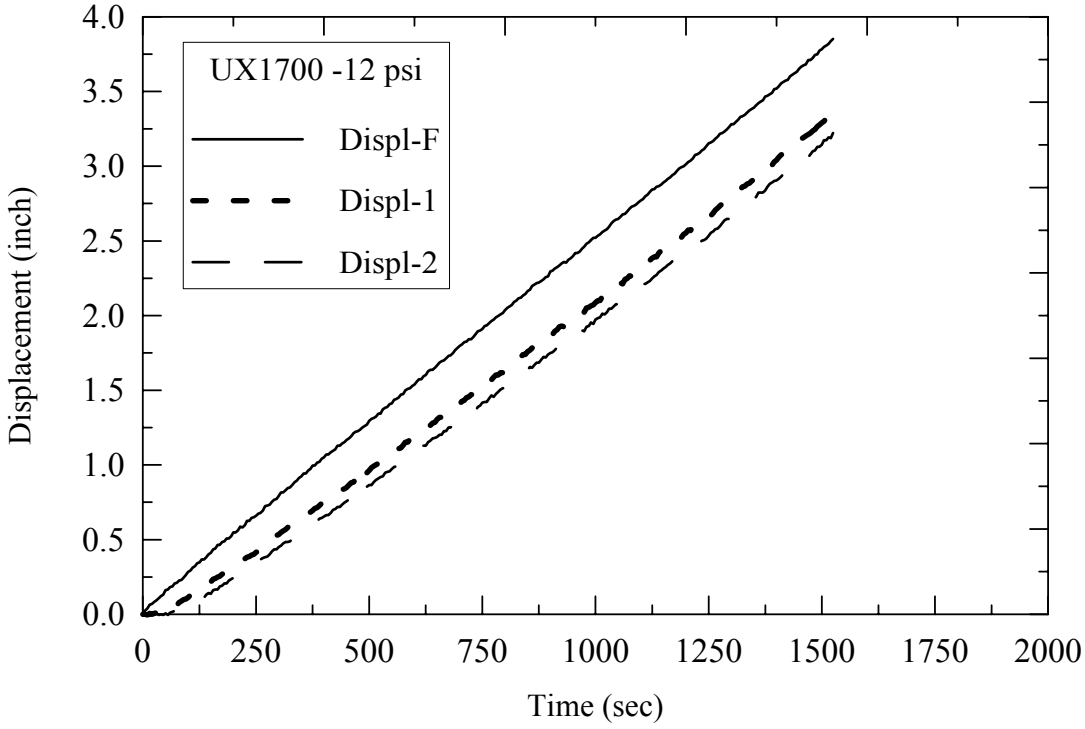

Figure 5.1.19: UX1700 under a confining pressure of 12 psi.

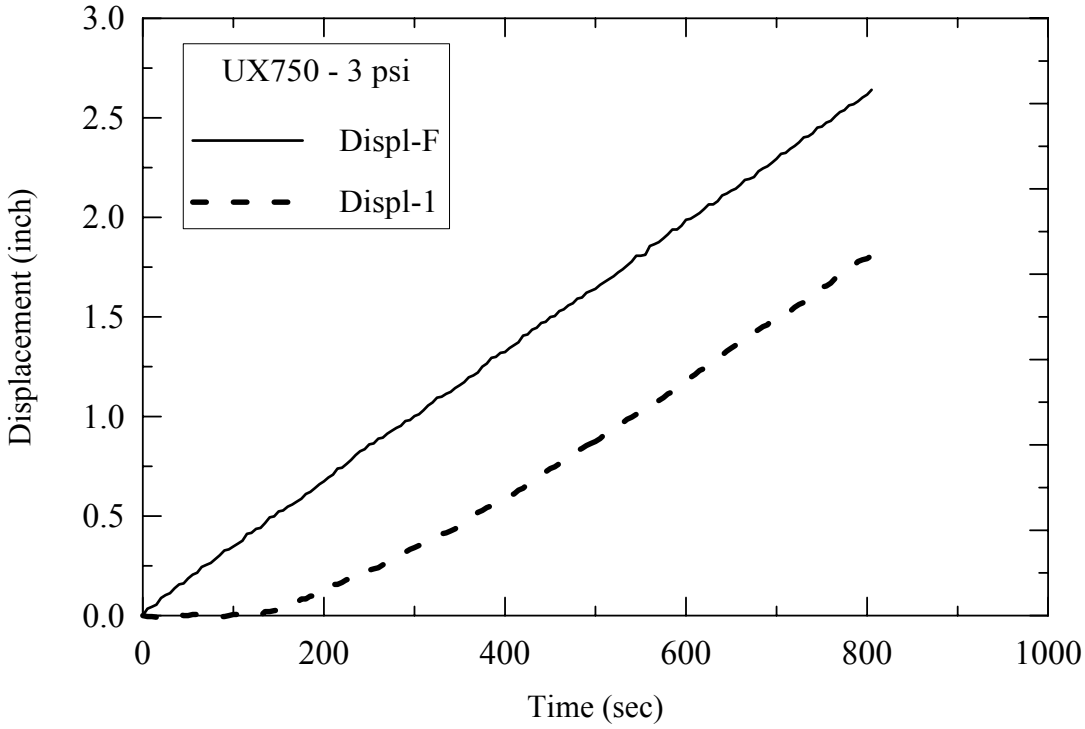

Figure 5.1.20: UX750 under a confining pressure of 3 psi.

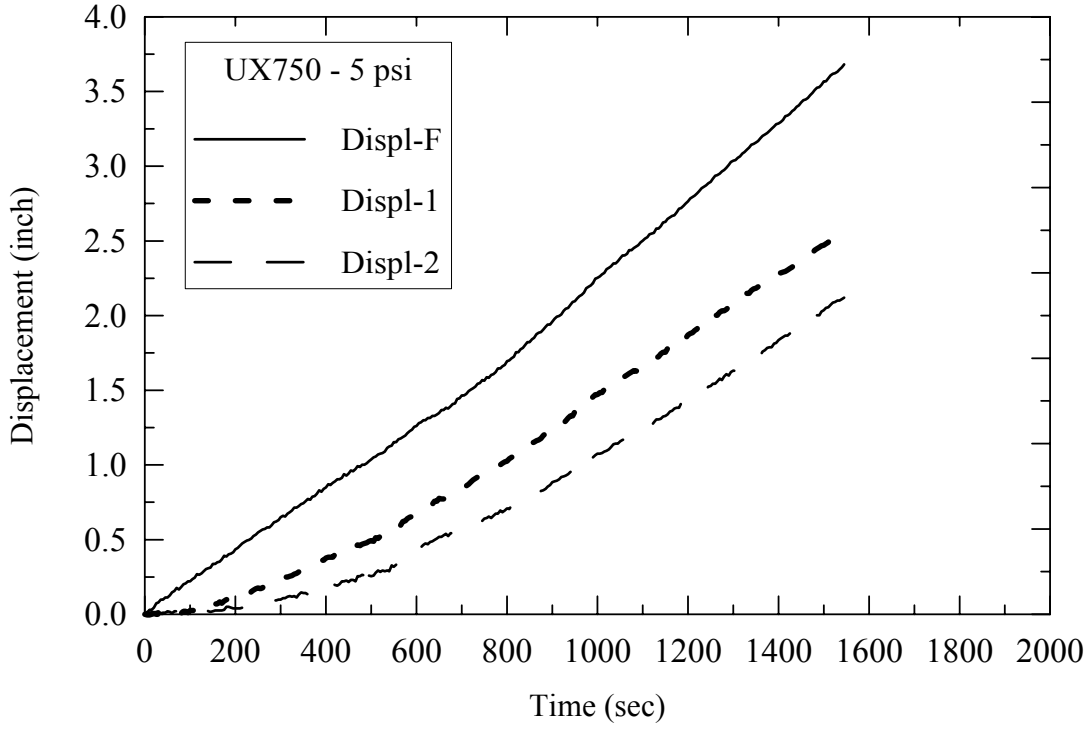

Figure 5.1.21: UX750 under a confining pressure of 5 psi.

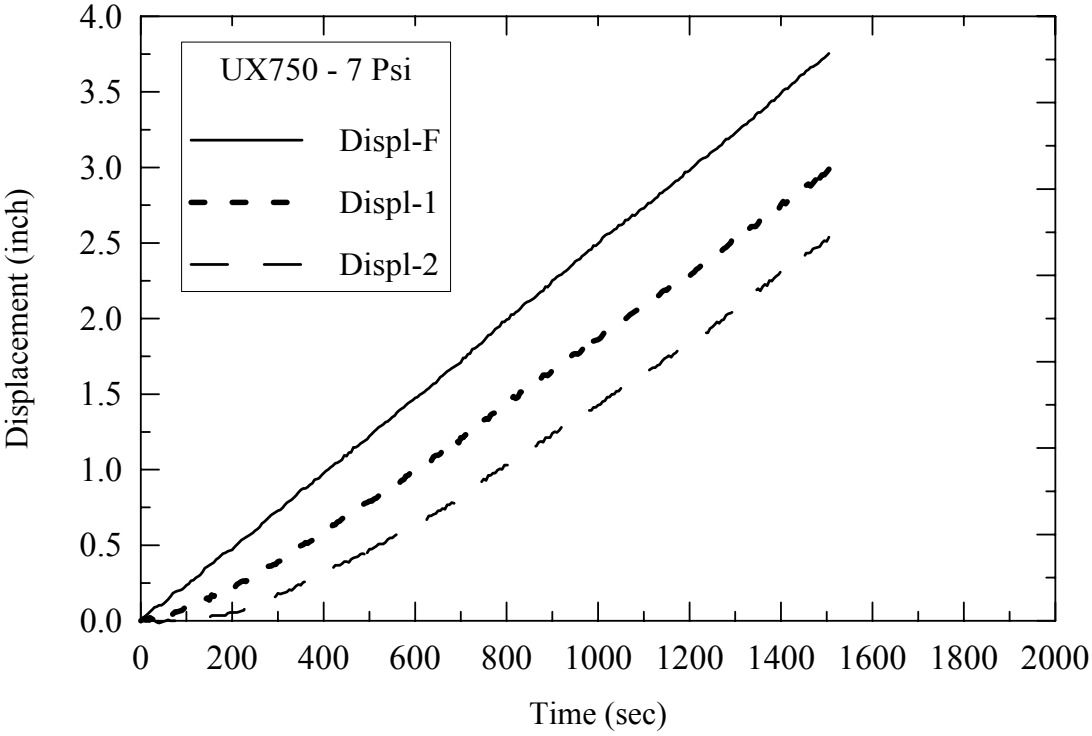

Figure 5.1.22: UX750 under a confining pressure of 7 psi.

5.2 Field Pull-out Test Results

Field pull-out tests were conducted to investigate the pull-out resistance of different geosynthetic embedded at different overburden pressures and densities. The pull-out testing mechanism in field was same as that of the laboratory, with all the arrangements made on a platform that was movable to facilitate easy testing at higher levels. The overburden pressure was calculated using soil unit weight (γ), and was calculated as γH, where H is the height of the backfill above the test point. Strain gauges and extensometers were instrumented to record the displacements and axial strains along the length of the specimen.

Figures 5.2.1 through 5.2.7 show the results for the pull-out load versus displacement for different confining pressures. These figures include all the seven different types of geosynthetics, subjected to different confining pressures. It can be clearly seen that the pull-out load increases with increasing confining pressure. However, Figures 5.2.1 and 5.2.2 show some inconsistency with respect to increasing confining pressure. For example, 4D > 4B, this might be due the soil dilation, which is higher at the top of the wall (lower overburden pressure) than that at the bottom of the wall (higher overburden pressure). The legend text shown in all figures, for example 4A-8.34 psi represents the geosynthetic specimen of length 4ft, tested at level A (where level A starts at the bottom and moves up to level E, respectively), and 8.34 psi is the estimated overburden pressure at that level.

Figures 5.3.1 through 5.3.3 show the strain measurement along the geosynthetic strip tested in the field. These results were obtained by placing strain gages at different locations along the length of the specimen at respective heights of the test wall.

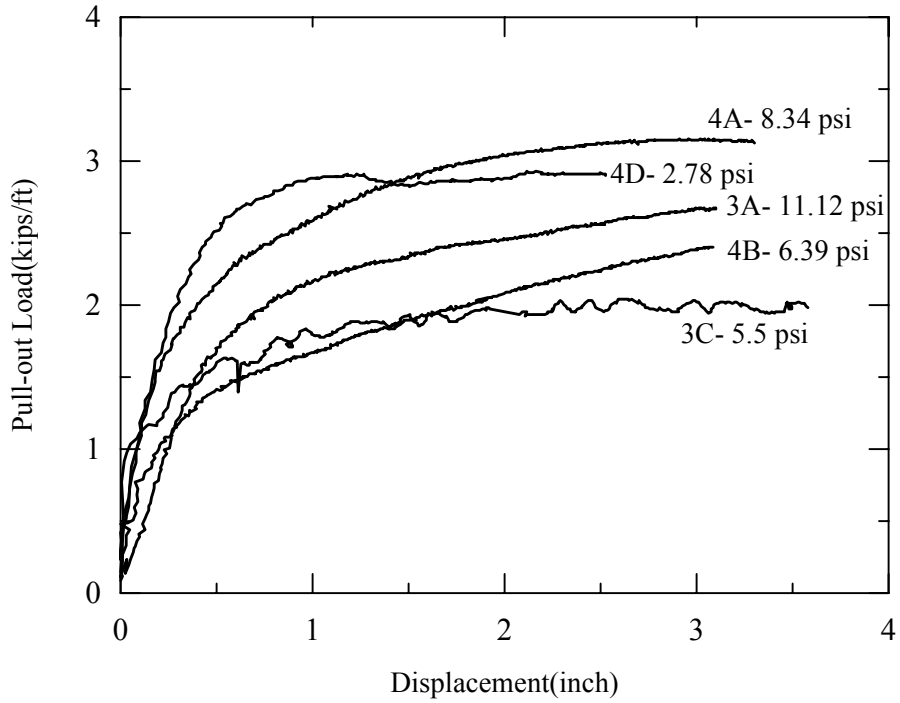

Figure 5.2.1: Displacement versus pull-out load for Non-Woven Geotextile.

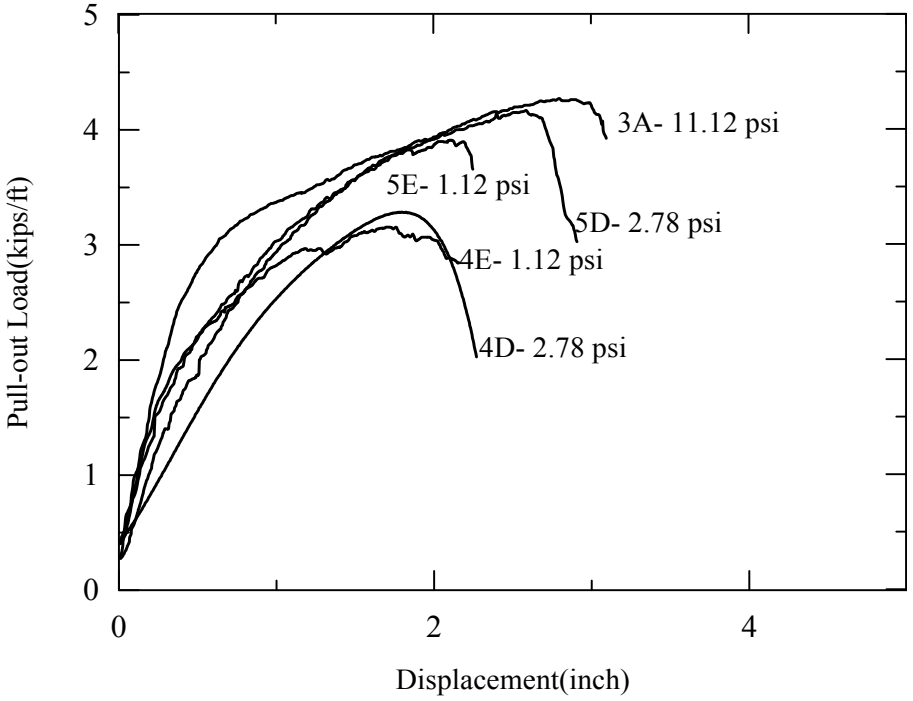

Figure 5.2.2: Displacement versus pull-out load for Woven (4x4) Geotextile.

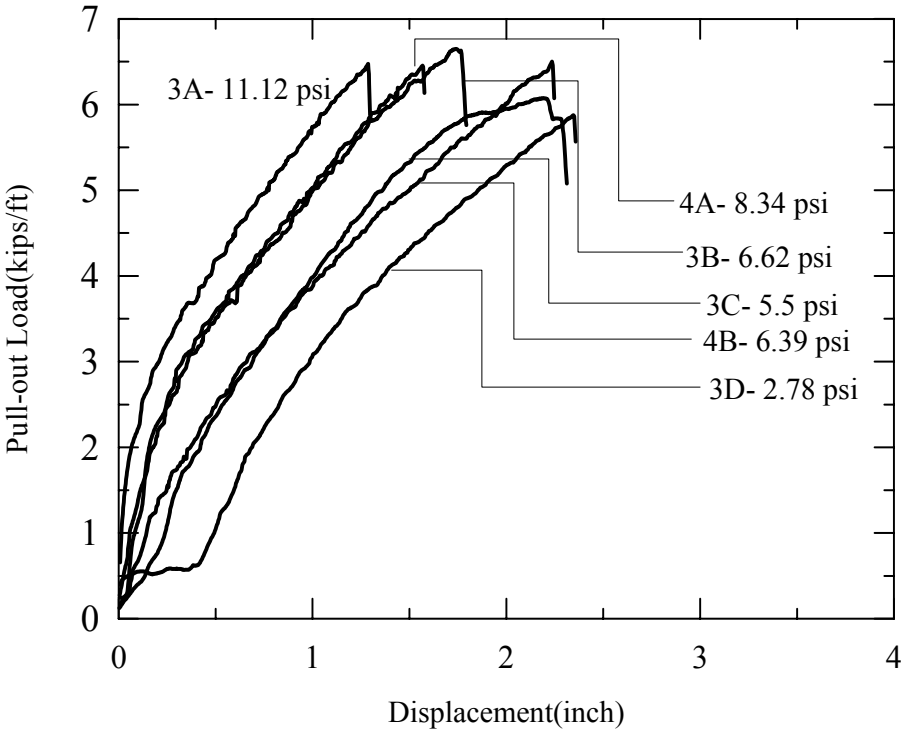

Figure 5.2.3: Displacement versus pull-out load for Woven (6x6) Geotextile.

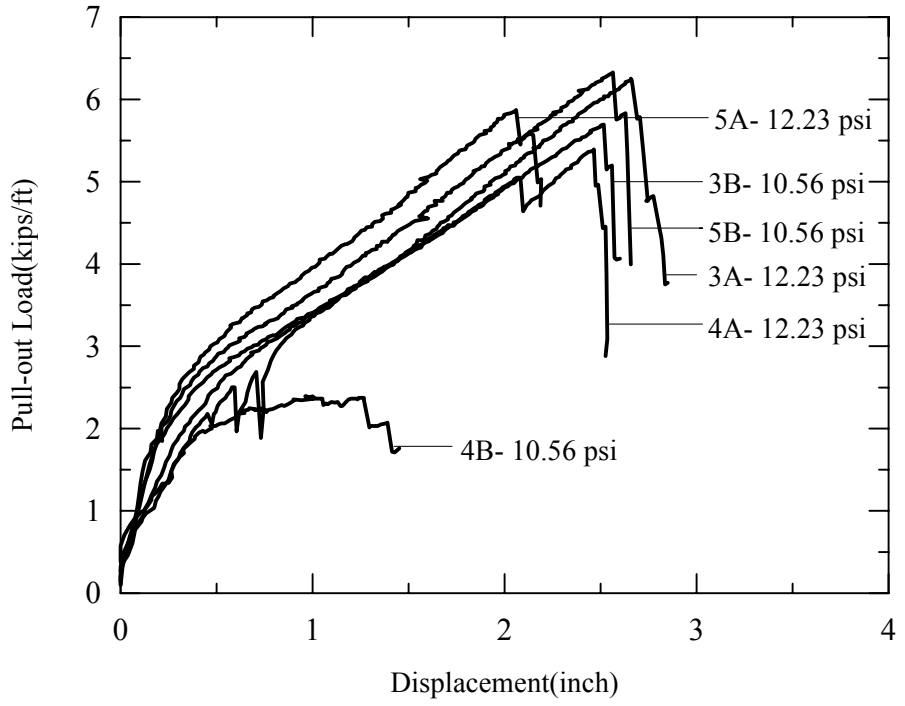

Figure 5.2.4: Displacement versus pull-out load for Stratagrid-500.

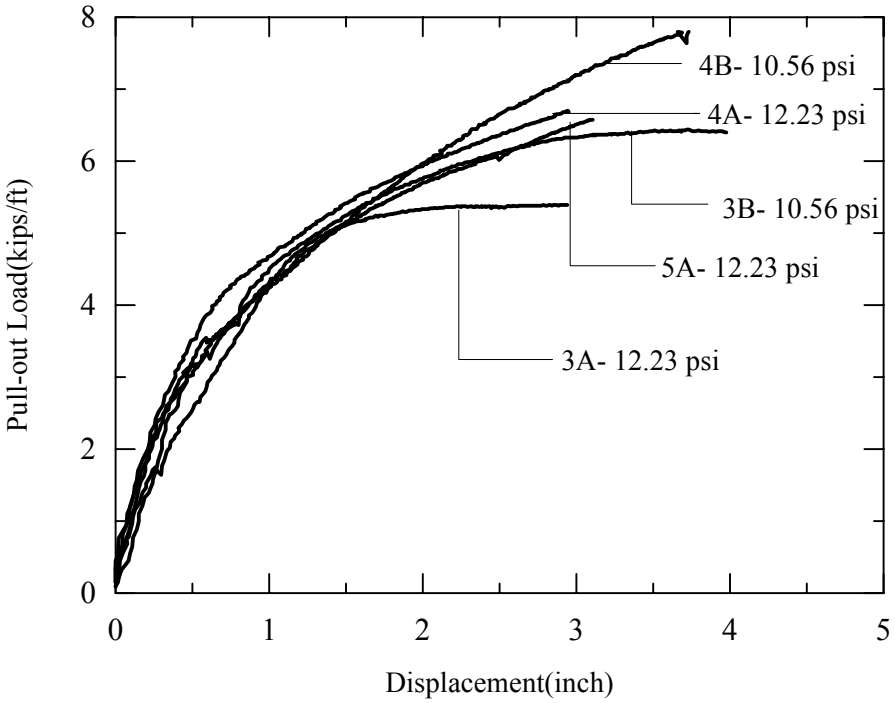

Figure 5.2.5: Displacement versus pull-out load for UX1700

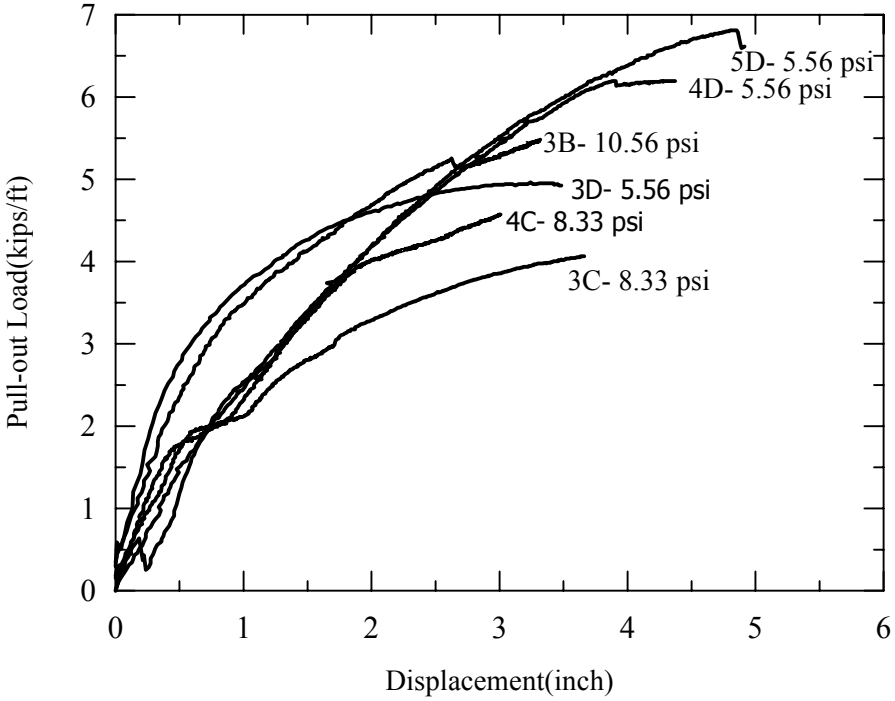

Figure 5.2.6: Displacement versus pull-out load for UX1500.

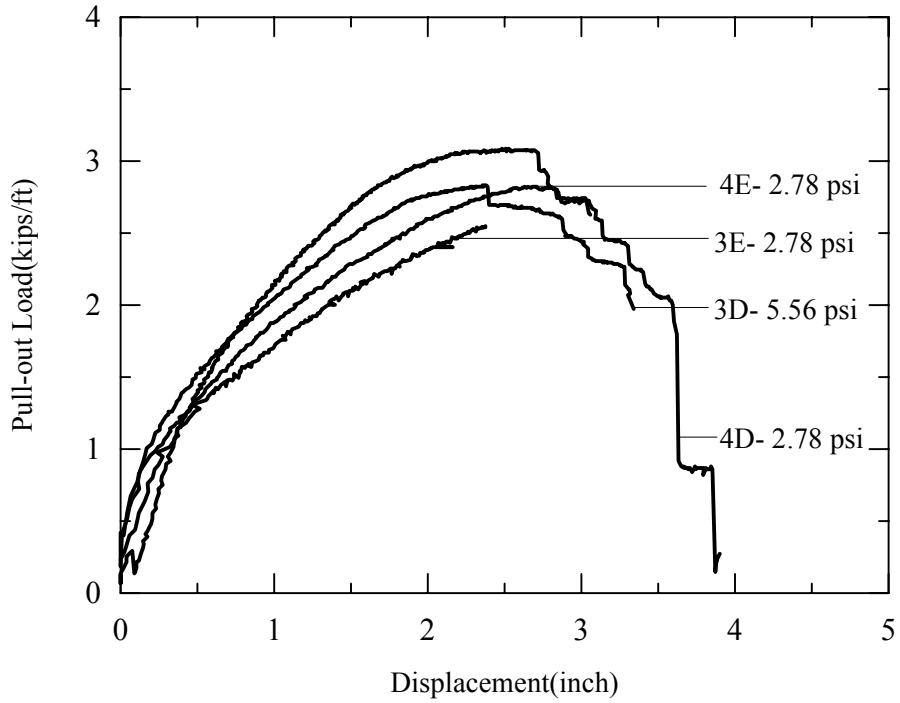

Figure 5.2.7: Displacement versus pull-out load for UX750.

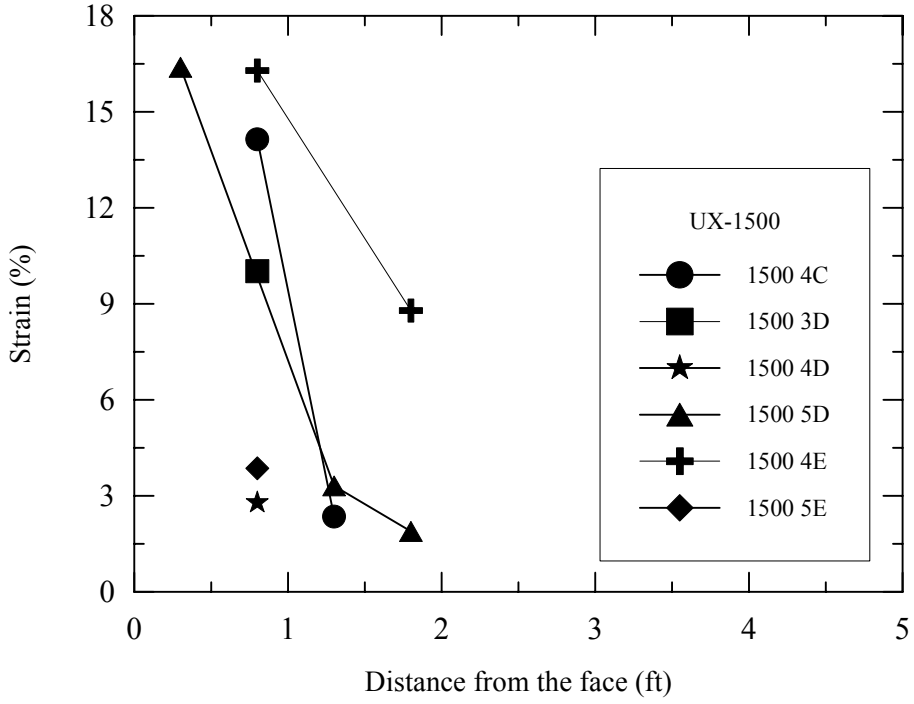

Figure 5.3.1: Strain (%) along the length for UX1500.

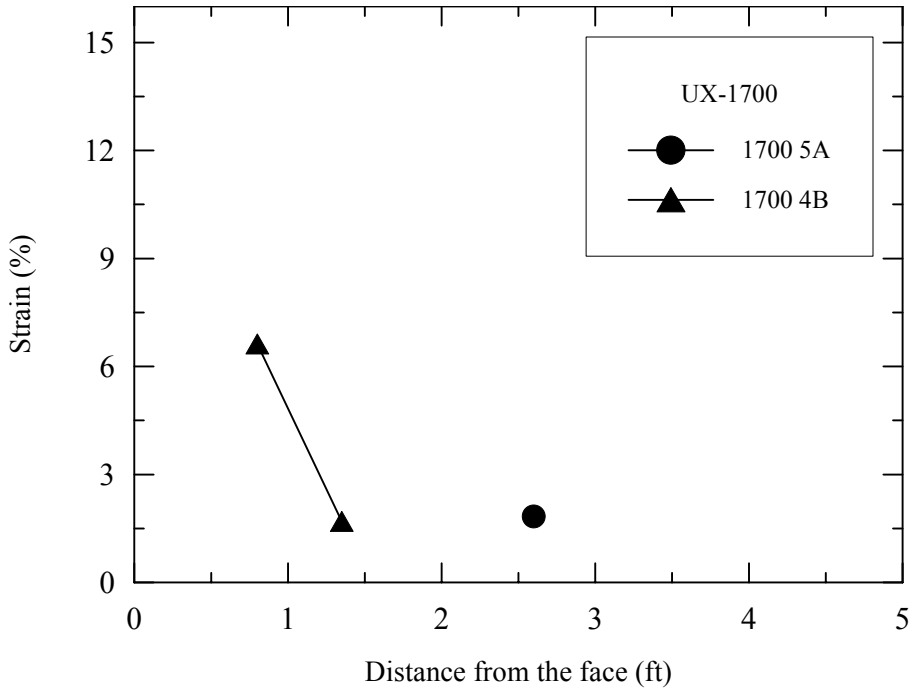

Figure 5.3.2: Strain (%) along the length for UX1700.

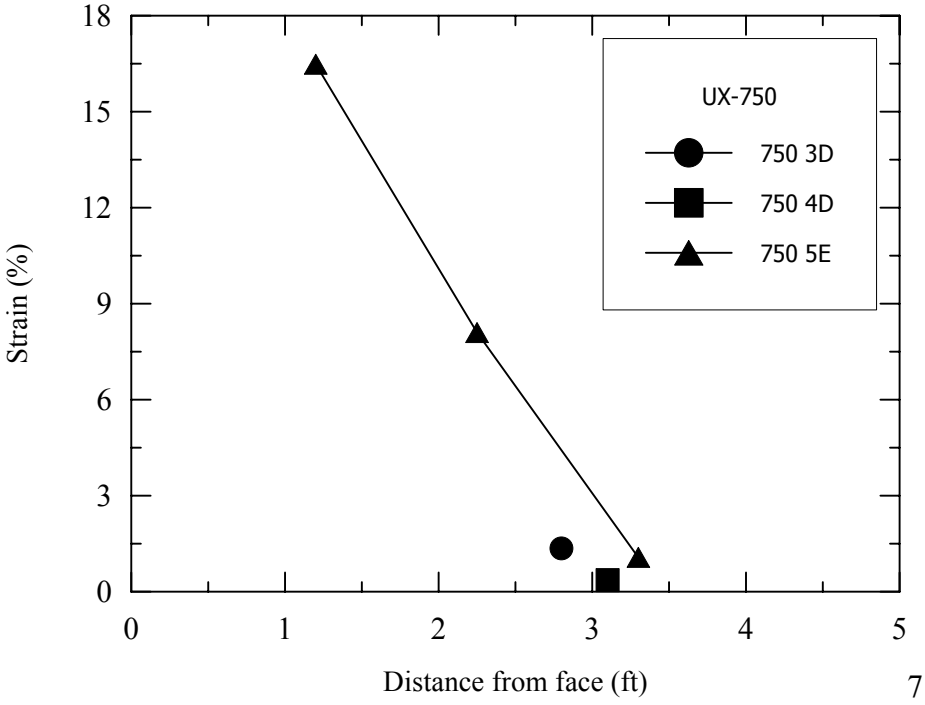

Figure 5.3.3: Strain (%) along the length for UX750.

CHAPTER 6

ANALYSIS OF PULL-OUT TEST RESULTS

6.1 General

As in any conventional reinforced soil structures, the stability of the geosynthetic reinforced soil structure depends on two basic components. First is due to the development of high tensile stresses in the geosynthetics, which makes the geosynthetic to elongate excessively or break, leading to large movements and possible collapse of the structure. This mode of failure is called the tension failure or elongation failure. The second is the pull-out failure of the geosynthetic. The first component is well understood, since it is mainly dependent upon the tensile modulus and the cross sectional area of the embedded specimen. However, the pull-out failure mechanism is not well understood, especially when cohesive soils are used as the backfill material. In order to understand the pull-out phenomena, laboratory and field pull-out tests were conducted, and the results will be analyzed and presented in the proceeding sections of this chapter.

6.2 Pull-out Resistance

In pull-out tests geosynthetic extensibility results in a non-uniform distribution of shear stresses and shear displacement along the length of the geosynthetic specimen. This makes the interpretation of the test results difficult. In interpreting the pull-out test results, it is common practice to assume that the apparent shear stress or pull-out resistance (τ_a) is developed on planar surfaces adjacent to each face of the reinforcement. This apparent shear stress or pull-out resistance (τ_{ap}) of a geosynthetic can be computed using the following Equation:

$$\tau_{ap} = \frac{T_{ult}}{2 \cdot A} \tag{6.2.1}$$

Where T_{ult} = ultimate pull-out load

A = embedded area of the geosynthetic specimen.

This empirical relation is defined as the average resistance method, and the formulation of this relation will be discussed in the later sections of this chapter.

6.3 Comparison of Laboratory and Field Pull-out Test Results

Figures 6.3.1 through 6.3.7 show the influence of confining pressure on the apparent pull-out resistance for the different geosynthetics. Both field and laboratory test results are compared in order to study the influence of in -situ conditions on pull-out resistance of geosynthetics. All results are consistent with respect to increase in pull-out resistance due to the increase in confining pressure. The laboratory and field tests are close to each other and show more consistency for high strength geogrids compared to weak geotextiles, which show less consistency. The apparent pull-out resistance is related to the confining pressure as follows:

$$\tau_a = C_{ap} + \sigma_n \tan\delta_{ap} \qquad (6.3.1)$$

Where: C_{ap} = the apparent adhesion intercept,

σ_n = the confining pressure, and

δ_{ap} = the apparent interface friction angle.

The parameters C_{ap} and δ_{ap} are dependent upon the physical (geometry and roughness) and chemical properties of geosynthetics, as well as the soil properties. Equation 6.3.1 shows that the apparent pull-out resistance (τ_{ap}) is almost linearly proportional to the confining pressure (σ_n). This proportionality is evident from the Figures 6.3.1 through 6.3.7 (i.e. pull-out resistance is increasing with increase in confining pressure).

Considering, the comparison of laboratory and field pull-out tests for different geosynthetics. As the soil tested in both the field and laboratory pull-out tests was same, the results for a particular geosynthetic are compared in the same figure. This comparison brings out the difference between the in-situ and the laboratory test results, and also provides evidence about the dependency of the laboratory tests, so that in future one can just use the laboratory test results and use them in design. Therefore this comparison gives the luxury of using the laboratory test results for designing the bond length for resisting the pull-out of geosynthetic.

In the case of Stratgrid-500 (Figure 6.3.1), the laboratory pull-out test results shows higher values of peak pull-out resistance compared to the field pull-out test results. The best fit line for the field test results is much lower to the best fit line for the laboratory test results, this difference might be due to inclusion of 4ft and 5ft samples that give the lower values of apparent pull-out resistance (as the calculations were carried out using the empirical relation defined as average resistance method). The reason for the lower values of 4ft and 5ft samples is discussed in the later sections of this chapter. Similarly, the test results for UX750 (Figure 6.3.2) has the similar trend as that of startagrid-500. The laboratory test result shows a steep increase in the pull-out resistance with respect to increase in confining pressure. Since both Stratagrid-500 and UX750 are the weaker geogrids among the set of geosynthetics, they exhibit similar trend.

In the case of stronger geogrids such as UX1500 (Figure 6.3.3), the peak pull-out resistance values for laboratory tests were lower compared to the field tests. The interface friction angle (δ_a) is almost equal, and the best fits for both the laboratory tests and the field tests are parallel. There is not much variation in the test result values for both the

laboratory and field tests. The higher values for the field tests may be attributed due to the fact that there might be non-uniform (greater) compaction and due to the assumed overburden pressure calculation (γH) for the field tests. Similarly, the pull-out test results for UX1700 (Figure 6.3.4) has the similar trend as that of UX1500. Both the laboratory and field test values for peak pull-out resistances for UX1700 are almost the same. Therefore the best fits for both the laboratory tests and field tests are very close and almost parallel to each other. Since UX1500 and UX1700 are the stronger geogrids, they exhibit similar trends.

The same apparent shear stress was used in calculating the coefficient of interaction, which is discussed later in this Chapter. Now by comparing the laboratory and field tests, the dependency of the test method, the quality of the construction work, the effect of different lengths, and the performance of the geogrids under different confining pressures can be discussed. But the actual pull-out resistance depends on the friction of the soil, the friction between the grid surface and the soil, and the passive bearing resistance of the soil on the transverse members of the grid reinforcement.

By seeing the comparative graphs of field tests and laboratory tests, it can be seen that field results show a higher pull-out resistance (not in all cases, but in general). Again there are many reasons; the reasons may be the dilation at lower confining pressures, the length embedded, or the variations in compaction, boundary effects in pull-out apparatus, arching effect in field. In some cases, there is some unusual increase or decrease in pull-out resistances that could be due to the development of lateral pressures against the rigid front face, leading to the arching of the soil over the reinforcement near the front face,

which reduces the local vertical stresses on the reinforcement, and thereby making an unusual increase in the pull-out resistance.

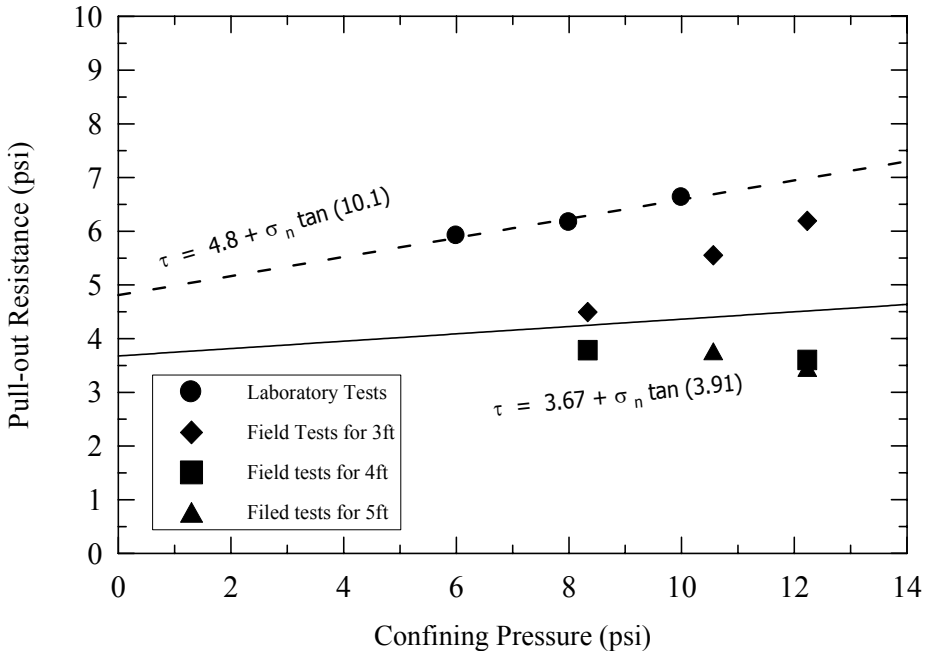

Figure 6.3.1: Pull-out resistance versus confining pressure for Stratagrid-500

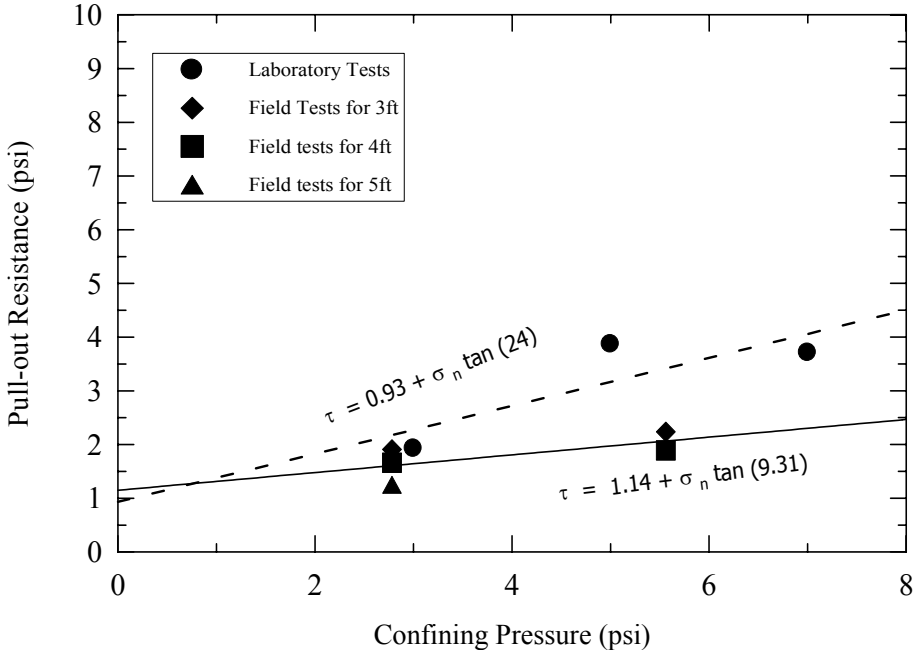

Figure 6.3.2: Pull-out resistance versus confining pressure for UX750

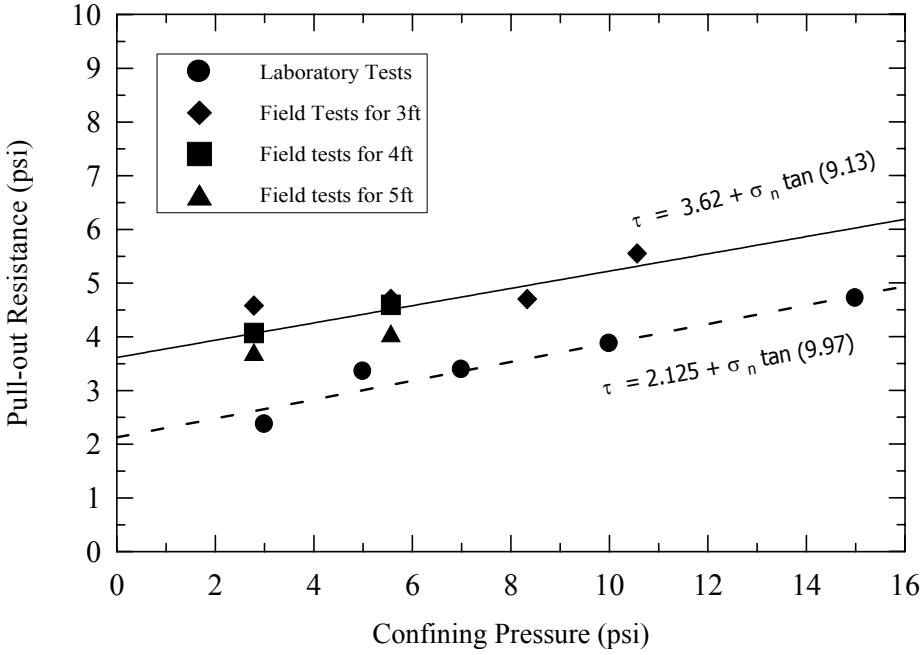

Figure 6.3.3: Pull-out resistance versus confining rressure for UX1500

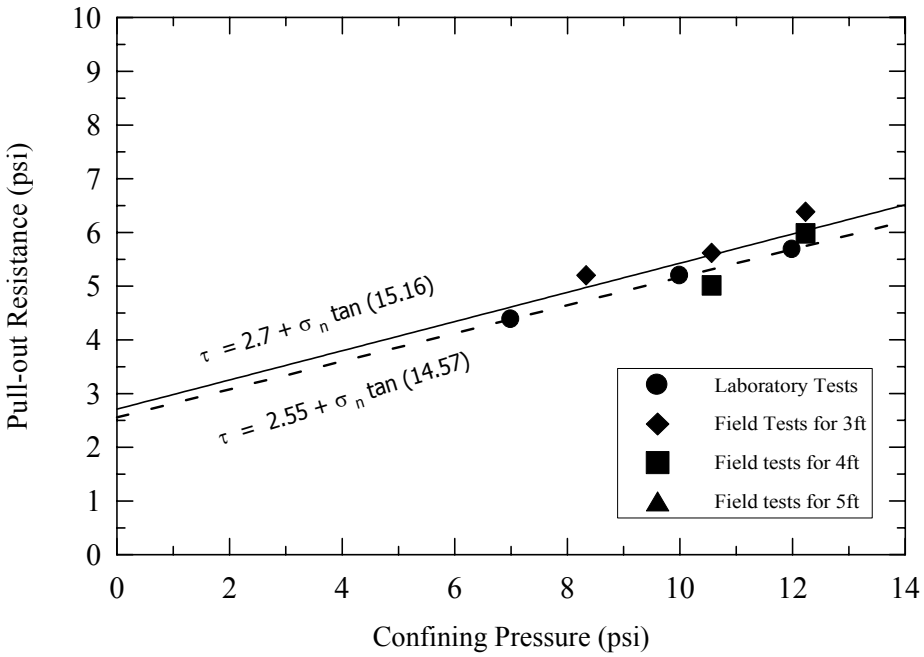

Figure 6.3.4: Pull-out resistance versus confining pressure for UX1700

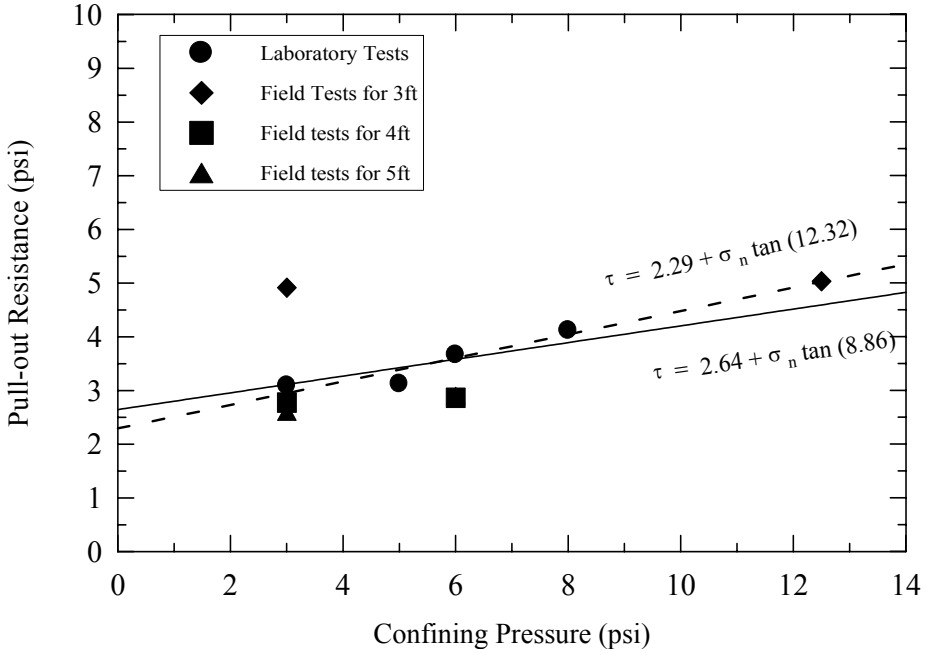

Figure 6.3.5: Pull-out resistance versus confining pressure for Woven (4x4) Geotextile

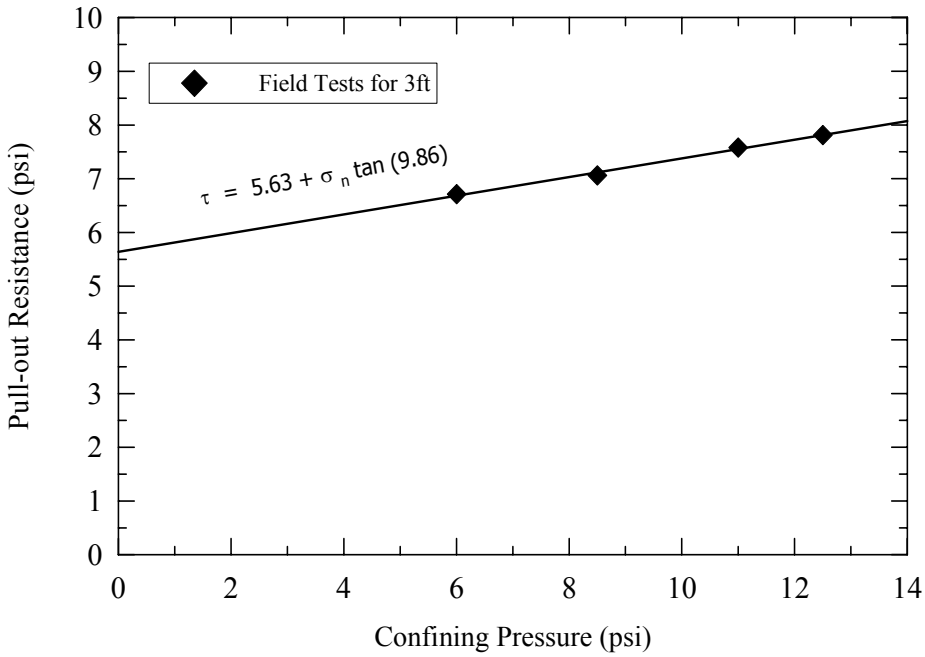

Figure 6.3.6: Pull-out resistance versus confining pressure for Woven (6x6) Geotextile

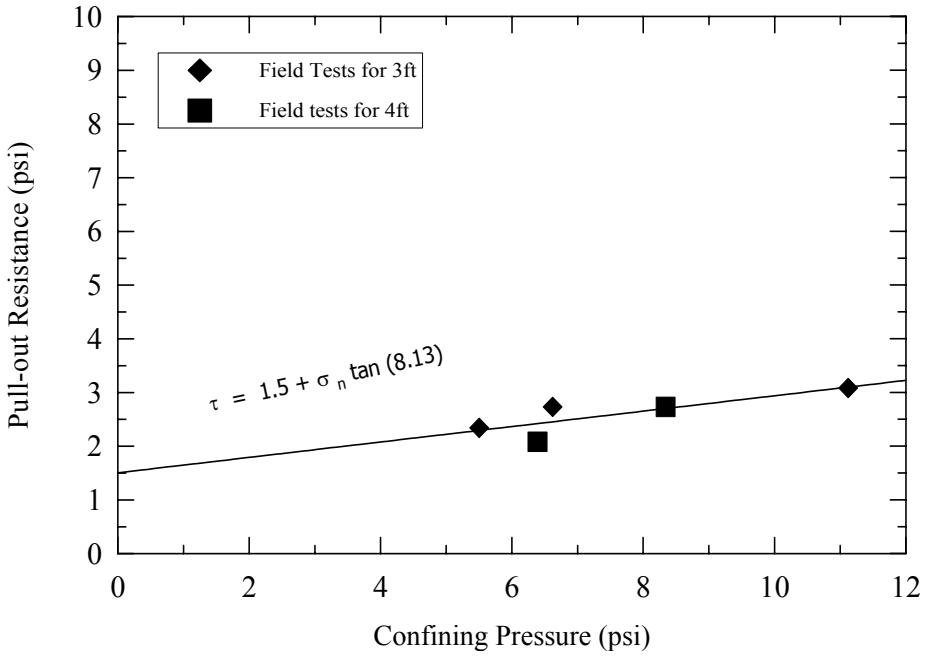

Figure 6.3.7: Pull-out resistance versus confining pressure for Non-woven Geotextile

Table 6.3.1**:** Comparison between laboratory and field pull-out test results

Geosynthetic type	Adhesion Intercept (psi) C_{ap}		Interface Friction Angle δ_{ap} (degrees)	
	Lab Tests	Field Tests	Lab Tests	Field Tests
Stratagrid- 500	4.8	3.67	10.1	3.91
UX750	0.93	1.14	24	9.31
UX1500	3.62	2.125	9.13	9.97
UX1700	2.55	2.7	14.57	15.16
Woven (4x4)	2.29	2.64	12.32	8.86
Woven (6x6)	NA	5.63	NA	9.86
Non-woven (TG700)	NA	1.5	NA	8.13

NA – Not Available.

6.4 Pull-out Phenomenon

The pull-out mechanism can be classified depending on the structure and geometry of the geosynthetic. For geosynthetics like woven and non-woven geotextiles, the contribution to the total pull-out is provided only by the frictional resistance (friction between the soil and the geosynthetic). On the other hand, for geosynthetics like geogrids, the contribution to the pull-out resistance is provided by two main components, the frictional resistance offered mainly by the longitudinal members of the geogrid, and the passive bearing resistance offered by the transverse members of the geogrid. Figure 6.4.1, illustrates the contribution of frictional resistance and passive bearing resistance in the case of geogrids.

Therefore, the total pull-out force can be given as:

$$F_t = F_f + F_b \tag{6.4.1}$$

Where: F_f = frictional force and this can be formulated using Mohr-coulomb criterion as:

$$F_f = \tau_f * 2A = (C_a + \sigma_n \tan\delta_a) * 2A \tag{6.4.2}$$

Where: τ_f = the actual frictional resistance,

C_a = the actual adhesion intercept,

σ_n = the confining pressure,

δ_a = the friction angle between soil and geosynthetic

A = the embedded area of the specimen.

The frictional force discussed here has the same formulation as that of the apparent shear stress or pull-out resistance (τ_a) discussed in Section 6.2, but the pull-out was apparent and the respective parameters were apparent. While the friction force

discussed here is the actual frictional force corrected for passive bearing in the transverse members of geogrids. However the frictional force discussed here is same as that of the apparent pull-out force discussed in Section 6.2 for geotextiles, which do not have the transverse bearing members.

In Equation 6.4.1, F_b is the bearing resistance, which is not measured in this study. However there are many empirical formulas that estimate the value of bearing resistance using bearing capacity factors (N_q and N_c). The passive bearing force (F_b) of the transverse members is related to the cohesion, friction angle and the bearing capacity factors in the Terzaghi-Buisman bearing capacity equation, which was modified in the following form (Peterson and Anderson, 1980)

$$F_b \big/ nwd = CN_c + \sigma_v N_q \qquad (6.4.3)$$

Where:

n = the number of transverse members

w = the width of the reinforcement

d = the thickness of the transverse members, and

N_c and N_q = bearing capacity factors.

The expression for N_q depends on the assumed failure mechanism. Two bearing capacity models were proposed to explain the passive bearing resistance in front of the transverse members. The first model is the general bearing capacity failure model (Figure 6.4.2) proposed by Peterson and Anderson (1980). In this model, the proposed N_q is expressed as follows:

$$N_q = e^{\pi \tan\phi} \cdot \tan^2\left(45 + \frac{\phi}{2}\right) \qquad (6.4.4)$$

The second model is the punching shear failure model (Figure 6.4.3) proposed by Jewell et al. (1984). In this model, the proposed N_q is expressed as follows:

$$N_q = e^{(\frac{\pi}{2}+\phi)\tan\phi} \tan(45+\frac{\phi}{2}) \qquad (6.4.5)$$

The other bearing capacity factor N_c was originally derived by Prandtl (1921), and it is expressed as follows:

$$N_c = \cot \Phi \, (N_q\text{-}1) \qquad (6.4.6)$$

Later, the equation for passive bearing force F_b (equation 5.3.7) was modified by Bergado and Anderson (1992) for weathered Bangkok clay, and suggested the following:

$$F_b = A_b N_c C_u \qquad (6.4.7)$$

where: A_b = (nwd) the bearing area offered by the thickness of the transverse member of the geogrid. This represents the sum of all the areas close to the latitudinal member along the numerous apertures present in the geogrid. Since the passive bearing force is offered by the thickness and the width of the aperture (i.e., the soil interlocks within the aperture width with the help of the thickness of the transverse member). Therefore, it is the product of the number of apertures, width of the aperture and the thickness of the transverse member. In order to have a maximum benefit from the passive bearing resistance, it is better to have more apertures with enough thickness of the transverse members.

In Equation 6.4.8, C_u is the apparent undrained strength of soil and is expressed as:

$$C_u = C+\sigma_n \tan\Phi \qquad (6.4.8)$$

Where: C = the cohesion intercept (obtained from direct shear test),

σ_n = the confining pressure and

Φ = the soil friction angle (obtained from direct shear test)

A study by Ospina (1988) based on X-ray monitored pull-out tests conducted on wire mesh embedded in sand indicated that the failure mechanism was a function of the allowed deformation of the wire mesh and the normal confining pressure. It was observed that the mechanism of failure in front of a transverse member embedded in loose sand is the bearing capacity failure. At the dense state, a punching failure seemed to develop in front of the transverse member at low deformations, which became a bearing capacity failure at larger deformations. Furthermore, at low normal confining pressures, the failure mechanism was closely related to punching type failure while bearing capacity failure was noted for high normal confining pressures.

The general bearing capacity failure and the punching failure modes for the soil friction angle of $\phi = 24^\circ$ appear to be an apparent upper bound envelope and an apparent lower bound envelope for the pull-out capacities of the geogrid reinforcements, respectively. However, for a geosynthetic reinforcement (which exhibits larger deformations) with lower confining pressures, it is assumed that the type of failure is a bearing capacity failure. Therefore, the bearing capacity model proposed by Peterson and Anderson (1980) (Equation 6.4.4) is used in this study to calculate the bearing capacity factor N_q. In calculating the bearing capacity factor (N_c and N_q), the soil properties given in Table 3.3.1 are taken.

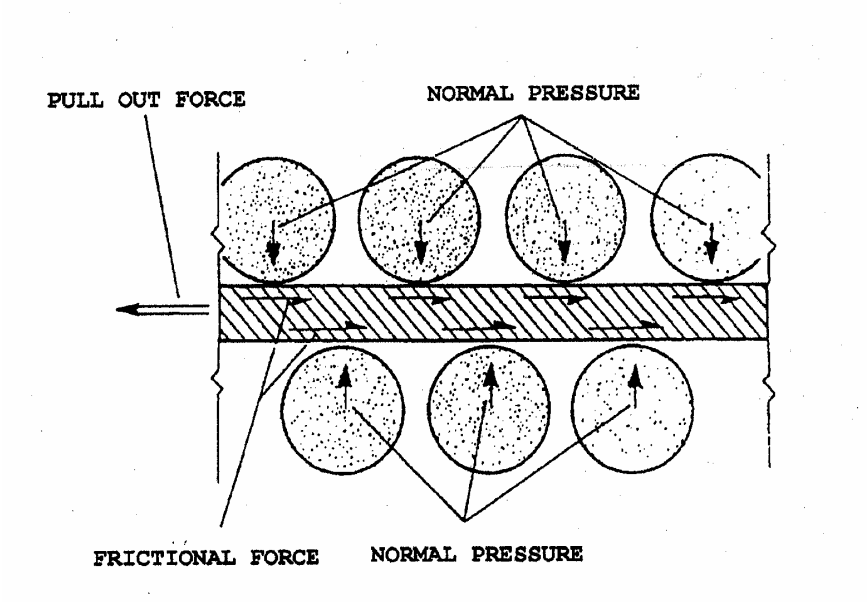

(a)

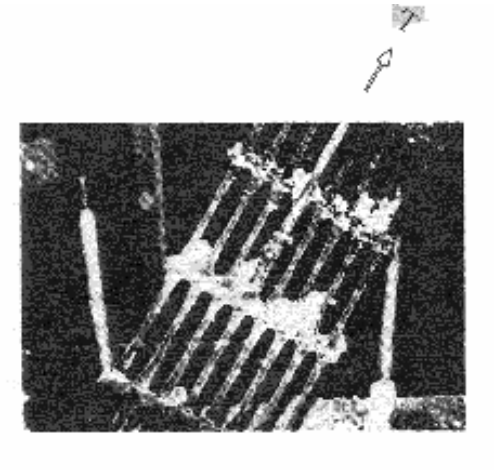

(b)

Figure 6.4.1(a) Mechanism of frictional resistance (Christopher et al. 1996)
Figure 6.4.1(b) Mechanism of passive bearing resistance (Tensar Ltd).

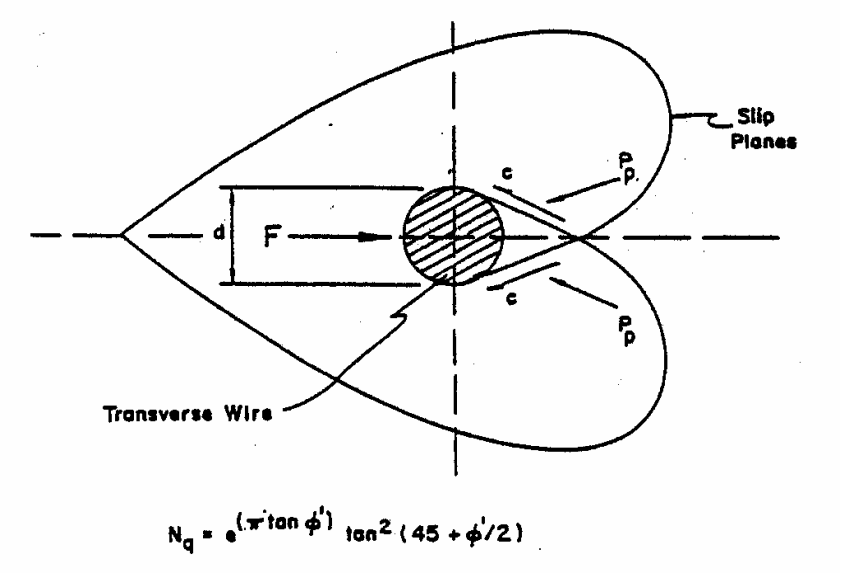

Figure 6.4.2: General bearing capacity failure mechanism (Peterson and Anderson, 1980)

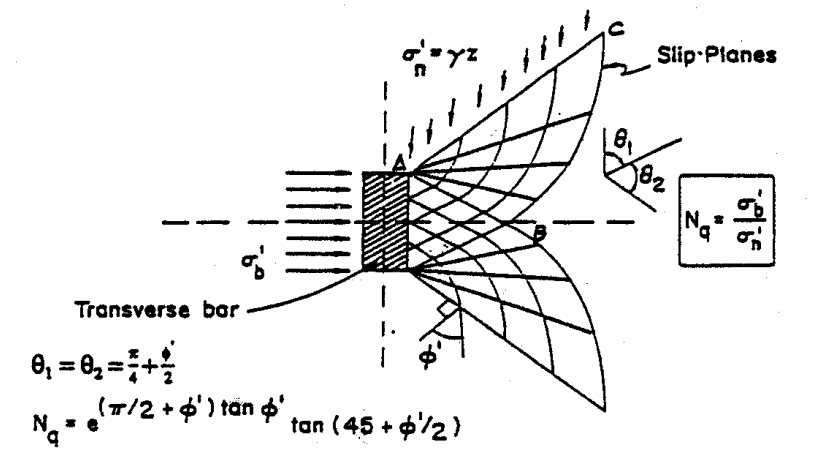

Figure 6.4.3: Punching shear failure mechanism (Jewell et al. 1984).

Figures 6.4.4 through 6.4.17 illustrate the contribution of bearing resistance to total pull-out resistance for the different geosynthetics used in this study. After inspection of these figures, one can see that the contribution of passive bearing resistance ranges from 5-30 percent of the total pull-out resistance. Figures 6.4.4 through 6.4.17 show the contribution of bearing force (in pounds) with respect to confining pressure. Moreover, the bearing resistance increases with increase in confining pressure, as it is an important factor that influences the undrained cohesion, and thereby it is directly proportional to the bearing resistance.

Consider Stratagrid-500, Figures 6.4.4 through 6.4.7, this geogrid is not that strong, and its thickness is moderate, but it is exhibiting a greater percentage of passive bearing, thereby increasing the total pull-out resistance. As explained earlier, the bearing increases with the increase in the thickness of the transverse member, and it increases with increase in the number of apertures per unit length. Therefore, as Stratagrid-500 has many apertures within the given length, it exhibits greater passive bearing resistance. Whereas UX750, it is weak, and the thickness of the transverse members is low, and even it has less number of apertures per unit length compared to Stratagrid-500, thereby exhibiting low bearing resistance. But to have good compatibility in contributing both the bearing and the friction, the geogrid should have enough surface area that could provide proper interface friction with the soil layers, and the ribs should be strong enough to withstand greater passive bearing forces. Therefore, it is important to select the appropriate geometry of the geogrid, to make it more efficient.

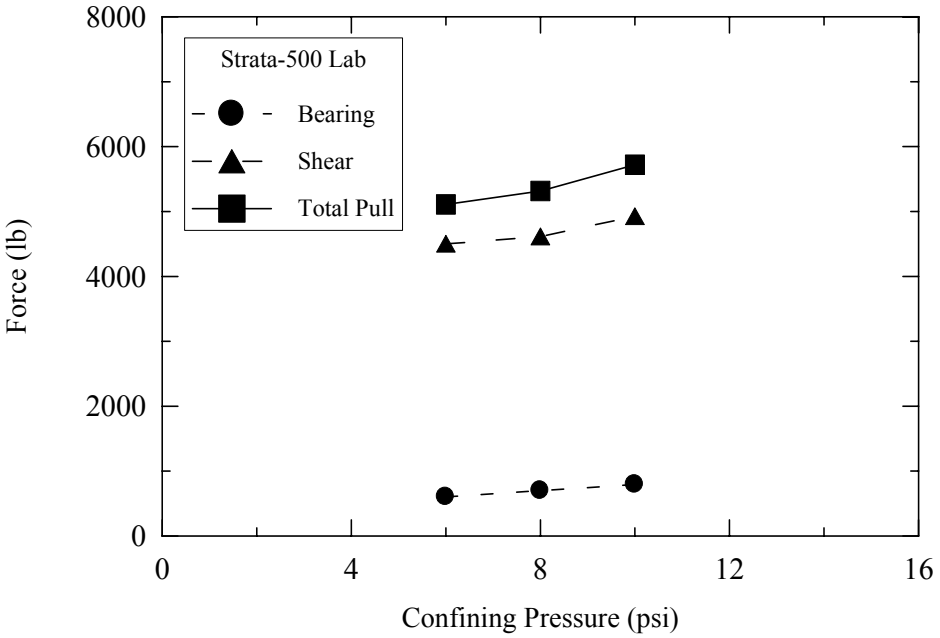

Figure 6.4.4: Contribution of bearing for Stratagrid-500 of 3ft length tested in laboratory.

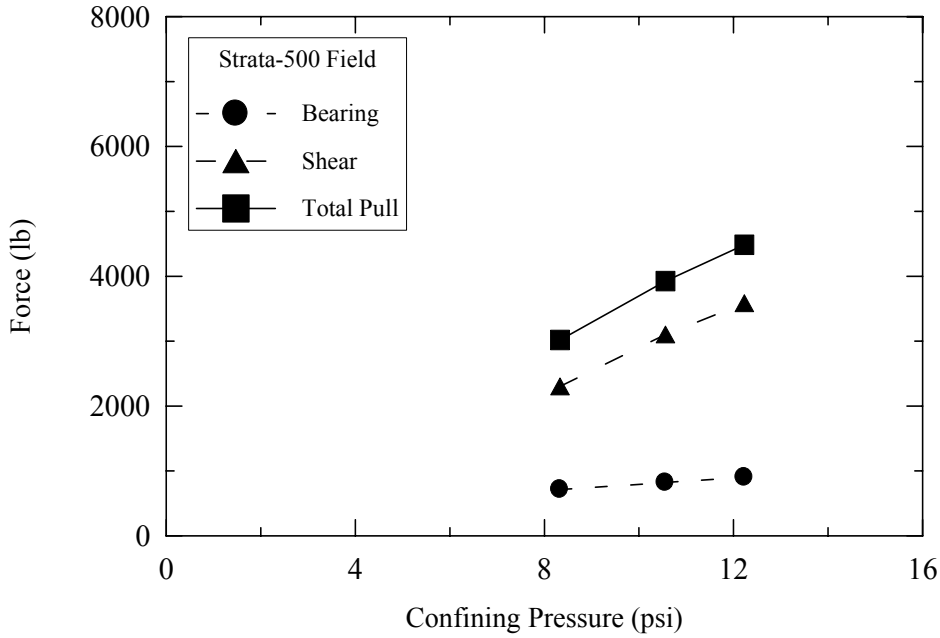

Figure 6.4.5: Contribution of bearing for Stratagrid-500 of 3ft length tested in field.

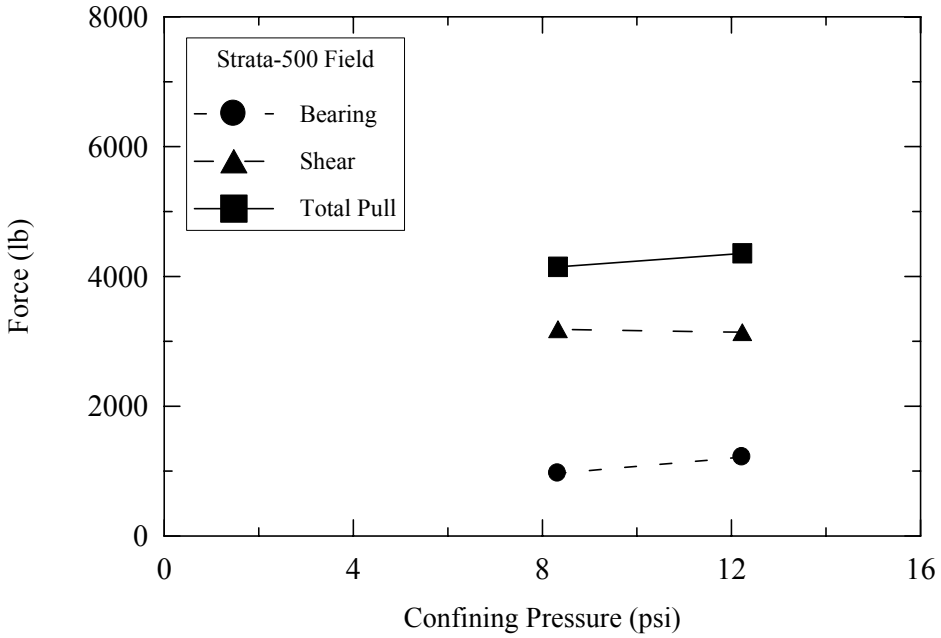

Figure 6.4.6: Contribution of bearing for Stratagrid-500 of 4ft length tested in field.

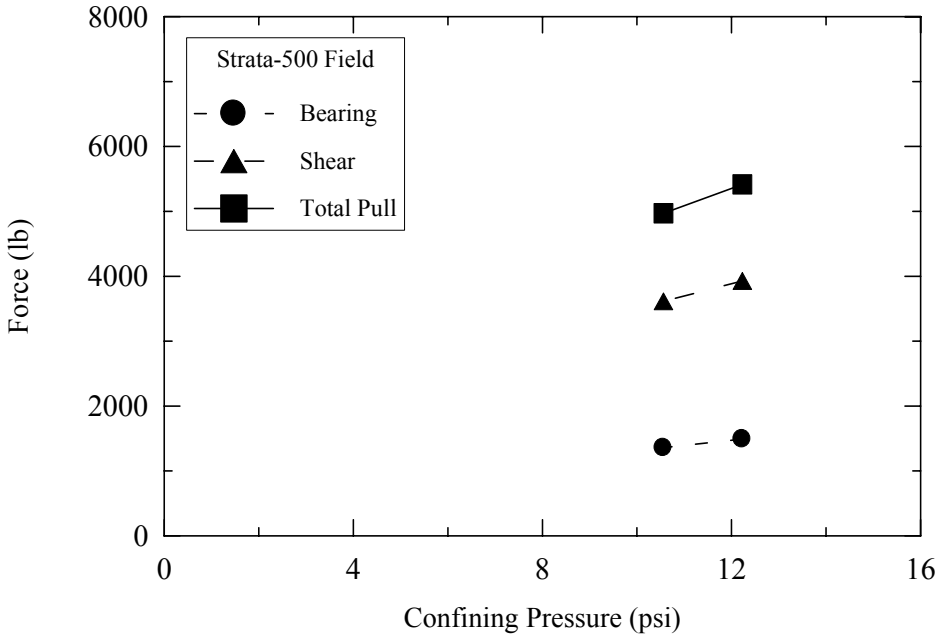

Figure 6.4.7: Contribution of bearing for Stratagrid-500 of 5ft length tested in field

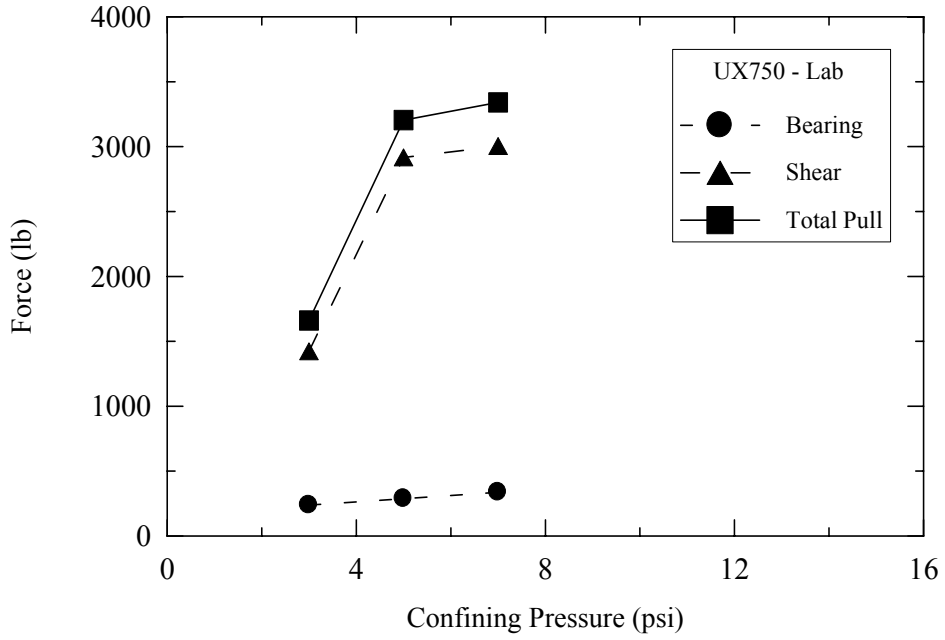

Figure 6.4.8: Contribution of bearing for UX750 of 3ft length tested in laboratory.

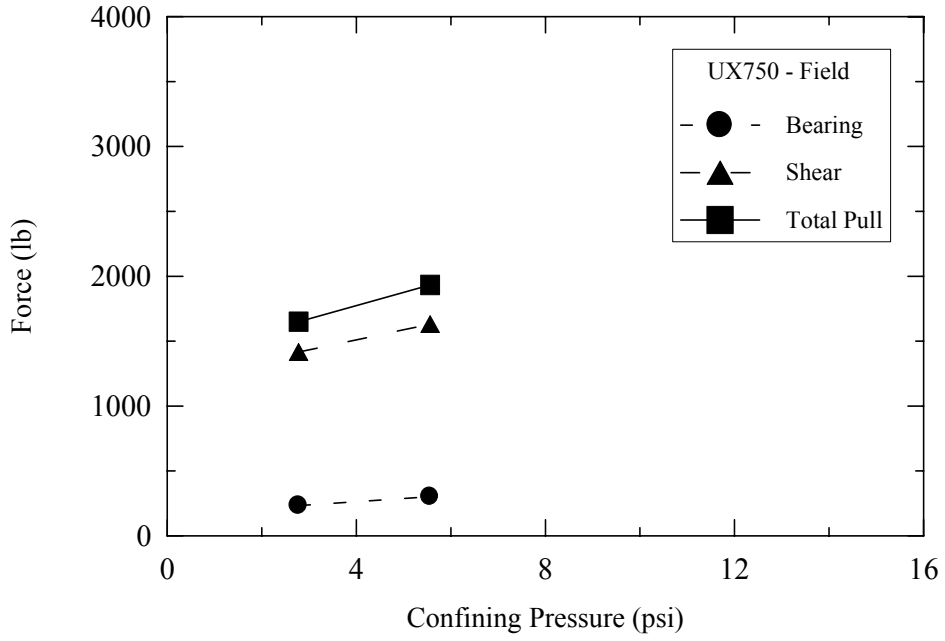

Figure 6.4.9: Contribution of bearing for UX750 of 3ft length tested in field.

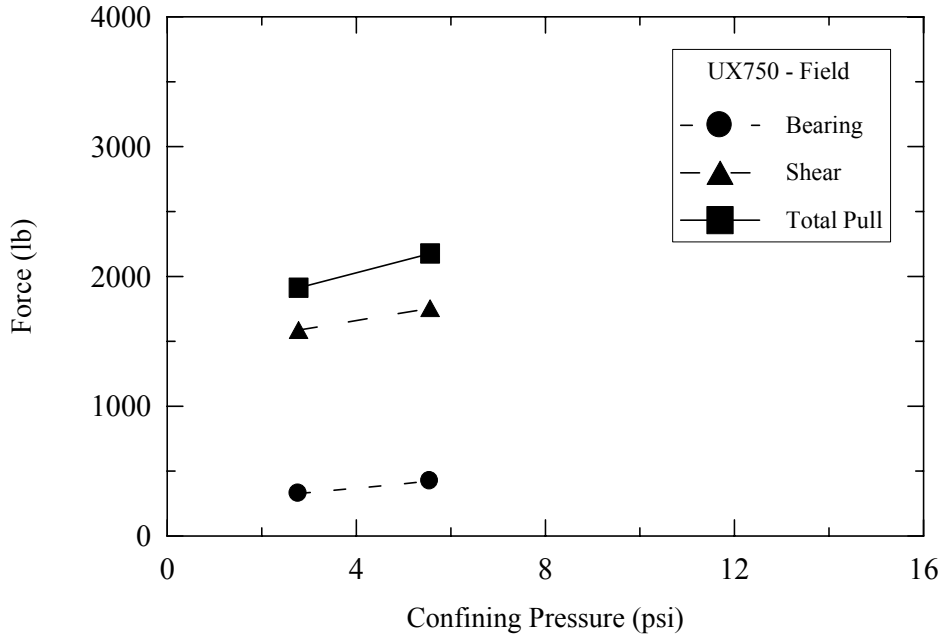

Figure 6.4.10: Contribution of bearing for UX750 of 4ft length tested in field.

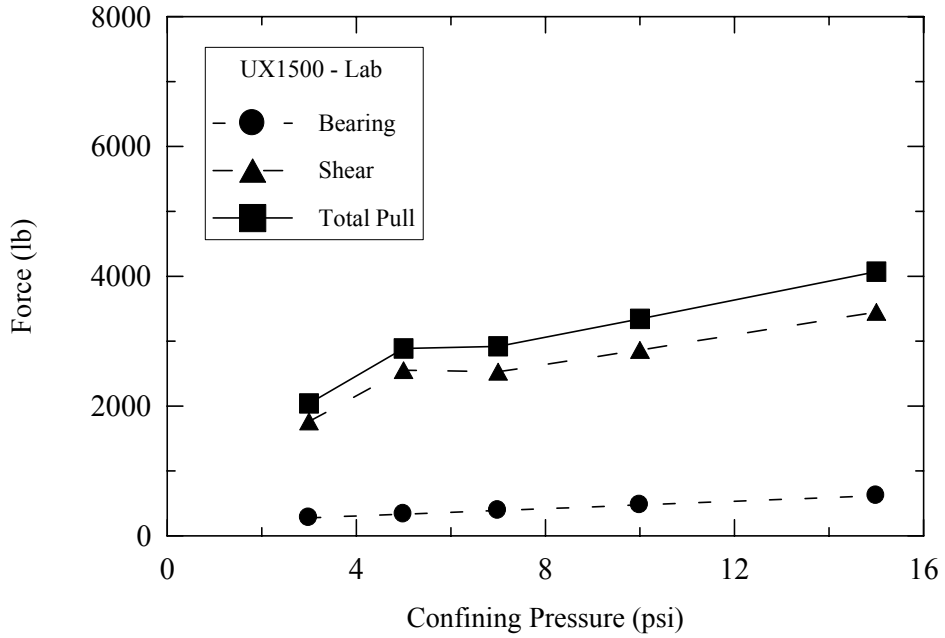

Figure 6.4.11: Contribution of bearing for UX1500 of 3ft length tested in laboratory.

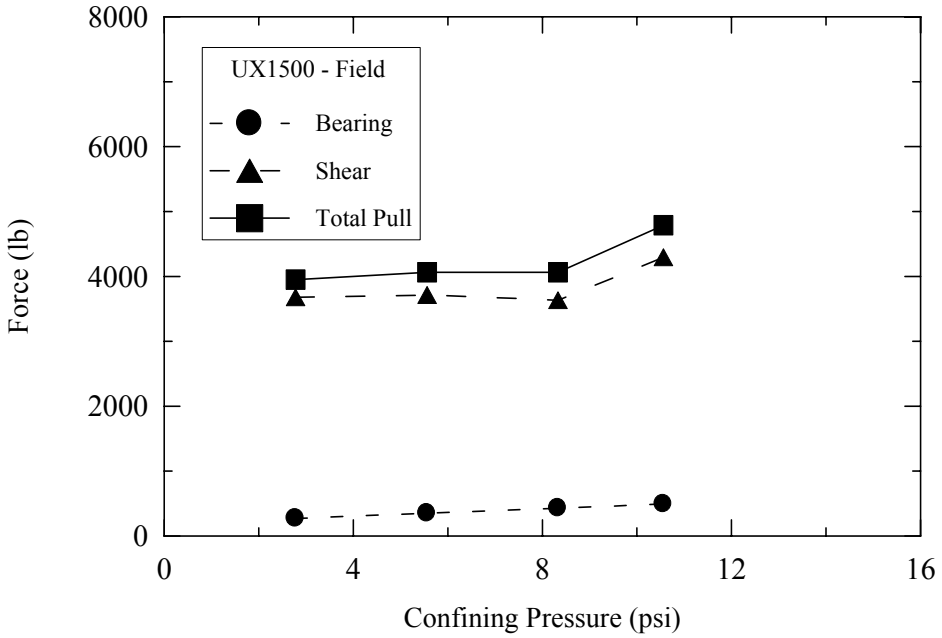

Figure 6.4.12: Contribution of bearing for UX1500 of 3ft length tested in field.

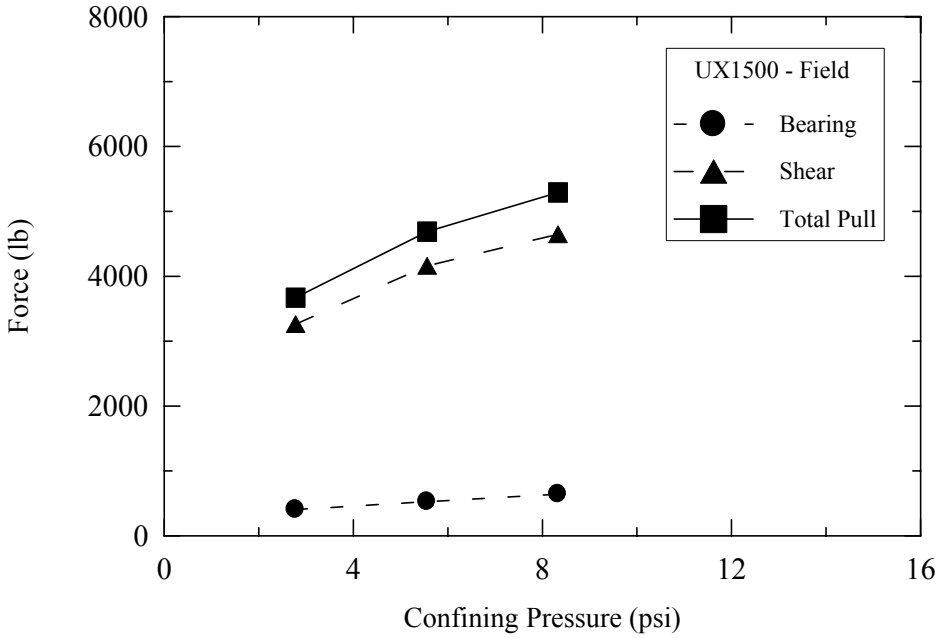

Figure 6.4.13: Contribution of bearing for UX1500 of 4ft length tested in field.

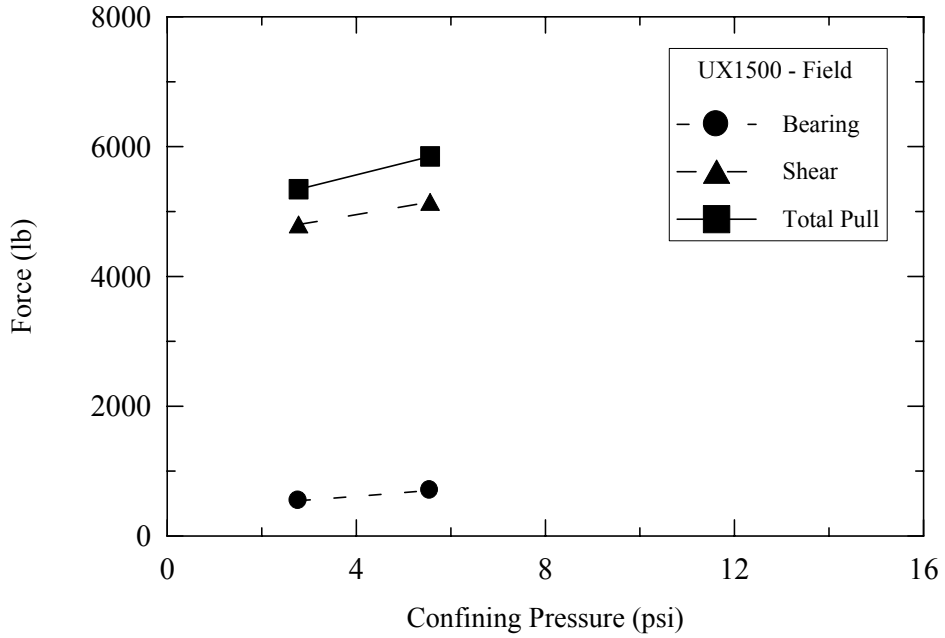

Figure 6.4.14: Contribution of bearing for UX1500 of 5ft length tested in field.

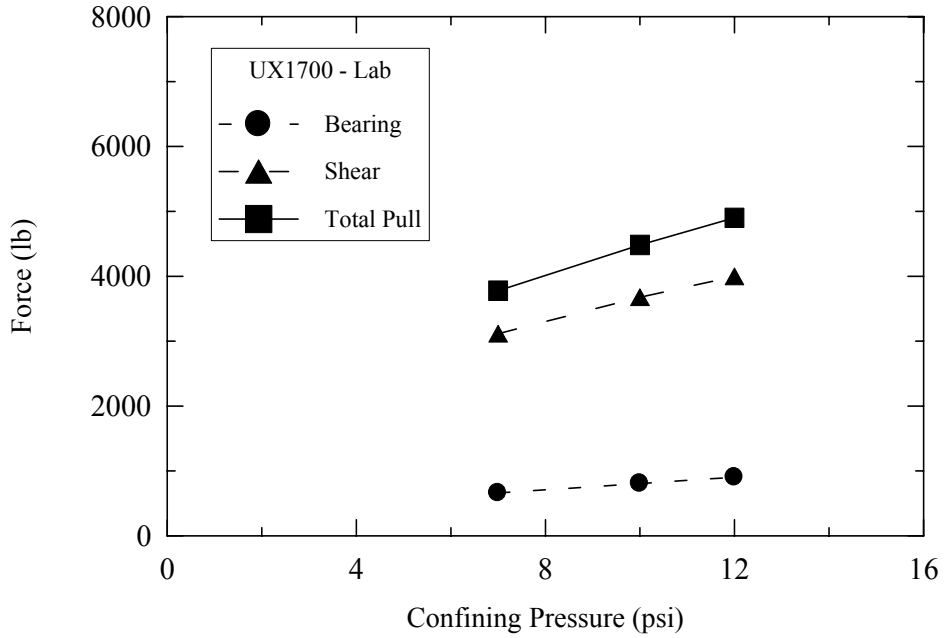

Figure 6.4.15: Contribution of bearing for UX1700 of 3ft length tested in laboratory.

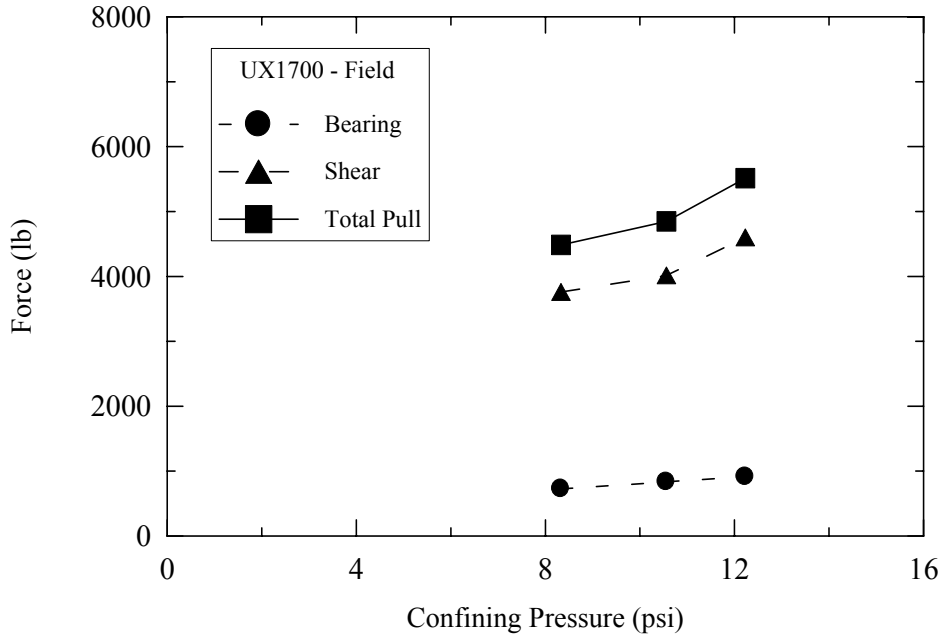

Figure 6.4.16: Contribution of bearing for UX1700 of 3ft length tested in field.

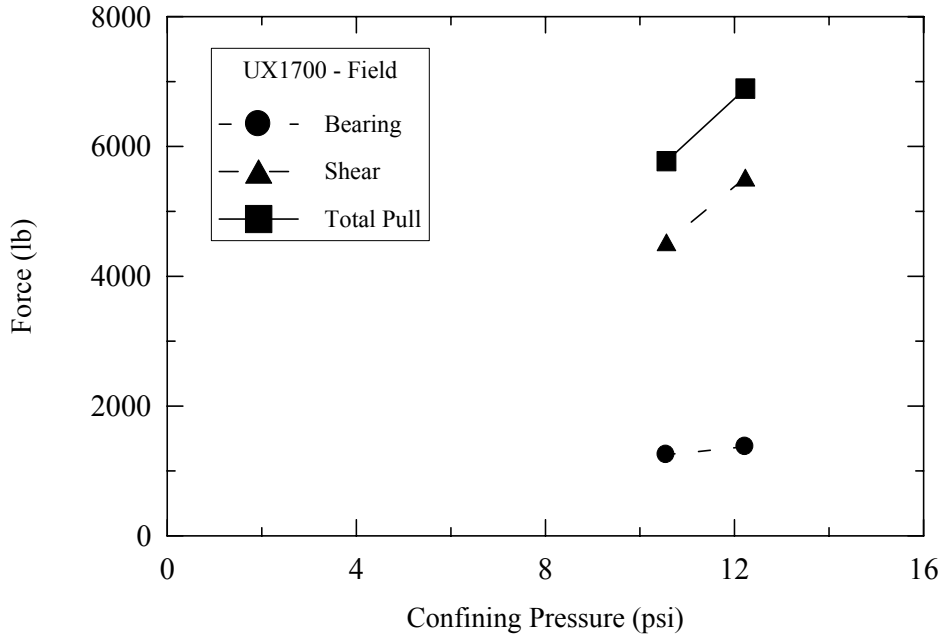

Figure 6.4.17: Contribution of bearing for UX1700 of 4ft length tested in field.

Table 6.4.1: Percentage bearing of Stratagrid-500

(a) Stratagrid-500 in laboratory tests for 3ft length

N_c	Σa	σ_v (psi)	C_u	Bearing (lb)	Total (lb)	% Bearing
19.32	5.52	6	5.67	604.7	5107.1	11.84
		8	6.56	699.6	5313.6	13.16
		10	7.45	794.5	5719.6	13.89

(b) Stratagrid-500 in field tests for 3ft length

N_c	Σa	σ_v (psi)	C_u	Bearing (lb)	Total (lb)	% Bearing
19.32	5.52	8.33	6.70	714.53	3015.36	23.69
		10.56	7.70	821.17	3922.56	20.93
		12.23	8.45	900.62	4484.16	20.08

(c) Stratagrid-500 in field tests for 4ft length

N_c	Σa	σ_v (psi)	C_u	Bearing (lb)	Total (lb)	% Bearing
19.32	7.44	8.33	6.70	963.06	4147.2	23.22
		12.23	8.45	1213.89	4353.48	27.88

(d) Stratagrid-500 in field tests for 5ft length

N_c	Σa	σ_v (psi)	C_u	Bearing (lb)	Total (lb)	% Bearing
19.32	9.12	10.56	7.70	1356.72	4968	27.31
		12.23	8.445	1487.95	5415	27.47

Table 6.4.2: Percentage bearing for UX750

(a) UX750 in Laboratory tests for 3ft length

N_c	Σa	σ_v (psi)	C_u	Bearing (lb)	Total (lb)	% Bearing
19.32	2.85	3	4.335	238.69	1660	14.3
		5	5.226	287.75	3203	8.98
		7	6.116	336.79	3340	10.08

(b) UX750 in field tests for 3ft length

N_c	Σa	σ_v (psi)	C_u	Bearing (lb)	Total (lb)	% Bearing
19.32	2.85	2.78	4.237	233.29	1649	14.14
		5.56	5.475	301.46	1932	15.6

(c) UX750 in field tests for 4ft length

N_c	Σa	σ_v (psi)	C_u	Bearing (lb)	Total (lb)	% Bearing
19.32	3.99	2.78	4.237	326.61	1912	17.08
		5.56	5.475	422.05	2176	19.39

(d) UX750 in field tests for 5ft length

N_c	Σa	σ_v (psi)	C_u	Bearing (lb)	Total (lb)	% Bearing
19.32	5.13	2.78	4.237	419.93	1794	23.4

Table 6.4.3: Percentage bearing for UX1500

(a) UX1500 in Laboratory tests for 3ft length

N_c	Σa	σ_v (psi)	C_u	Bearing (lb)	Total (lb)	% Bearing
19.32	3.315	3	4.335	277.64	2040	13.60
		5	5.226	334.7	2885.8	11.6
		7	6.116	391.7	2919.5	13.41
		10	7.452	477.26	3340.13	14.28
		15	9.678	619.83	4069.8	15.22

(b) UX1500 in field tests for 3ft length

N_c	Σa	σ_v (psi)	C_u	Bearing (lb)	Total (lb)	% Bearing
19.32	3.315	2.78	4.237	271.36	3948.5	6.87
		5.56	5.475	350.65	4060.8	8.63
		8.33	6.708	429.62	4062.5	10.57
		10.56	7.70	493.15	4786.5	10.3

(c) UX1500 in field tests for 4ft length

N_c	Σa	σ_v (psi)	C_u	Bearing (lb)	Total (lb)	% Bearing
19.32	4.974	2.78	4.237	407.16	2787.51	14.6
		5.56	5.475	526.13	3545.97	14.83
		8.33	6.708	644.62	3894.2	16.55

(table con'd.)

(d) UX1500 in field tests for 5ft length

N_c	Σa	σ_v (psi)	C_u	Bearing (lb)	Total (lb)	% Bearing
19.32	6.63	2.78	4.237	542.96	5342.4	10.16
		5.56	5.475	701.30	5846.4	11.99

Table 6.4.4: Percentage bearing for UX1500

(a) UX1700 in laboratory tests for 3ft length

N_c	Σa	σ_v (psi)	C_u	Bearing (lb)	Total (lb)	% Bearing
19.32	5.60	7	6.116	661.70	3775.68	17.52
		10	7.452	806.24	4482	17.98
		12	8.342	902.53	4898.88	18.42

(b) UX1700 in field tests for 3ft length

N_c	Σa	σ_v (psi)	C_u	Bearing (lb)	Total (lb)	% Bearing
19.32	5.60	8.33	6.708	725.75	4484.16	16.18
		10.56	7.70	833.07	4847	17.18
		12.23	8.445	913.68	5512.32	16.57

(c) UX1700 in field tests for 4ft length

N_c	Σa	σ_v (psi)	C_u	Bearing (lb)	Total (lb)	% Bearing
19.32	8.40	10.56	7.70	1249.61	6888.96	19.89
		12.23	8.45	1370.52	5771.52	21.65

6.5 Coefficient of Interaction:

One of the primary input parameters required in the design of soil structures reinforced with geosynthetics is the coefficient of interaction (C_i) of the geosynthetic with the soil. It is an important design parameter, which is used to calculate the bond length of the reinforcement required beyond a critical failure plane. The coefficient of interaction for cohesive soils is defined as (Tatlisoz et al., 1998):

$$C_i = \frac{C_a + \sigma_n \tan \delta_a}{C + \sigma_n \tan \phi} \tag{6.5.1}$$

The coefficient of interaction depends on: the percent open area of the geosynthetic, area of bearing surfaces perpendicular to tensile loading, bearing capacity of the surrounding soil, soil type, and the length of the embedded specimen.

The numerator in the Equation 6.5.1 is nothing but the apparent shear stress or the apparent pull-out resistance (τ_a) discussed in Section 6.2, and the denominator is the undrained shear strength (C_u) of the soil. Therefore it is the ratio of the apparent pull-out resistance or apparent shear stress to the internal shear strength of the back fill.

6.5.1 Average Resistance Method

Most of the design methods for geosynthetic reinforced soil structures are based on the limit equilibrium method (will be discussed later in Chapter 6), in which the interaction property between soil and reinforcing material is evaluated by the average resistance method (Ochiai et al., 1996). In this method the distribution curve at the maximum value of pulling force is taken into consideration and the average values are used for the evaluation. This average resistance method is further subdivided in to three methods, as described in Figure 6.5.1, and summarized below:

1. Total Area Method

In this method the pulling force at the front and the whole area of the geosynthetic in the pull-out box (in case of laboratory tests) are taken into consideration for the resistance evaluation. The average pull-out resistance is calculated using Equation 6.5.2, in which F_{Tmax} is the maximum value of pull-out force at the front of the geosynthetic, and L and B are the length and width of the geogrid, respectively. This equation is the same as that of Equation 6.2.1, discussed in the Section 6.2.

$$\tau_{av} = \frac{F_{T\max}}{2BL} \tag{6.5.2}$$

This method gives a reasonable average value of the pull-out resistance when the geosynthetic is wholly pulled out with slight elongation (Ochiai et al., 1996). The advantage of this method is that only the pulling force at the front of the geogrid needs to be measured.

2. Effective Area Method

This method is defined by the effective force with the related area for evaluating the pull-out resistance. The pull-out resistance is calculated by Equation 6.5.3, where L_T is the effective length of the geosynthetic and the value of ($F_{Tmax} - F_r$) is the effective tensile force, which corresponds to L_T, as shown in Figure 6.5.2.

$$\tau_{av} = \frac{F_{T\max} - F_r}{2BL_T} \tag{6.5.3}$$

In order to determine effective length (L_T), the displacements of each grid junction in the soil have to be measured in the test, as well as the pulling force at the geogrid front. However, the effective area method agrees with the total area method when the whole geogrid is totally pulled out (Ochiai et al., 1996).

3. **Maximum Slope Method**

In this method the slope of the tangent at a point of maximum tangent of the slope on distribution curve is used to evaluate the pull-out resistance. The pull-out resistance is calculated by Equation 6.5.4, which expresses the maximum slope of the tangent to the tensile force distribution curves.

$$\tau_{av} = \left(\frac{dF}{dL} \right)_{\max} \tag{6.5.4}$$

However, this method gives an over estimation of the average pull-out resistance.

Coefficient of interaction is an important design parameter, and gives a rough estimate of the frictional resistance of a particular geosynthetic specimen. It compares the effective strength of the soil-geosynthetic interface to the shear strength of the soil. Coefficient of interaction was calculated with different confining pressures, and for several geosynthetics with different lengths.

In this study, the total area method is used to calculate the coefficient of interaction for the different geosynthetics. The interaction coefficients for the investigated geosynthetics are summarized in Table 6.5.1 for laboratory tests and in Table 6.5.2 for field tests.

An interaction coefficient of less than 0.5 normally indicates weak bonding between the soil and the geosynthetic or breakage of the geosynthetic specimen. An interaction coefficient of greater than unity ($C_i > 1$) indicates that there is a strong bonding between the soil and the geosynthetic. The value of $C_i > 1$ indicates that the frictional resistance between the geosynthetic and the soil is greater than the inner shear

strength of the soil. Most of the investigated geosynthetics have C_i values range between 0.5 and unity.

The C_i values for the geogrids (Strata-500, UX750, UX1500, UX1700) either decrease or remain steady as the confining stresses increase. But geotextiles give inconsistent values with respect to increasing confining pressure. Comparing the field and the laboratory tests, the laboratory tests show the consistency in the values of coefficient of interaction. However, they are decreasing with increase in confining pressure.

6.5.2 Variation of Coefficient of Interaction (C_i) With Respect to Length

The variation of coefficient of interaction with respect to length is an important correlation to show the dependability of the total area method used to calculate the coefficient of interaction (C_i). The variation of the coefficient of interaction with specimen length for the geogrids and geotextiles are presented in Figure 6.5.3 and 6.5.4, respectively.

Figures 6.5.3 and 6.5.4 show that the value of coefficient of interaction decreases with increase in length of the geosynthetic specimen. The reason for decrease in C_i values with length might be due to the methodology applied while calculating C_i from the evaluated pull-out resistance using the total area method. This method assumes that the whole area of the geosynthetic is mobilized during pull-out of the geosynthetic (this is true for low confining pressures). However, Figure 6.5.1 illustrates the difference in the three methods, and the resulting forces are illustrated in Figure 6.5.2. It is clear from Figure 6.5.3 that the stronger geogrids (i.e. UX1500 and UX1700) shows greater values of C_i and weaker geogrids (i.e. UX750 and Stratagrid-500) showed lower values of C_i.

The variations of C_i with respect to confining pressure are also presented in Figures 6.5.5 and 6.5.6. This shows that the coefficient of interaction decreases with increasing confining pressure for a particular geosynthetic.

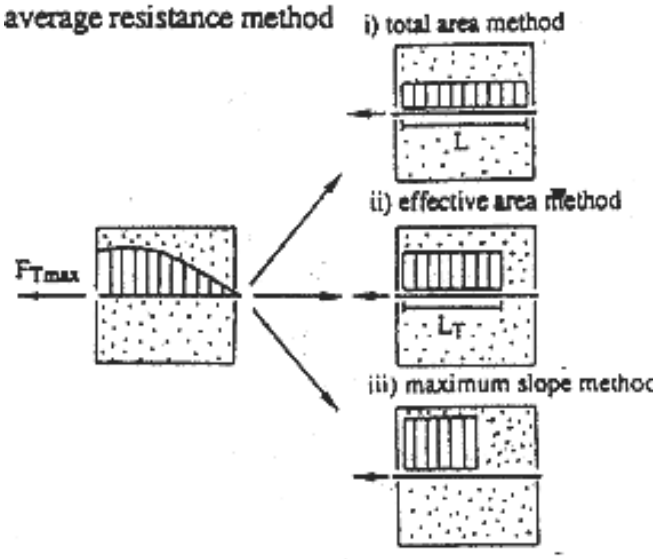

Figure 6.5.1: Evaluation methods for pull-out resistance (Ochiai et al., 1996)

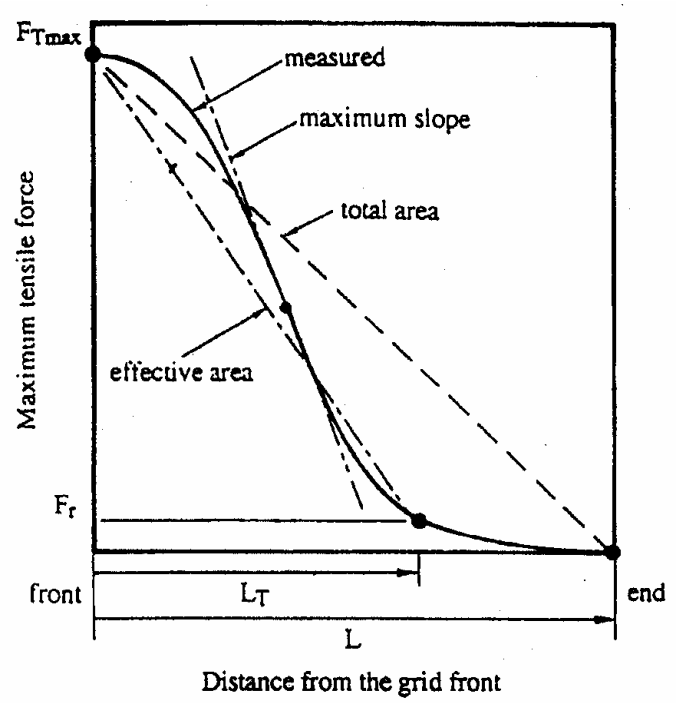

Figure 6.5.2: Sketches of the evaluation methods for pull-out resistance (Ochiai et al., 1996)

Table 6.5.1: Values of Coefficient of interaction (C_i) for different geosynthetics that were tested in the laboratory.

Test	Geosynthetic	Normal Stress(σ_n) (Psi)	Shear Strength(τ_s) (Psi)	Apparent shear strength (τ_i) (Psi)	length of the specimen (ft)	Coefficient of interaction C_i
Lab	Sratagrid-500	6	5.67	5.91	3	1.04
		8	6.56	6.15	3	0.93
		10	7.45	6.62	3	0.88
	UX750	3	4.33	1.92	3	0.44
		5	5.22	3.70	3	0.70
		7	6.11	3.86	3	0.63
	UX1500	3	4.33	2.36	3	0.54
		5	5.22	3.34	3	0.64
		7	6.11	3.37	3	0.55
		10	7.45	3.86	3	0.51
		15	9.67	4.70	3	0.48
	UX1700	7	6.11	4.37	3	0.71
		10	7.45	5.18	3	0.69
		12	8.34	5.67	3	0.67
	Woven (4x4)	3	4.33	3.08	3	0.71
		5	5.22	3.11	3	0.59
		6	5.67	3.66	3	0.64
		8	6.56	4.11	3	0.62

Table 6.5.2: Values of Coefficient of interaction (C_i) for different geosynthetics that were tested in the field.

Test	Geosynthetic	Normal Stress(σ_n) (psi)	Shear Strength(τ_s) (psi)	Apparent shear strength (τ_i) (psi)	length of the specimen (ft)	Coefficient of interaction C_i
Field	Sratagrid-500	8.33	6.70	4.49	3	0.67
		10.56	7.70	5.54	3	0.72
		12.23	8.44	6.19	3	0.73
		8.33	6.70	3.60	4	0.53
		12.23	8.44	3.77	4	0.44
		10.56	7.70	3.45	5	0.448
		12.23	8.44	3.76	5	0.445
	UX750	2.78	4.23	1.90	3	0.45
		5.56	5.47	2.23	3	0.40
		2.78	4.23	1.66	4	0.39
		5.56	5.47	1.88	4	0.34
		2.78	4.23	1.24	5	0.30
	UX1500	2.78	4.23	4.57	3	1.07
		5.56	5.47	4.70	3	0.86
		8.33	6.70	4.71	3	0.70
		10.56	7.70	5.54	3	0.71
		2.78	4.23	3.18	4	0.75
		5.56	5.47	4.06	4	0.74
		8.33	6.70	4.59	4	0.68
		2.78	4.23	3.71	5	0.87
		5.56	5.47	4.06	5	0.74
	UX1700	8.33	6.70	5.19	3	0.77
		10.56	7.70	5.61	3	0.72
		12.23	8.44	6.38	3	0.75
		10.56	7.70	5.01	4	0.65
		12.23	8.44	5.98	4	0.71
	Woven (4x4)	3	4.33	4.91	3	1.13
		12.50	8.56	5.03	3	0.59
		3	4.33	2.77	4	0.63
		6	5.67	2.86	4	0.50
		3	4.33	2.60	5	0.60
		6	5.67	2.90	5	0.51
	Woven (6x6)	6	5.67	6.71	3	1.18
		8.5	7.06	7.06	3	1.04
		11	7.89	7.58	3	0.96
		12.5	8.56	7.81	3	0.91
		11	7.89	5.55	4	0.70
		12.5	8.56	5.60	4	0.65

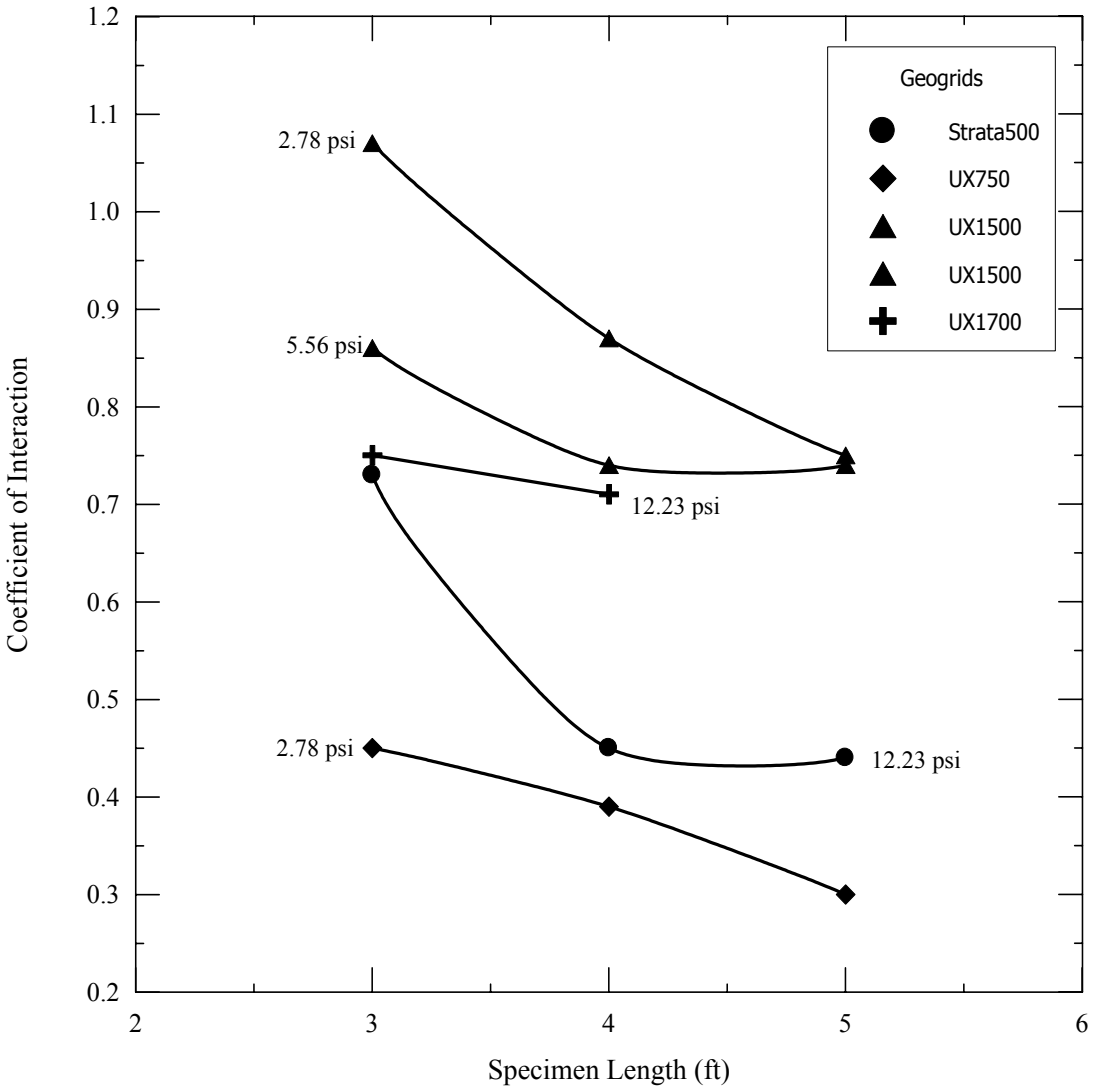

Figure 6.5.3: Variation of coefficient of interaction (C_i) with respect to length for all geogrids.

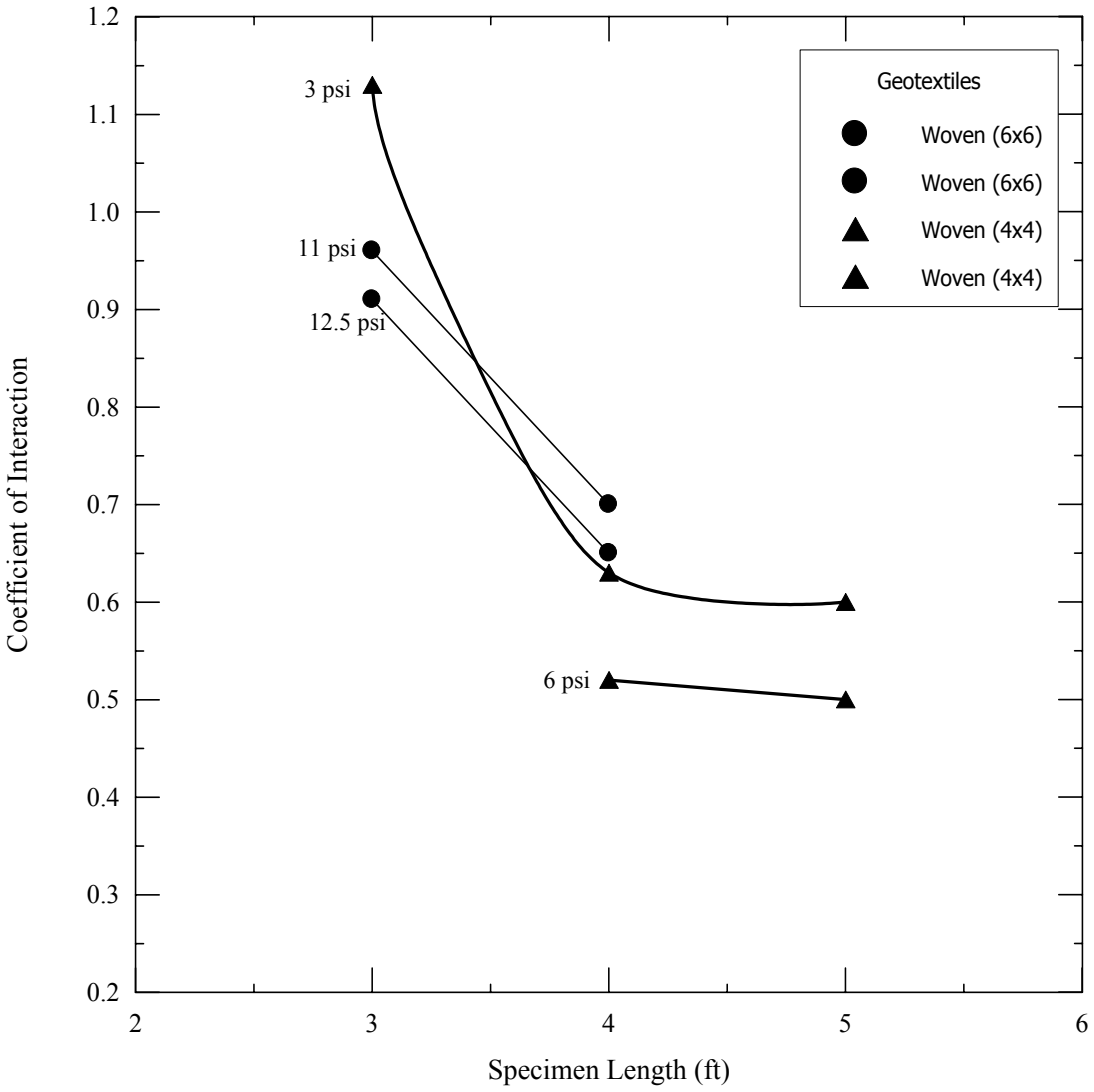

Figure 6.5.4: Variation of coefficient of interaction (C_i) with respect to length for all geotextiles.

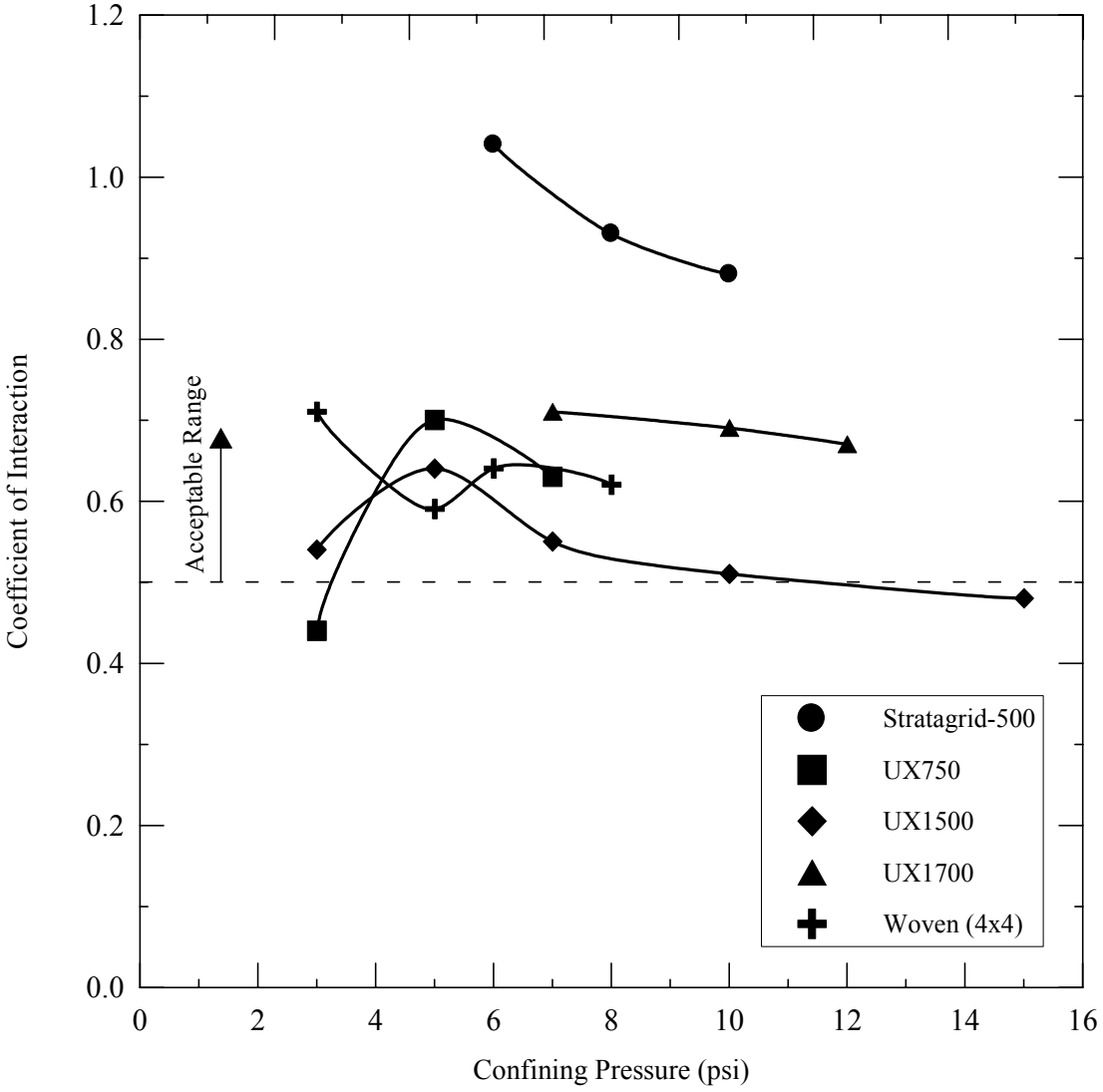

Figure 6.5.5: Variation of Coefficient of interaction (C_i) with confining pressure for the geosynthetics of 3ft length tested in the laboratory.

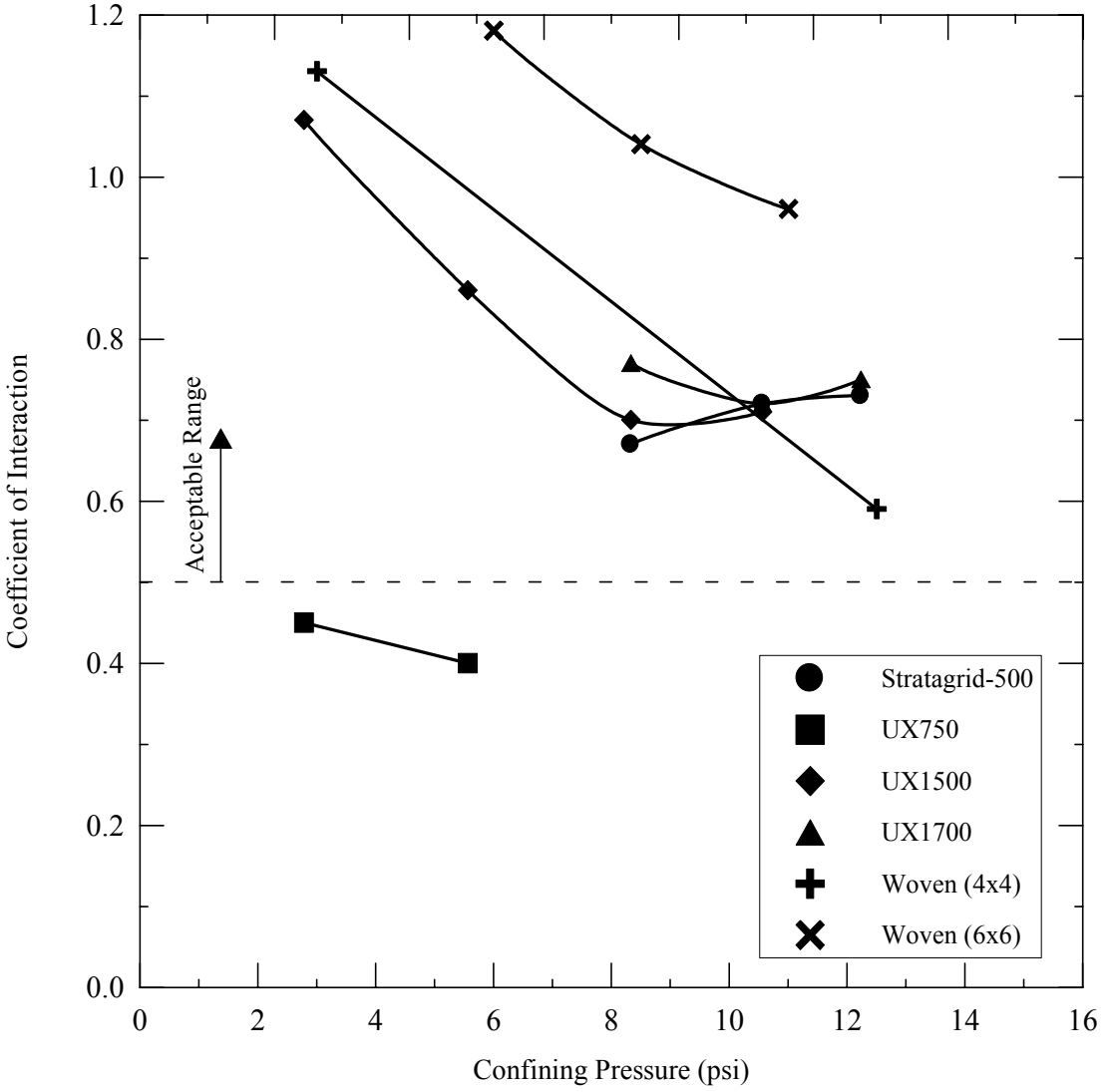

Figure 6.5.6: Variation of Coefficient of interaction (C_i) with confining pressure for the geosynthetics of 3ft length tested in the field.

6.6 Distribution of Shear Stress

In order to analyze the distribution of shear stress along the length of the geosynthetic specimen, it is important to know the displacements and/or strains at different locations along the length of the geosynthetic, and the stress-strain behavior of the geosynthetic specimen. LVDTs were installed in the laboratory pull-out tests with a spacing of 1ft in order to measure the displacements at the respective positions (i.e., the average displacement between two positions). The difference between the displacements gives the elongation, and from basic mechanics, the average strain within the segment can be calculated as the ratio of elongation to the total length of the segment selected. After estimating the average strain within the specified segment, the average tensile load is then calculated from the load-strain relation (see Figures 6.6.1a through 6.6.4a). The resulting average tensile force within the segment is then divided by the average embedded area to estimate the average shear stress within the segment. Now one can select the specified sections and continue the above mention steps to get the average shear stresses within the desired sections.

The analysis for the average shear distribution was done on four different geogrids that were tested in the laboratory. The average shear distribution for geogrids, Strata-500, UX750, UX1500 and UX1700 is presented in Figures 6.6.1 through 6.6.4, respectively. Unfortunately, there were not enough data points (i.e. less number of LVDTs to measure the displacements) to exactly show the shear distribution. However, with the available data, the average shear stress within every 1 ft section is illustrated. The Figures also illustrate the effect of different confining pressures.

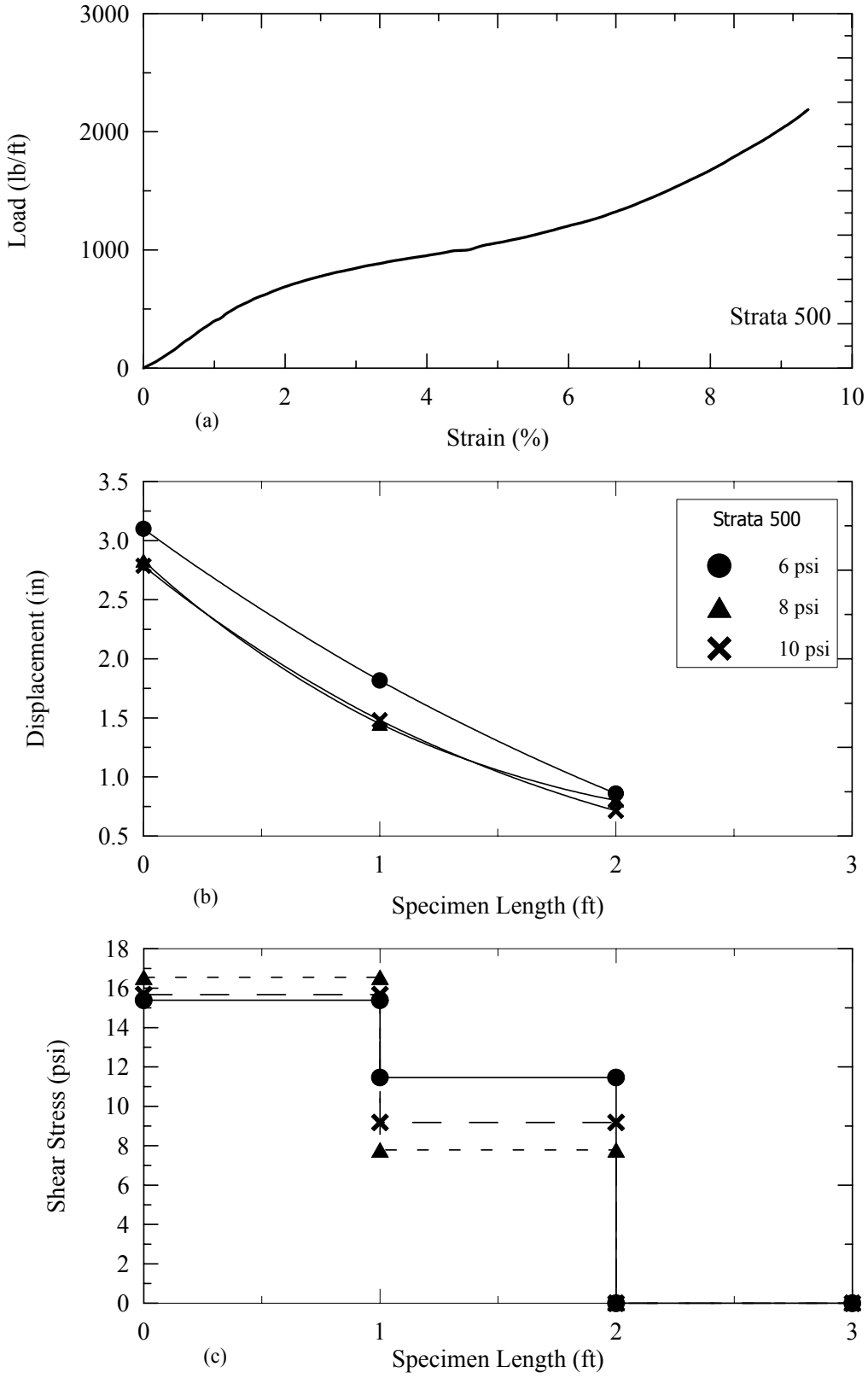

Figure 6.6.1: Evaluation of shear distribution for Stratagrid-500

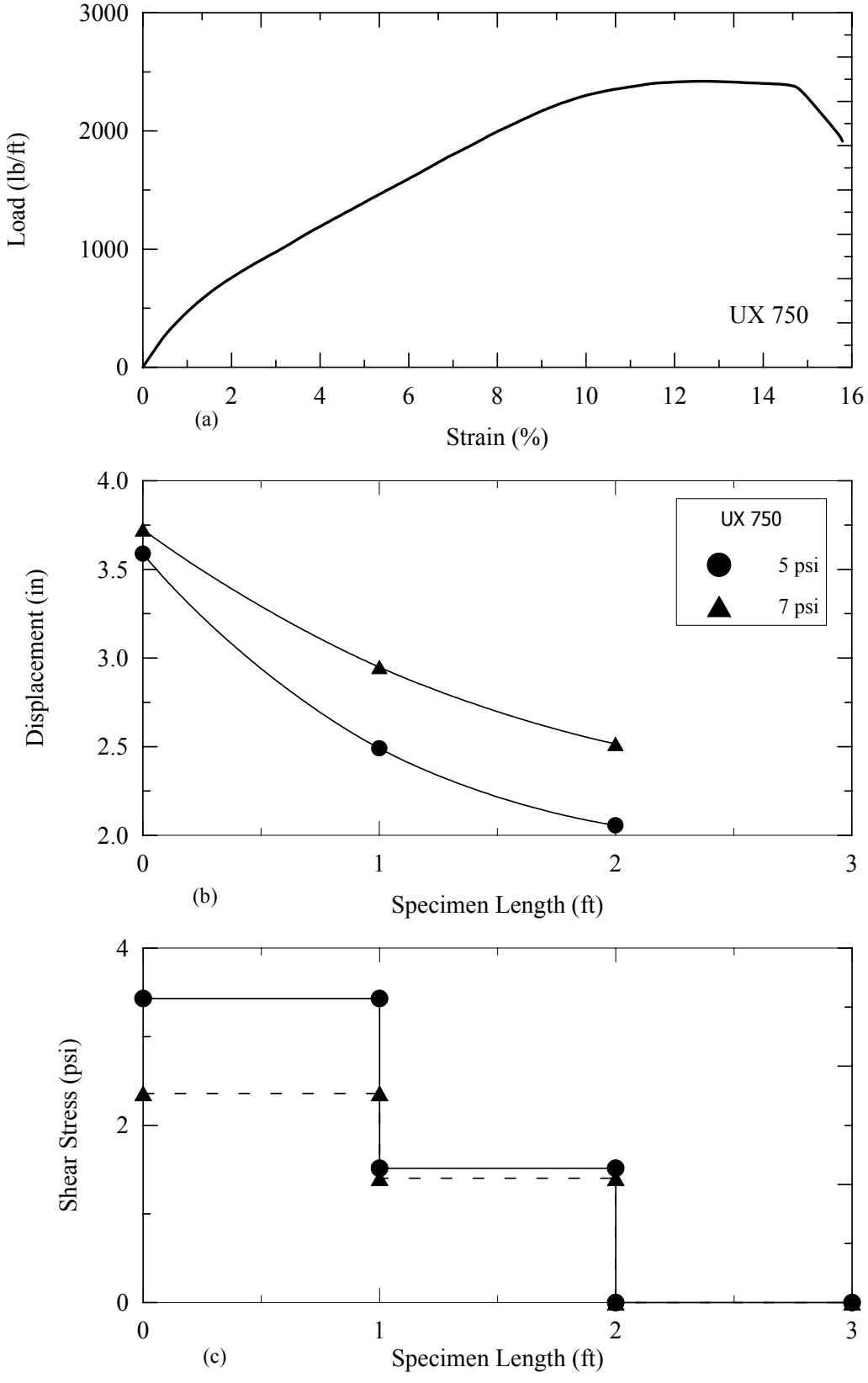

Figure 6.6.2: Evaluation of shear distribution for UX750

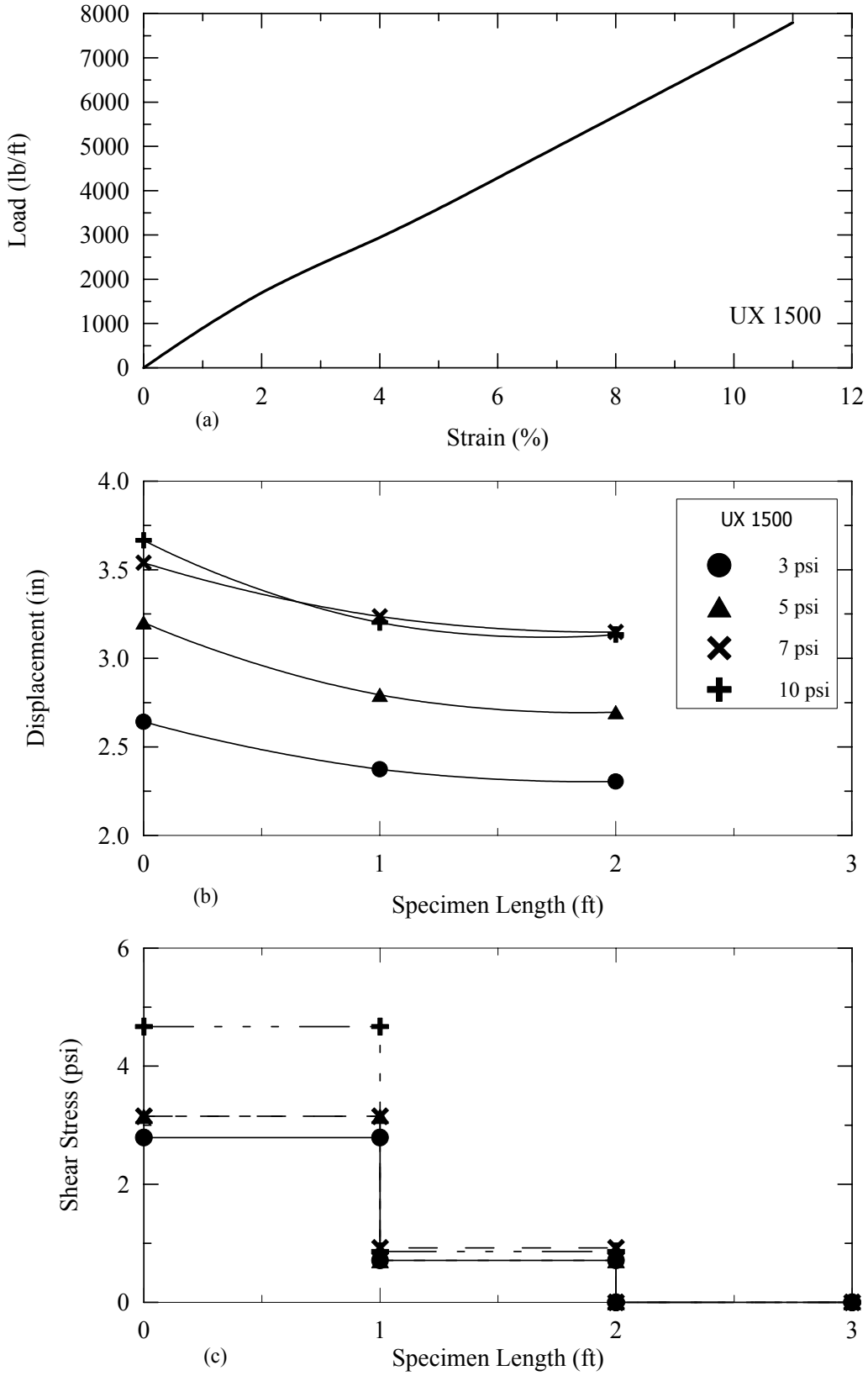

Figure 6.6.3: Evaluation of shear distribution for UX1500

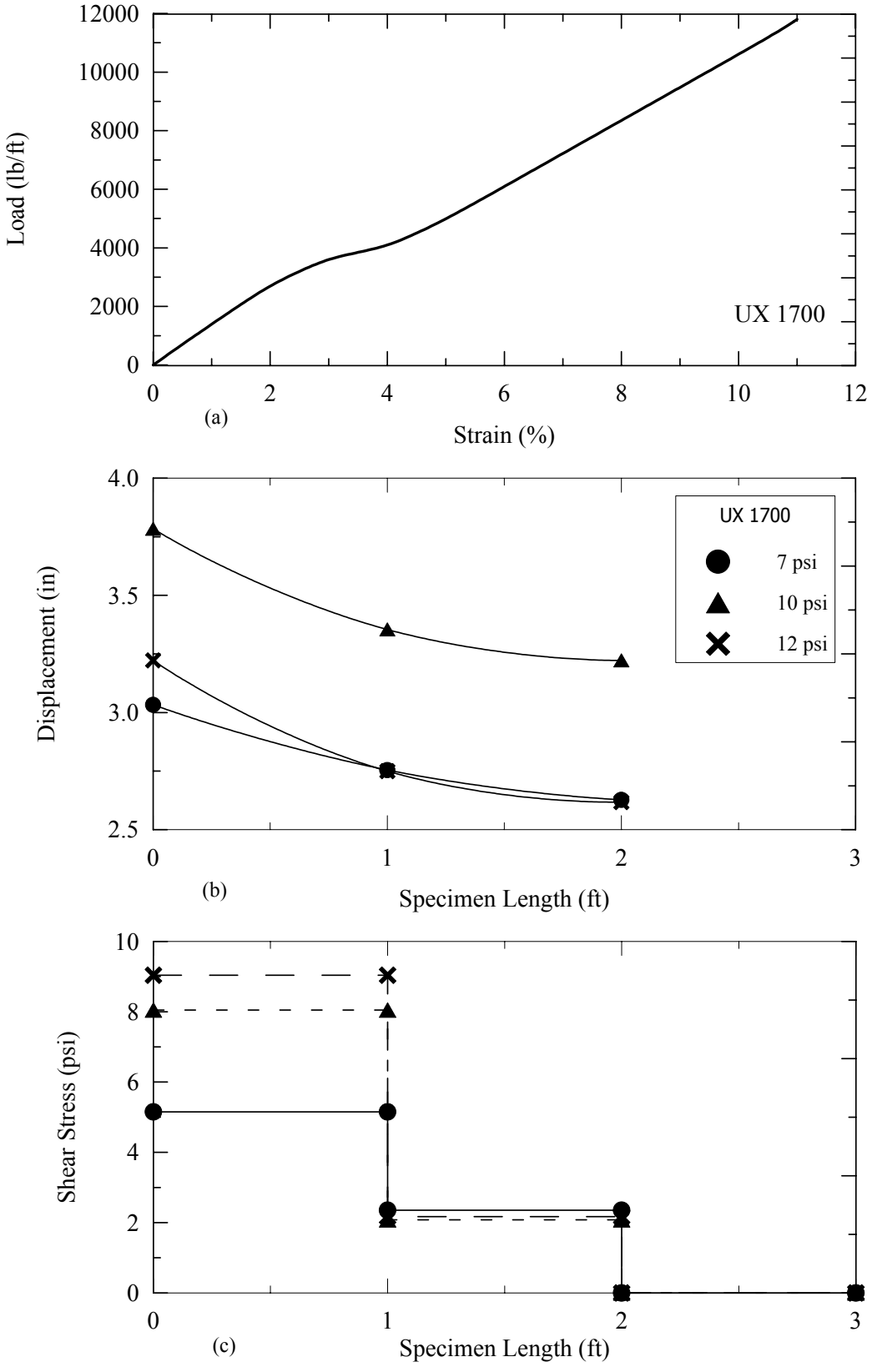

Figure 6.6.4: Evaluation of shear distribution for UX1700

After, examining the average shear distribution curves, one can see that the maximum average shear stress occurs near the face and decreases gradually along the length of the geosynthetic specimen. One can even see that the shear stress increases with increasing confining pressure for all four types of geogrids

The shear distribution in the extensible reinforcements is shown in Figure 6.6.5 (FHWA 96). The shear distribution obtained in this study is not the same, but it does follow the trend with the maximum average shear stress near the face. Since, there were very few LVDTs instrumented along the specimen length, the actual shear distribution was not obtained, and instead an average shear distribution within every one feet segment was calculated.

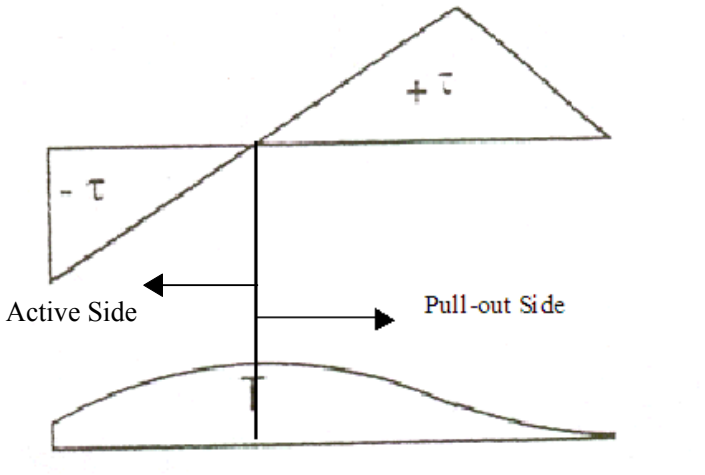

Figure 6.6.5: Shear distribution for actual reinforcement (after FHWA, 1996).

For the field pull-out tests, unfortunately the shear distribution was not estimated as there were not enough strain gauges to sketch the shear distribution along the specimen length.

6.7 Pull-out Resistance Factors (F^* and α)

For design and comparison purposes, a normalized definition of pull-out resistance is used by FHWA (FHWA 1996 manual). The pull-out resistance, P_r, of the reinforcement per unit width of reinforcement is given as:

$$P_r = F^*.\alpha.\sigma_v'.L_e.C \qquad (6.7.1)$$

where:

$L_e.C$	=	the total surface area per unit width of the reinforcement in the resistive zone behind the failure surface
L_e	=	the embedment or adherence length in the resisting zone behind the failure surface
C	=	the reinforcement effective unit perimeter, and C = 2 for strips, grids and sheets
F^*	=	the pull-out resistance factor (or friction-bearing interaction)
α	=	a scale effect correction factor to account for a non-linear stress reduction over the embedded length of highly extensible reinforcements
σ'_v	=	the effective vertical stress.

The correction factor α depends primarily upon the strain softening of compacted backfill material, the extensibility and the length of the reinforcement. For inextensible reinforcements, α is approximately 1.0, but it can be substantially smaller than 1.0 for extensible reinforcements (FHWA, 1996). The α factor (a scale correction factor) can be obtained from pull-out tests on reinforcement with different lengths. According to FHWA, if pull-out test data is not available, a default value of 1.0 can be used for α for

inextensible reinforcements and a default value of 0.6 to 0.8 can be used for extensible reinforcements.

The pull-out resistance factor F^* can be obtained most accurately from the laboratory or field pull-out tests performed in the specific backfill to be used on the project. Alternatively, F^* can be derived from empirical or theoretical relationships developed for each soil-reinforcement interaction mechanism and provided by the reinforcement supplier. For any reinforcement, F^* can be estimated using Equation 6.7.2:

$$F^* = \text{Passive resistance} + \text{Frictional resistance} \quad (6.7.2)$$

For geosynthetic reinforcement, pull-out resistance factor (F^*) is often referred to as an Interaction factor (C_i) (FHWA, 1996). The determination of the coefficient of interaction is described in the earlier section of this study (i.e., in Section 6.5 of this Chapter).

6.7.1 Procedure to Determine α

The method for determining scale effect correction factor, α, consists of normalized approach mentioned in FHWA 1996 manual (Elias and Christopher, 1996). The method provided in this study is known as corrected area method. The scale effect correction factor, α, is a function of nonlinearity in the pull-out load-mobilized reinforcement length relationship observed in the pull-out tests. To estimate the scale effect correction factor, α, the displacements along the length of the geosynthetic specimen need to be measured for all the pull-out tests, and the pull-out tests must be run at several confining pressures and/or at different lengths to develop the P_r versus $\sigma_v L_p$ plot as described in the Figures 6.7.1 through 6.7.4. Where, P_r is the applied pull-out load

per unit width of the reinforcement, and L_p is the assumed mobilized length of the reinforcement.

For a deflection of 1.0 inch at front of each pull-out test, the respective pull-out load per unit width is taken, and it is assumed that the total length was mobilized for every 1.0 inch deflection at front. Therefore, the L_p value for 3ft length was assumed to be 3ft, and similarly the L_p values for 4ft and 5ft were assumed to be 4ft and 5ft, respectively. After selecting the P_r values and assuming the L_p values for the selected geosynthetic, the plot for P_r versus $\sigma_v L_p$ for different L_p values and confining pressures is plotted. The secant tangent is drawn for the initial development of the curve, and the slope is taken as F^*_{peak}, and then the secant tangent is drawn for the respective mobilized reinforcement lengths with slope values taken as F^*_m. After estimating the respective F^*_m values, the secant tangent is drawn to the residual point of the curve to obtain $F^*_{resi.}$.

A relation is plotted with α value of 1.0 for the zero mobilized length, and then the value of $\frac{F^*_m}{F^*_{peak}}$ is calculated for the respective mobilized lengths. After reaching a point where the curve tends to form a residual behavior, the value of $\frac{F^*_{resi.}}{F^*_{peak}}$ is calculated. According to the developers of this method, for design purposes, the value of α is taken as $\frac{F^*_{resi.}}{F^*_{peak}}$. The scale correction factor (α) values estimated for the geogrids Strata-500, UX1500 and UX1700 ranges from 0.32 to 0.82, which is almost within the range set by FHWA standards, i.e. ranging from 0.6 to 0.8. The reason for lower values might be due

to the selection of the pull-out load with a front displacement of 1.0 inch, which was selected in order to assume that the total length of the geogrid is mobilized.

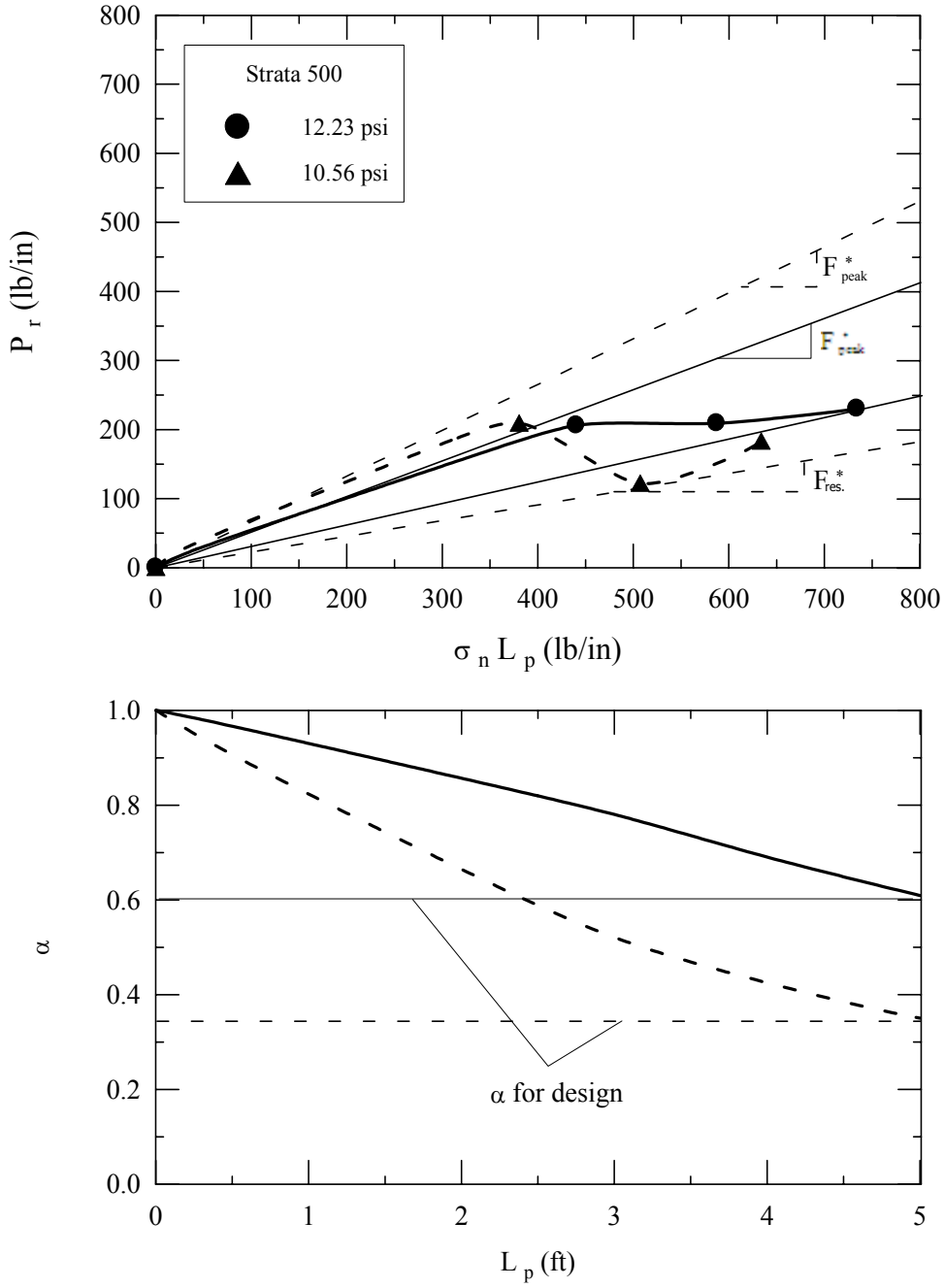

Figure 6.7.1: Procedure to determine α for Stratagrid-500 using field pull-out tests

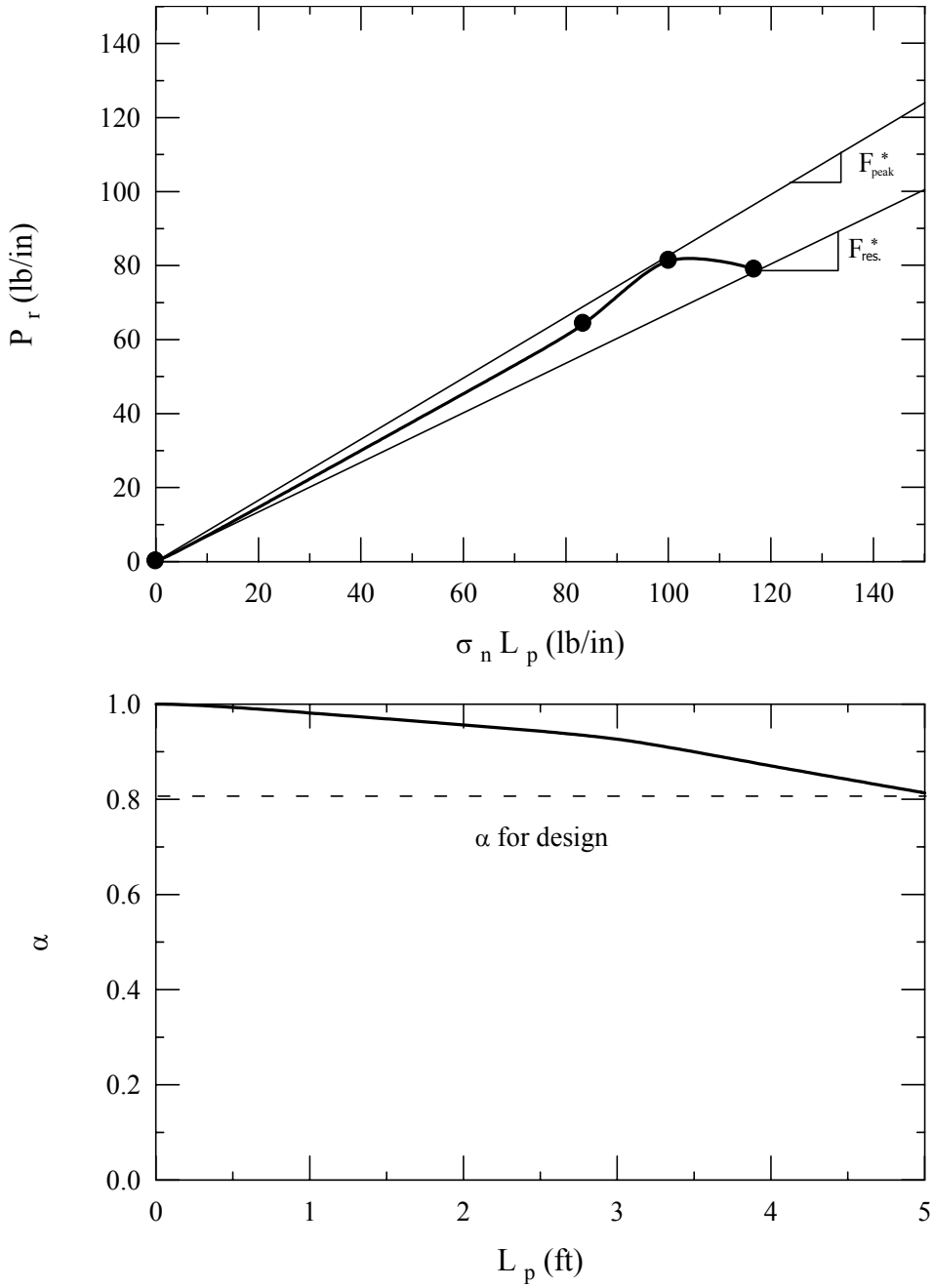

Figure 6.7.2: Procedure to determine α for UX750 using field pull-out tests

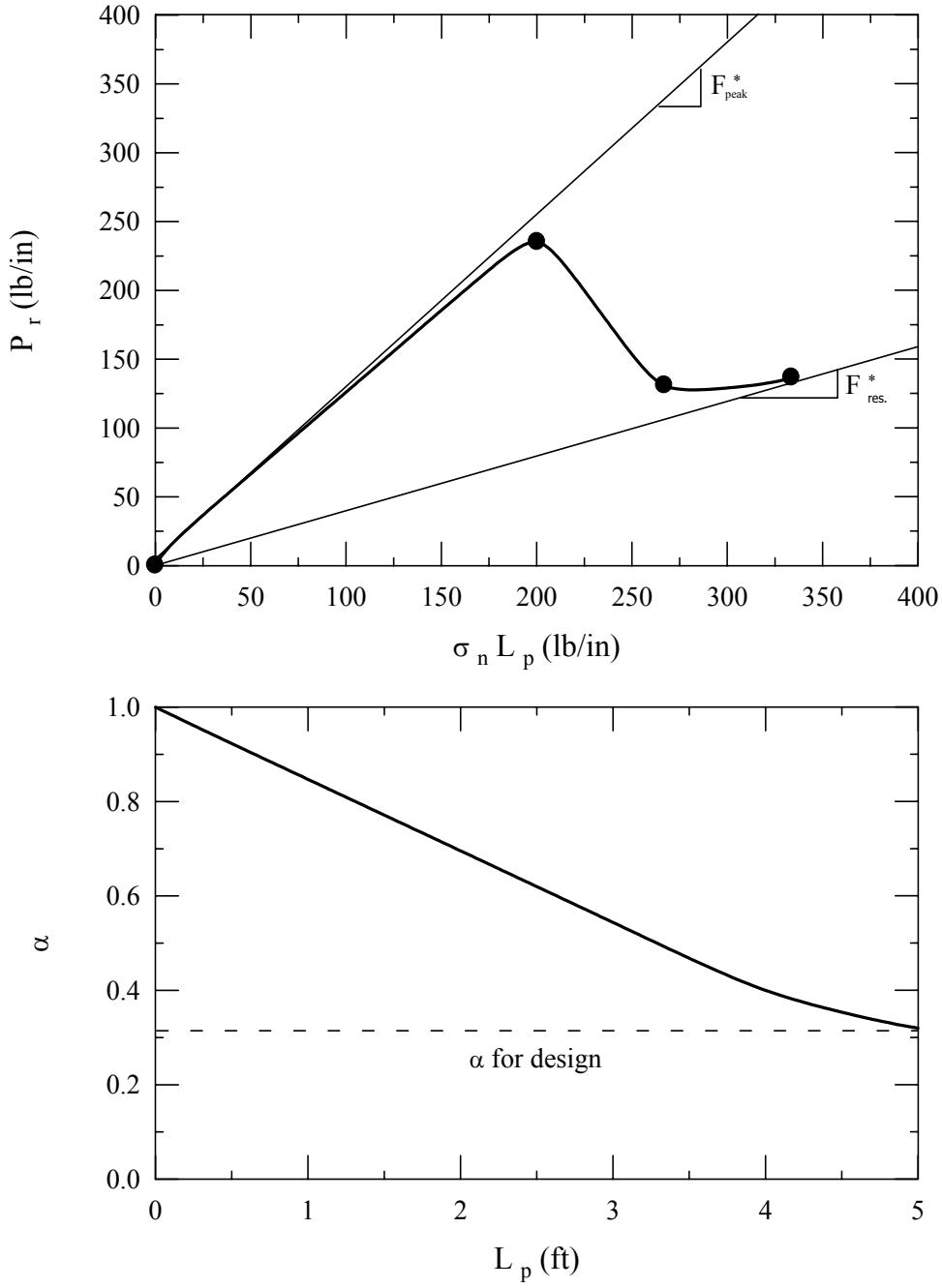

Figure 6.7.3: Procedure to determine α for UX1500 using field pull-out tests

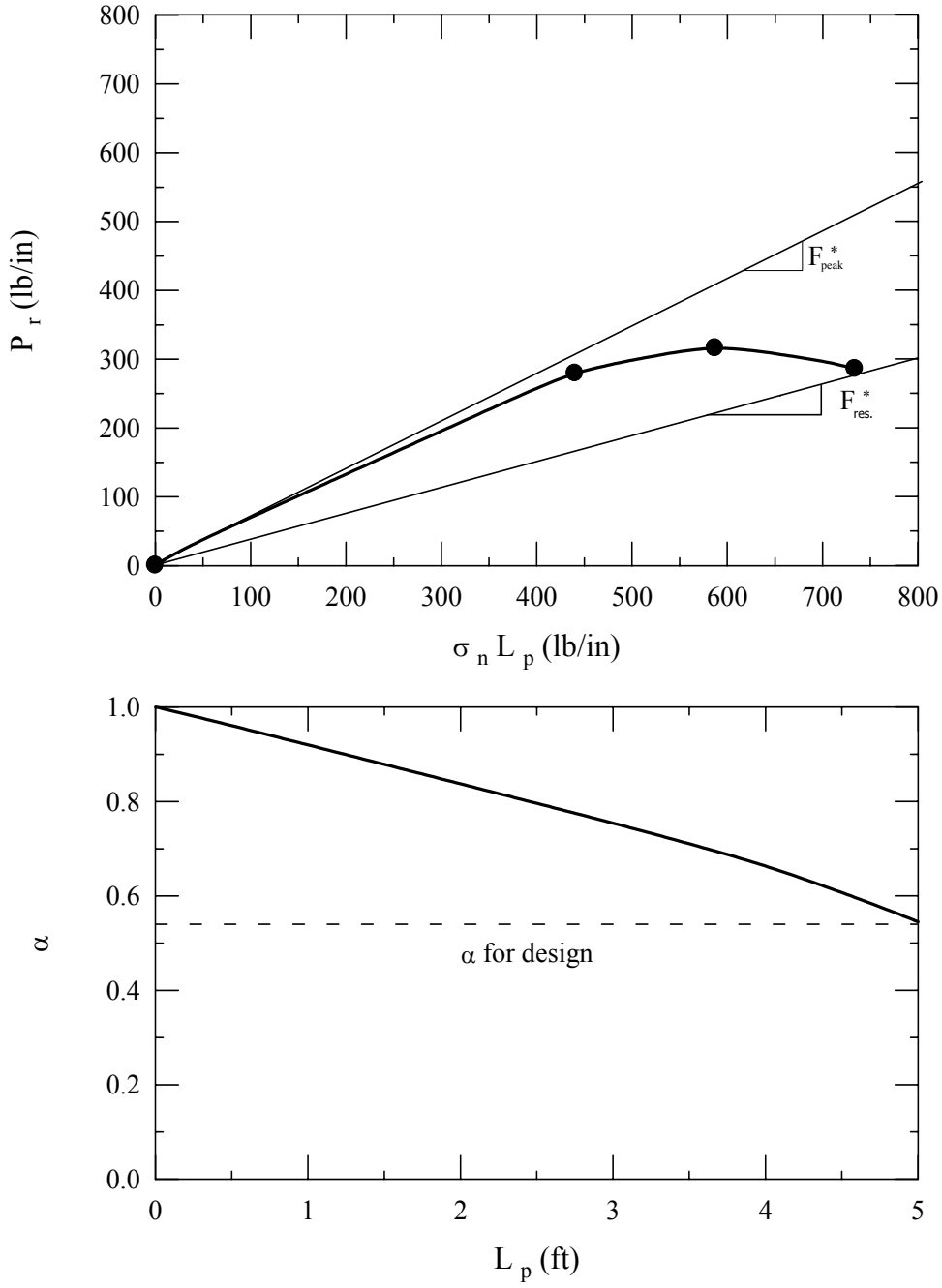

Figure 6.7.4: Procedure to determine α for UX1700 using field pull-out tests

CHAPTER 7

CONCLUSIONS AND RECOMMENDATIONS

7.1 Conclusions

- Laboratory and field pull-out test results are close to each other and show more consistency for high strength geosynthetics compared to weak geosynthetics, which show less consistency. The values of apparent coefficient of adhesion and apparent interface friction angle are similar for high strength geosynthetics (UX1500 and UX1700) as compared to weak geosynthetics (UX750, Stratagrid-500 and Woven (4x4)).

- The stronger geogrids (i.e. UX1500 and UX1700) have greater values of coefficient of interaction (C_i), while weaker geogrids (i.e. UX750 and Stratagrid-500) have lower values of C_i.

- The coefficient of interaction (C_i) ranged from 0.5 to 1.0 for laboratory pull-out tests and from 0.3 to 1.2 for field pull-out tests.

- In general, the coefficient of interaction (C_i) decreases with increasing confining pressure and with increase in geosynthetic length.

- Based on the theoretical calculation of passive bearing resistance for geogrids UX750, UX1500, UX1700 and Stratgrid-500, the contribution of passive bearing resistance ranges from 5-30 percent of the total pull-out resistance. The geogrid Stratagrid-500 (10% - 30%) has higher passive bearing resistance because it has more apertures and regarding the geogrid UX1700 (15% - 22%), it has greater thickness.

- The maximum average shear stress occurs at the front of specimen (1ft behind the face) and decreases gradually along the length of the geosynthetic specimen.
- The scale correction factor (α) values estimated for the geogrids Strata-500, UX1500 and UX1700 ranges from 0.32 to 0.82, which is almost within the range set by FHWA standards, i.e. ranging from 0.6 to 0.8.

7.2 Recommendations

- For the field pull-out tests, the displacements should be measured at the end of each specimen length (by gluing a strain gage) so as to account the effect of pull-out load at the tip, thereby providing additional point to have a good interpretation of the test results.
- Proper locations of the pressure cells to know the appropriate overburden pressure through the height of the wall.
- Better to perform pull-out tests in the laboratory with different lengths.
- Since it is an experimental project, better to perform more than three tests under similar conditions to have accurate predictions of all the test results.
- For estimating the contribution of passive bearing resistance, it is better to perform pull-out tests by removing the junctions (transverse members).
- A finite element modeling might provide a better solution in understanding the interaction behavior and internal stability concern of the wall.

REFERENCES

Bergado, D.T., Hardiyatimo, H.C., Cineros, C.B., Chun, C.J., Alfaro, M.C., Balasubramaniam, A.S., and Anderson, L.R. (1992). "Pull-out Resistance of Steel Geogrids with Weathered Clay as Backfill Material." *Geotechnical Testing Journal,* Vol. 15, No. 1., pp 33-46 (Mar).

Chan, D.H., Yi, C.T. and Scott, J.D. (1993). "An Interpretation of the Pull-out Test." *Geosynthetics* '93, pp 593-605.

Chang, D.T.-T., Wey, W. T. and Chen, T.C. (1993). "Study on Geotextiles Behaviors of Tensile Strength and Pull-out Capacity under Confined Condition." *Geosynthetics '93,* pp 607-618.

Chen, R.H. and Lee, Y.S. (1998). " A Model for the Ultimate Pull-out Resistance of Geogrids." *Geosynthetics* '98, pp 721-724.

Christopher, B.R., and Berg, R.R. (1990). "Pull-out Evaluation of Geosynthetics in Cohesive Soils." *Geotextiles, Geomembranes and Related Products, Den Hoedt (ed.), Balkema Publishers,* pp 731-736.

Christopher, B.R., Holtz, B.R. and Bell W.D. (1986). "New Tests for Determining the In-Soil Stress-Strain Properties of Geotextiles." *Third International conference on Geotextiles 1986, Vienna, Austria*, pp 683-688.

Cowell, M.J., and Sprague, C.J. (1993). "Comparison of Pull-out Performance of Geogrids and Geotextiles." *Geosynthetics '93,* pp 579-592.

Elias, V and Christopher, B.R. (1997). "Mechanically Stabilized earth Walls and Reinforced Soil Slopes, Design and Construction Guidelines," FHWA-SA-96-071.

Fannin, R.J., and Raju,D.M. (1993). "Large-Scale Pull-out Test Results on Geosynthetics." *Geosynthetics '93,* pp 633-643.

Farrag, K.A. and Griffin, P. (1993). "Pull-out Testing of Geogrids in Cohesive Soils." *American Society for Testing and Materials,* ASTM*, Philadelphia*, pp 76-89.

Farrag, K. (1995). "Evaluation of the Effect of Moisture Content on the Interface Properties of Geosynthetics." *Geosynthetics* '95, pp 1031-1041.

Farrag, K. (2003). "Laboratory and Field Pull-out Test Results", *Personal Communication.*

Garbulewski, K., (1990). "Direct Shear and Pull-out Frictional Resistance at the Geotextile-Mud Interface." *Geotextiles, Geomembranes and Related Products, Den Hoetd (ed.) Balkema Publishers*, pp 737-742.

Gurung, N. and Iwao, Y. (1999). "Pull-out Test Analysis for Geo-Reinforcement." *Geotextiles and Geomembranes,* Vol. 17, pp 157-170.

Hayashi, S., Shahu, J.T., and Watanabe, K. (1999) "Changes in Interface Stresses During Pull-out Tests on Geogrid Strip Reinforcement." *Geotechnical Testing Journal, GTJODJ,* Vol. 22, pp 32-38 (Mar).

Holtz, R.D. (1977). "Laboratory Studies of Reinforced Earth Using a Woven Polyester Fabric." *C.R. Coll. Int. Sols Textiles. Paris 1977,* pp 149-154.

Holtz, R.D. and Lee W.F. (2000). "Internal Stability Analyses of Geosynthetic Reinforced Retaining Walls." *Final Research Report Prepared for WSDOT (Jan 2002).*

Ingold, T.S. (1983). "Laboratory Pull-out Testing of Grid Reinforcements in Sand." *Geotechnical Testing Journal,* GTJODJ, Vol. 6, No. 3, pp 101-111 (Sept.).

Juran, I., Farrag, K.H. and Richmond. L. (1991). "Short and Long Term Performance of Polymeric Geogrids." *Geosynthetics '91.*

Juran, I. and Chen, C.L. (1988). "Soil-Geotextile Pull-out Interaction Properties, Testing and Interpretation," *Transportation Research Record,* 67th Annual Meeting.

Karmokar, A.K. and Kabeya, H. (1998). " An Approach to Analyze the Pull-out Resistance of Woven Geotextiles." *Geosynthetics* '98, pp 725-728.

Khera, R.P., Kasturi, R. M. and Khairul Alam, M. (1997). " Depth and Width Effect on Pull-out Resistance of Woven Geotextiles in Sand." *Geosynthetics* '97, pp 851-862.

Koerner, R.M. (1999). "Designing with Geosynthetics." Fourth edition.

Koutsourais, M., Sandri, D. and Swan, R. (1998). "Soil Interaction Characteristics of Geotextiles and Geogrids." *Geosynthetics* '98, pp 739-744.

Lee W.F. (2000). "Internal Stability Analyses of Geosynthetic Reinforced Retaining Walls." Dissertation, Doctor of Philosophy, Civil and Environmental Engineering, University of Washington.

Liu, S.S., Liu, C.L., Liu, J.C. and Kuo, S.H. (1996). "Short Term Pull-out Tests of Geogrid in a Compacted Lateritic Soil." *Journal of Geotechnical Engineering*, ASCE, pp 543-559.

Lopes, M.L and Ladeira, M. (1997). "Influence of the Confinement, Soil Density and Displacement Rate on Soil-Geogrid Interaction." *Geotextiles and Geomembranes*, Vol. 14, pp 543-554.

Mallick, S.B., Zhai, H., Adanur, S. and Elton, D.J. (1995). "Pull-out and Direct Shear Testing of Geosynthetic Reinforcement: State-of-the-Art Report." *Transportation Research Record 1534*, pp 80-90.

Mallick, S.B., Elton, D.J. and Adanur, S. (1997). "An experimental Characteriztion of Soil-Woven Geotextile Interface in Large Box Pull-out Tests." *Geosynthetics* '97, pp 927-940.

Mallick, S.B., Elton, D.J. and Adanur, S. (1998). " A New Approach in Modeling of Soil-Geotextile Interface Behavior in Pull-out Tests." *Geosynthetics* '98, pp 729-732.

Ochiai, H., Otani, J., Hayashic, S. and Hirai T. (1996). "The Pull-out Resistance of Geogrids in Reinforced Soil." *Geotextiles and Geomembranes,* Vol. 14, pp 19-42.

Ospina, R. I. (1988). "An Investigation on the Fundamental Interaction Mechanism of Non-Extensible Reinforcement Embedded in Sand," *Master of Science thesis*, Georgia Institute of Technology, Atlanta, GA.

Palmeira, E.M., and Milligan, G.W.E. (1991). "Large Scale Pull-out Test on Geotextiles and Geogrids." *Geosynthetics '91,* pp 743-746.

Peterson, L.M. and Anderson, L.R. (1980). "Pull-out Resistance of Welded Wire Mats Embedded in Soil," *Master of Science thesis*, Utah State University, Logan, UT.

Rowe, R.K., Ho, S.K. and Fisher, D.G. (1985). "Determination of Soil-Geotextile Interface Strength Properties." *Second Canadian Symposium on Geotextiles and Geomembranes,* pp 25-34 (Sept).

Sugimoto, M., Alagiyawanna, A.M.N. and Kadoguchi, K. (2001). "Influence of Rigid and Flexible Face on Geogrid Pull-out Tests." *Geotextiles and Geomembranes,* Vol. 19, pp 257-277.

Tatlisoz, N., Edil, T.B. and Benson, C.H. (1998). "Interaction Between Reinforcing Geosynthetics and Soil-Tire Chip Mixtures." *Journal of Geotechnical and Geoenvironmental Engineering,* pp 1109-1119

VITA

Ather Mohiuddin was born on March 25th, 1980 in Nizamabad, India, to Khader Mohiuddin and Qaiser-unisa Begum. He received his Bachelor of Engineering in Civil Engineering from Muffakham Jah College of Engineering and Technology, Osmania University, Hyderabad, India, in July 2001. He came to United States in the fall of 2001 to pursue a master's degree in civil engineering, majoring in geotechnical engineering at Louisiana State University, Baton Rouge, Louisiana. The degree of Master of Science in Civil Engineering will be conferred on Ather Mohiuddin in August 2003.